Diss. ETH No. 18807

Response of maize (*Zea mays* L.) seedlings to low and high temperature: association mapping of root growth and photosynthesis-related traits

A dissertation submitted to the
ETH Zurich

for the degree of
Doctor of Sciences

presented by

Regina Reimer
M.Sc., Justus-Liebig-University Giessen, Germany
born July 3rd, 1977
citizen of Germany

accepted on the recommendation of
Prof. Dr. Peter Stamp, examiner
Dr. Andreas Hund, co-examiner
Prof. Dr. Albrecht E. Melchinger, co-examiner

2010

Niemand darf seine Wurzeln vergessen. Sie sind Ursprung unseres Lebens.
Federico Fellini

Table of contents

Abbreviations

AFLP	Amplified fragment length polymorphism
ANOVA	Analysis of variance
Bin	Segment of a chromosome located between two core markers
BLUP	Best linear unbiased predictor
BPH	Better-parent heterosis
CER	Carbon exchange rate expressed as µmol m^{-2} s^{-1}
cM	CentiMorgan. A unit for measuring genetic distance. One cM corresponds to approximately 1% recombination, if double and high level crossovers are ignored
DAG	Days after germination
$D_{Ax,\ Lat}$	Median diameter of axile/lateral roots, respectively
DW_{Leaf}	Dry weight of the leaf blades
DW_{Rt}	Dry weight of the roots
DW_{RtSt}	Ratio of dry weight of root and shoot
DW_{St}	Dry weight of the shoot
ER_{Ax}	Elongation rate of the axile roots
F_v/F_m	Maximal quantum efficiency of PSII of a dark adapted leaf
GCA	General combining ability
h^2	Broad sense heritability
IRGA	Infrared gas analyzer
k_{Lat}	Rate constant of lateral roots
k_{Lat}/ER_{Ax}	Elongation rate ratio of lateral roots to that of axile roots
LA	Leaf area
$L_{Ax,\ Lat}$	End length of the axile/lateral roots, respectively
L_{Rt}	Total root length
MPH	Mid-parent heterosis
PAM	Pulse amplitude modulation
PPFD	Photosynthetic photon flux density expressed as µmol m^{-2} s^{-1}
Φ_{PSII}	Operating quantum efficiency of the photosystem II
QTL	Quantitative trait loci
RLDD	Root length in diameter-class distribution
SCA	Specific combining ability
SPAD	Leaf greenness (Soil plant analysis development)
SSR	Simple sequence repeat, micro satellite
V2/3	Vegetative stage of 2/3 fully developed leaves

Expressions used:
associations with temperature treatment interaction effects = association-by-temperature interactions

Summary

Abiotic stress, like unfavorable temperature, is responsible for reduced yields throughout the world. Therefore, breeders aim to develop plants that are adapted to changing and challenging environments. In maize, breeders selected and developed heterotic groups of germplasm to take advantage of non-additive genetic variation. In cool regions of central and northern Europe these heterotic groups comprise the flints with European flint and Flint/Lancaster background and the dents with Iodent and Iowa/Stiff Stalk background. In this project a set of inbred lines from these backgrounds was used. It was derived from a breeding program of the University of Hohenheim, Stuttgart, Germany. Seedling growth was tested through a range of favorable and unfavorable temperatures in growth pouches, consisting of an A4-size germination blotter covered by a plastic sheet. As roots stopped growing at the extremes of 12°C and 40°C, limits were set accordingly and plants were tested at chilling stress of 16°C, close-to-optimal conditions of 28°C and heat stress of 36°C.

The first part of this study aimed to assess root elongation and photosynthesis-related traits with regard to temperature performance. Temperature stress affected all measured physiological and morphological traits. Elongation of both axile and lateral roots, shoot growth and photosynthesis were strongly affected by chilling. Heat stress effects occurred but were less severe than chilling stress effects. Flints and dents were clearly separated according to principle coordinate analysis, which justified a separate analysis for both groups. The flints had greener, smaller leaves and an increased photosynthesis under chilling stress. They grew thicker roots and less seminal roots than the dents. The dents developed axile roots elongating faster at optimum temperature than the flints and accumulated more leaf dry weight at optimum temperature and under heat stress. The association mapping yielded 1 to 50 associations, dependent on the trait, and explained proportions of the genetic variance ranging from 27.3 to 92.6%. The individual effect per association averaged at 30%. The flints were genetically less diverse at temperature-tolerance loci than the dents, but carried the chilling tolerance alleles for Φ_{PSII} more frequently. The dents carried the trait increasing alleles for axile root length and heat tolerance alleles for k_{Lat}/ER_{Ax}. A higher number of associations for the root elongation traits like $ER_{Ax,}$ was detected compared to the static traits, like the total root length at the end of experiment. This increased power of using elongation rates to detect association-by-temperature interaction effects justifies the greater time expense for the

repeated measurements. The altered root morphology was mostly caused by the response of ER_{Ax} to temperature, as an increase of k_{Lat}/ER_{Ax} was frequently collocated with a decrease of ER_{Ax}. Candidate genes have been selected according to their assumed function in temperature stress tolerance. A major proportion of those genes are related to the sugar metabolism. Therefore, the cytosolic glycolysis pathway was identified as a candidate pathway based on its metabolic adaptability, which facilitates plant acclimation to challenging environments.

The second part of the study aimed to examine temperature-dependent heterosis for physiological and morphological traits by using a diallel cross of two flint and two dent inbred lines. It was hypothesized that i) temperature dependent combining ability could be used to establish a wider temperature range in the hybrids and ii) that mid-parent heterosis (MPH) and better-parent heterosis (BPH) could serve as predictors for hybrid performance from inbred performance. The first hypothesis was met for treatment-by-SCA (specific combining ability) interactions meaning that one inbred line was conferring chilling or heat tolerance in a specific combination with another inbred line. The second hypothesis was not met since MPH and BPH regressions on genotypic mean values were not significant for most traits. In general, hybrids performed better than the inbreds. Inbred lines differed in their physiological and morphological performance and all performed best at optimum conditions. Heterosis was more expressed at the temperature extremes for the photosynthetic traits and was greatest at optimum conditions for shoot growth traits.

The third part of this study aimed to improve the separation of axile from lateral roots after the digital image analysis. The image analysis software supplies a distribution of root lengths in diameter classes, which is typically bimodal in case of maize seedling roots. The peak at the smaller diameter classes represents the lateral roots; the one for the lager diameter classes represents the axile roots. Finding the appropriate threshold to separate the two peaks is a critical step in the analysis of root morphology. So far this step was not automated and the threshold had to be selected manually. To improve the procedure, different non-parametric and parametric functions were evaluated to automate the separation of the putative peaks of axile and lateral roots. A Gaussian mixture model of two normal distributions was most suitable to determine this threshold.

In conclusion, the phenotyping platform successfully allowed for a precise application of the desired temperature stress and a high throughput screening of the study material as it is required for an association mapping approach. The association-by-temperature interaction

model was successful in detecting significant associations especially for the root elongation rates. The flint heterotic group was genetically less divers than the dent group and their allelic contribution to tolerance differed with regard to chilling and heat stress. The map projection with a publicly available genetic map revealed candidate genes involved in the sugar metabolic pathway to play a key role in root elongation under unfavorable temperature conditions.

Zusammenfassung

Ernteerträge von Mais werden weltweit durch abiotischen Stress, wie z. B. ungünstige Wachstumstemperaturen, stark reduziert. Das Ziel des Züchters ist es daher, Pflanzen zu entwickeln, die an wechselnde und ungünstige Umweltbedingungen angepasst sind. Im Falle von Mais haben Züchter heterotische Gruppen selektiert und entwickelt, um die nicht-additive genetische Variation zu nutzen. In den kühlen Lagen Zentral- und Nordeuropas bestehen diese Gruppen aus dem Hartmais, mit europäischer und „Flint/Lancaster“ Herkunft, und aus dem Zahnmais, mit „Iodent“ und „Iowa/Stiff Stalk“ Herkunft. Das ausgewählte Material enthält europäische Inzuchtlinien aus beiden heterotischen Gruppen. Das Material stammt aus einem Zuchtprogramm der Universität Hohenheim in Stuttgart (Deutschland). Die Jugendentwicklung unter optimalen und ungünstigen Temperaturbereichen wurde in sogenannten Wachstumshüllen getestet. Diese bestehen aus einem A4 Keimpapier, welches mit einer schwarzen PET-Folie bedeckt ist. Da das Wurzelwachstum bei 12°C und 40°C stagnierte, wurden Testtemperaturen von 16°C als unterer Schwellenwert (Kühlestress), 36°C als oberer Schwellenwert (Hitzestress) und 28°C als Kontrolle (Optimum) ausgewählt.

Der erste Teil der Dissertation hatte zum Ziel, Wurzelwachstum und Photosyntheseparameter im Hinblick auf ihr Temperaturverhalten zu bewerten. Der Temperaturstress beeinträchtigte alle physiologischen und morphologischen Parameter. Das Haupt- und Seitenwurzelwachstum, die Sprossentwicklung und die Photosynthese waren stark durch die kühlen Temperaturen beeinträchtigt. Der Hitzestress hatte ebenfalls negative Auswirkungen, wobei diese weniger gravierend waren als die des Kühlestresses. Hartmais und Zahnmais Linien waren laut der Faktorenanalyse genetisch voneinander verschieden was eine separate Auswertung der beiden Gruppen erlaubte. Der Hartmais entwickelte grünere, kleinere Blätter und hatte eine höhere Photosyntheseleistung in der Kühle, im Vergleich zum Zahnmais. Des Weiteren entwickelte er weniger, aber dafür dickere Hauptwurzeln. Der Zahnmais entwickelte Hauptwurzeln mit einer erhöhten Wachstumsrate unter optimalen Temperaturen im Vergleich zum Hartmais. Ebenso bildete er mehr Blatttrockenmasse bei optimalen Temperaturen sowie in der Hitze. Die Assoziationskartierung ergab 1 bis 50 signifikante Assoziationen, abhängig von den untersuchten Parametern, welche 27,3 bis 92,6% der genotypischen Varianz erklären. Der Einfluss der einzelnen Assoziation lag im Durchschnitt bei 30%. Der Hartmais war an den Genorten für Temperaturtoleranz weniger divers, trug jedoch das Kühletoleranzallel für

die Quanteneffizienz des Photosystems II eines lichtadaptierten Blattes (Φ_{PSII}) häufiger als der Zahnmais. Der Zahnmais wiederum trug die merkmalserhöhenden Allele für die Hauptwurzellänge und auch die Hitzetoleranzallele für das Verhältnis von Seitenwurzel- zu Hauptwurzelwachstumsrate (k_{Lat}/ER_{Ax}). Es wurden mehr QTLs für die dynamischen Wurzelwachstumsmerkmale gefunden als für statische Merkmale, die nur am Ende des Experiments gemessen wurden. Dies deutet auf eine höhere Präzision der dynamischen Merkmale hin, was die zeitaufwendigeren wiederholten Messungen rechtfertigt. Die veränderte Wurzelmorphologie basierte meistens auf einer Reaktion seitens der Hauptwurzelwachstumsrate (ER_{Ax}). Das schliesst sich daraus, dass eine Erhöhung des Merkmals k_{Lat}/ER_{Ax} häufig mit einer Verminderung von ER_{Ax} einherging. Aufgrund ihrer mutmasslichen Funktion bei der Toleranz gegenüber Temperaturstress wurden Kandidatengene ausgewählt. Ein grosser Teil dieser Gene ist in den Zucker-Metabolismus, insbesondere die zytosolische Glykolyse, involviert. Eine gute Anpassungsfähigkeit der zytosolischen Glykolyse an schwankende Temperaturen ist für das Gleichgewicht des pflanzlichen Stoffwechsels wichtig.

Der zweite Teil dieser Arbeit zielte darauf ab, temperaturabhängige Heterosis für physiologische und morphologische Merkmale anhand einer Teilmenge von Hart- und Zahnmais Inzuchtlinien zu eruieren. Folgende Hypothesen wurden aufgestellt: i), dass temperaturabhängige Kombinationseignung zur Schaffung eines breiteren Temperaturoptimums in den Hybriden genutzt werden kann und ii), dass die Heterosis im Vergleich zum Elternmittel (MPH) und im Vergleich zum besseren Elter (BPH) die Hybridleistung aufgrund der Elternleistung vorhersagen kann. Die erste Hypothese konnte für die Umwelt × SCA Interaktion (SCA, spezifische Kombinationseignung) bestätigt werden, was bedeutet, dass eine bestimmte Inzuchtlinie in Kombination mit einer anderen bestimmten Inzuchtlinie die Kühle- oder Hitzetoleranz des Hybriden erhöhte. Die zweite Hypothese wurde nicht bestätigt, da die MPH und BPH Regression zum Mittelwert der Genotypen für die meisten Merkmale nicht signifikant war. Das bedeutet, dass die Hybridleistung in den meisten Fällen nicht durch die Eigenleistung der Eltern vorhersagbar war. Im allgemeinen zeigten die Hybriden eine bessere Leistung als die Inzuchtlinien. Letztere zeigten physiologische und morphologische Unterschiede und alle entwickelten sich unter optimalen Bedingungen am besten. Heterosis für die Photosynthese äusserte sich am stärksten in den

Extremtemperaturen, während Heterosis Effekte für das Sprosswachstum unter optimalen Bedingungen am grössten waren.

Der dritte Teil dieser Arbeit zielt darauf ab, die Trennung von Haupt- und Seitenwurzeln im Anschluss an die Bildanalyse zu verbessern. Das Bildanalyseprogramm liefert eine Verteilung der Wurzellängen in Durchmesserklassen, die im Falle von Mais typischerweise einen zweigipfligen Verlauf zeigt. Der Scheitelpunkt der niedrigen Durchmesserklassen repräsentiert die Seitenwurzeln und der Scheitelpunkt der hohen Klassen die Hauptwurzeln. Den adäquaten Schwellenwert zwischen beiden Scheitelpunkten zu finden, ist ein kritischer Schritt in der Analyse der Wurzelmorpholgie. Bislang war dieser Schritt nicht automatisiert und der Schwellenwert wurde manuell ausgewählt. Um dies zu automatisieren, wurden verschiedene nicht-parametrische und parametrische Modelle geprüft. Ein gemischtes Model von zwei Gauss'schen Normalverteilungen erwies sich dafür als am besten geeignet.

Schlussfolgernd kann gesagt werden, dass die Phänotypisierungs-Plattform, bestehend aus den Wachstumshüllen, eine präzise Einstellung des gewünschten Temperaturstresses erlaubte und eine Hochdurchsatz-Analyse des Materials ermöglichte. Das Model war geeignet zur Detektion von signifikanten Assoziation × Umwelt-Interaktionen insbesondere für solche im Zusammenhang mit dem Wurzelwachstum. Der Hartmais war genetisch weniger divers als der Zahnmais und der Beitrag ihrer jeweiligen Allele zur Toleranz unterschied sich für Kühle- und Hitzestress. Die Projizierung der Assoziationen auf eine öffentlich verfügbare genetische Karte führte zur Identifikation von Kandidatengenen des Zucker-Metabolismus, welche eine entscheidende Rolle für das Wurzelwachstum unter ungünstigen Temperaturbedingungen spielen.

Chapter 1

General introduction

MAIZE AND ITS EXPANSION TO NORTHERN LATITUDES

Today, maize (*Zea mays* L.) is the third important cereal crop beside wheat and rice. Low temperature is a major factor limiting the productivity and geographical distribution of important agricultural crops like maize (ALLEN and ORT 2001). But maize has high temperature needs for germination and growth and is, therefore, a thermophilic plant species (MIEDEMA 1982). Early development of maize is already affected by temperatures below 15°C (STAMP 1984). Accordingly, its seedling growth is limited in northern latitudes by low temperature in spring (VERHEUL *et al.* 1995). Despite this fact, the cultivation of maize has been extended to areas in cooler regions over the past 50 years and it has become a major crop in northern regions where its high temperature requirement is not always fulfilled (FRACHEBOUD *et al.* 1999). This northwards migration is a combined effect of global warming and breeding efforts to improve chilling tolerance in maize. Improving early vigor remains crucial for the adaptation of maize to the climatic conditions of central Europe and the northern Mediterranean zone, where early sowing is an important strategy for avoiding the effect of summer drought (HUND *et al.* 2004).

PLANTS RESPONSE TO CHILLING STRESS

The temperature optimum is 30°C for growth processes in maize. This is described for germination, shoot elongation (MIEDEMA *et al.* 1987), for leaf development (DUNCAN and HESKETH 1968), elongation and dry matter accumulation after emergence (MULDOON *et al.* 1984).

Many plant species have mechanisms to adapt to adverse environmental conditions like low temperature (THOMASHOW 1999), but as a chilling sensitive plant, maize shows limited capacity to acclimate to low growth temperature (FOYER *et al.* 2002). Adverse temperature affects the photosynthetic capacity of seedlings (FRACHEBOUD *et al.* 1999; VERHEUL *et al.* 1996), leading to a decreased dry matter accumulation and thus poor yields (STAMP 1986) due

to a disturbed root (ENGELS 1994a) and leaf development (STONE *et al.* 1999). Furthermore, the formation of destructive oxygen species increases (LEIPNER *et al.* 1997), leading to an increased expression of active-oxygen-scavenging enzymes. Changes in lipid composition (ALLEN and ORT 2001) and anthocyanin accumulation are known. STONE *et al.* (1999) demonstrated that soil temperature determines the rate of early maize development when the shoot meristem is still below ground. Plant growth at suboptimal root zone temperature is limited by both a direct temperature effect on shoot activity and an indirect effect via reduced nutrient supply (ENGELS and MARSCHNER 1990) and water uptake (BASSIRIRAD *et al.* 1991) by the roots. According to ENGELS (1994b), inhibition of root growth is the most limiting factor for the early acquisition of nutrients at low temperature. In a nutshell, almost every cellular process is altered during cold acclimation (BROWSE and XIN 2001). Thus, a chilling sensitive maize variety is affected by reduced photosynthesis and decreased root growth while a chilling tolerant variety can maintain growth during low temperature periods (RICHNER *et al.* 1996).

PLANTS RESPONSE TO HEAT STRESS

Temperate maize is usually not affected by high temperature during the seedling stage. But sown as a second main season crop, high soil temperature can harm the isolated young maize seedlings, a situation that has become real as winter cereals are harvested earlier and very early maturing hybrids are on the market. Since high soil temperature is considered to be more harmful than high air temperature (XU and HUANG 2001), maize seedlings are vulnerable to a heated soil surface before canopy closure. Heat stress can have direct damaging effects on the plant associated with hot tissue temperature or indirect effects associated with increased evaporative demands (HOWARTH 2005) resulting in plant-water-deficits due to high transpiration rates. Heat stress has been shown to lead to oxidative stress (KOCHHAR and KOCHHAR 2005) and damaged thylakoid membranes of the chloroplast and membrane properties (AL-KHATIB and PAULSEN 1999), which are components of the photosystem II. Such a situation leads to a decreased photosynthetic activity, reducing growth.

ROOT GROWTH AND ROOT MORPHOLOGY

The acquisition of water and nutrients from the soil and plant anchorage are the two major functions of plant roots (HOCHHOLDINGER *et al.* 2004a; TUBEROSA *et al.* 2002). The root system of maize consists of three root types with different origin. First an embryonic primary root is formed that becomes visible two or three days after germination (FELDMAN 1994; HOCHHOLDINGER *et al.* 2004b). The primary root has a very simple and defined anatomical structure with only little variability, thus representing a very stable morphological system (HOCHHOLDINGER *et al.* 2004a). It has a defined longitudinal sequence of developmental zones (ISHIKAWA and EVANS 1995) including the meristematic zone followed by the elongation and the differentiation zone (HOECKER *et al.* 2006). The primary root is followed by a variable number of seminal roots emerging from the scutellar node. Both root types are embryo-borne. Postembryonic shoot-borne roots are initiated from underground as well as aboveground nodes of the stem and are called crown and brace roots, respectively. These shoot-borne nodal roots represent the major part of the root system of a mature plant (FELDMAN 1994). Lateral root initiation starts approximately four days after germination (HOECKER *et al.* 2006). They emerge from all axile growing roots and furthermore from already existing first order lateral roots, forming a second order of lateral roots. Lateral roots are important for the root system architecture (LYNCH 1995) and they play a major role in water and nutrient uptake (e.g. MCCULLY and CANNY 1988). Plant species differ in root development in both the overall root system architecture and the anatomy of individual roots. An appropriate rootstock is an important factor of plant survival in response to environmental conditions such as unfavorable temperatures (STAMP *et al.* 1997) or drought (SHARP and DAVIES 1979). Knowledge about root characteristics such as root proliferation rate and rooting depth (SMIT and GROENWOLD 2005) is crucial if the efficiency of modern cropping systems in varying environments shall be optimized (DWYER *et al.* 1987).

DIFFERENCES OF FLINT AND DENT

Root morphology was found to be dependent on the heterotic group. Studies in the early 20th century (WIGGANS 1916) revealed that flint varieties often produced zero or one seminal root while dent varieties often produced between three or four seminal roots. Such a difference is

still described nowadays by HOECKER *et al.* (2006). Furthermore, this study revealed differences in lateral root density between the heterotic groups.

SOWINSKI *et al.* (1998) observed differences in rooting depth at cold temperature as flint varieties explored the upper soil layers, which was positively correlated with early vigor, while dent lines had a less dense upper root system but a deeper rooting profile. Similar differences in root morphology were also observed for a tropical dent (Penjalinan) compared to a temperate flint (Z7) in a field study at early spring sowing (RICHNER *et al.* 1996). Chilling-sensitive Penjalinan decreased its root length but had a greater proportion of its roots in deeper soil layers. Chilling-tolerant Z7 maintained its root length and had a greater proportion of roots in superficial soil layers (STAMP *et al.* 1997). The flint gene pool has a long history of adaptation to chilling conditions and is used as a source of cold tolerance (HALLAUER 1990). By contrast, plants from the dent pool are known to be better adapted to warmer climates and are associated with a high yield potential at optimal conditions. No comparable studies have been done for seedling root growth under heat stress.

ROOT RESEARCH SYSTEMS

Roots have mainly been studied in the field. Field investigations of root traits have major disadvantages like tedious work reducing sample size and loss of root material due to the excavation process. Various alternative sampling techniques and root imaging methods have been reported. Recent techniques provide improvements in labor, time and accuracy. Hydroponics (SANGUINETI *et al.* 1998) and sand columns (RUTA *et al.* 2010) for root growth in controlled environments offer alternative approaches of root traits investigations. Simplifying the image acquisition can be done using a camera (WALTER *et al.* 2002), camera in minirhizotrons (LIEDGENS and RICHNER 2001), photocopier (COLLINS *et al.* 1987), flatbed-scanner (DONG *et al.* 2003; HUND *et al.* 2009; MANSCHADI *et al.* 2008), or X-ray techniques (GREGORY *et al.* 2003). Limitations of recent techniques are still the low sample size or tedious and destructive root sampling. Furthermore, images taken from soil grown roots contain unavoidable noise that can never be eliminated (DONG *et al.* 2003), complicating the separation of root and background. A newly developed root phenotyping platform (HUND *et al.* 2009) aimed for digital measurement of early seedling root growth followed by an automated image analysis. It provides an eased handling, high throughput opportunity with a

non-destructive root observation. The latter overcomes the disadvantage of the strategy of 'minimizing the loss of roots' (MONK 1966) by growing roots on germination paper. Image series taken from one growing root over a certain time period is particularly attractive to quantify root growth with a temporal resolution.

ASSOCIATION MAPPING APPROACH

Breeding research has revealed that the expression of most traits of ecological and agricultural importance such as yield, quality and some forms of disease resistance (COLLARD *et al.* 2005) are based on the action of quantitative trait loci (QTL), i.e. influenced by multiple genes and the environment (*cf.* MALOOF 2003; 2006). The identification of QTLs for relevant traits and the availability of molecular markers linked to QTLs controlling variation for those traits would allow for the implementation of marker-assisted selection to improve plant productivity (*cf.* RIBAUT and HOISINGTON 1998). Selection for root traits could lead to important benefits for improving and stabilizing yield under special conditions (FRACHEBOUD *et al.* 2004; TUBEROSA *et al.* 2002), because information available on the genetic control of root traits under varying temperature conditions is limited. Corresponding QTLs for root performance are highly valuable as no breeder has routine access to roots. Up to now little research has been done for QTLs controlling root morphology under mild-chilling stress.

Traditionally linkage mapping approaches have been used to study QTLs in plants. Alternatively, QTLs can be mapped using the linkage disequilibrium (LD) in populations. Linkage refers to the correlated inheritance of loci through the physical connection on a chromosome, whereas LD refers to the correlation between alleles in a population. This method uses the non-random association of alleles at different loci within the material and utilizes DNA polymorphisms associated with phenotypic traits. It is a promising approach to overcome the limitations of conventional linkage mapping (KRAAKMAN *et al.* 2004) providing a higher mapping resolution (FLINT-GARCIA *et al.* 2003) and a higher number of alleles that can be captured simultaneously. Although association studies have been studied extensively in animal systems, research on plants has mostly only been done in *Arabidopsis thaliana* and maize. Successful association mapping depends on the possibility of detecting LD between marker alleles and alleles affecting the expression of phenotypic traits and it determines the resolution of an association study (FLINT-GARCIA *et al.* 2003). This is only feasible if LD is

present in the breeding material to be studied (STICH *et al.* 2005). Association analysis has the potential to identify a single polymorphism within a gene that is responsible for the difference in the phenotype (FLINT-GARCIA *et al.* 2003), which is a useful tool for fine mapping of candidate genes. Alternatively, it may also be used to perform genome-wide scans in case LD is large enough to enable an appropriate saturation of the genetic map with molecular markers.

PLANT MATERIAL

A set of 74 European maize inbred lines derived from a breeding program of the University of Hohenheim, Stuttgart, Germany was used for the experiments described in Chapters 2 and 3. The inbreds comprised 32 flints with European flint and Flint/Lancaster background and 42 dents with Iodent and Iowa/Stiff Stalk background (SCHRAG *et al.* 2006). Analyses of linkage disequilibrium (LD) indicate that the dent lines exhibit a higher LD (21.7%/14.9%) than the flints (11.1%/4.8%) for intrachromosomal and interchromosomal LD, respectively (SCHRAG, T., personal communications).

A set of selected elite inbred lines was used for the experiment described in Chapter 4. The set comprised the two flints (UH002 and UH005) and two dents (UH250 and UH301) maize inbred lines. Their genetic background is as follows: European flint (UH002 and UH005), Iodent (UH301) and Iowa Stiff Stalk synthetic (UH250). The lines have been developed in order to improve combining ability for earliness, yield of grain and stover as well as for stalk quality and root lodging resistance. They were selected for GCA (general combining ability) with European flint and with dents of B14/Stiff-stalk and Iodent origin, respectively. Genetic distances between the different hybrids were determined with 53 SSR markers at the University of Hohenheim. Distance measure was calculated with modified Roger's distance: UH002-UH005: 0.643; UH002-UH301: 0.791; UH002-UH250: 0.819; UH005-UH301: 0.772; UH005-UH250: 0.795; UH301-UH250: 0.714 (HOECKER *et al.* 2006).

TREATMENT SELECTION

A small set of selected genotypes was used to evaluate the limits and optimum of root growth in the new developed phenotyping platform (HUND *et al.* 2009). Seedlings were tested in

growth containers, which allowed for a precise control of root-zone temperature. Seedlings were tested at a temperature range from 12°C to 40°C with 4°C increments. As roots stopped growing at the extremes of 12°C and 40°C, limits were set accordingly at 16°C and 36°C. Therefore, plants were tested at chilling stress of 16°C, close-to-optimal conditions of 28°C and mild heat stress of 36°C.

STRUCTURE AND OBJECTIVES

Aim 1: providing a morpho-physiological and genetic characterization of the material under study by means of shoot and root parameters, unraveling the genetic basis of chilling or heat tolerance by tracing the effect of an allele throughout the whole temperature range.
Specific objectives:

1. evaluate temperature dependent early seedlings growth by means of optimal and extreme growth conditions
2. determine if the European breeding pools dent and flint differ for key traits regarding temperature sensitivity
3. map key loci controlling plant performance dependent on their environment and genetic basis

(***Chapter 2*** shoot parameters; ***Chapter 3*** root parameters)

Aim 2: examination of a physiological and morphological temperature dependent heterosis by means of seedling shoot parameters in hybrid combinations of flint and dent inbred lines (***Chapter 4***).
Specific objectives:

1. test the hypothesis whether temperature-dependent general and specific combining ability can serve as a basic assumption to establish a wider temperature range in the hybrids
2. test the hypothesis whether mid-parent and better-parent heterosis would serve as a predictor of hybrid performance from inbred performance.

Aim 3: determination of further improvements in separating lateral form axile roots. The aim was to evaluate an appropriate, more precise algorithm for separating axile and lateral roots based on diameter classes for future applications (***Chapter 5***).

Chapter 2

Association mapping of temperate maize (*Zea mays* L.) for seedlings response to temperature extremes

* A publication based on this chapter has been submitted.

ABSTRACT

The shoot growth of maize (*Zea mays* L.) is hampered by chilling and heat. An association mapping approach on a germplasm set of European flint and dent inbred lines was carried out. Photosynthesis-related traits and seedling growth were assessed under three temperature regimes. The flint lines were less diverse than the dent lines at loci for temperature tolerance and developed greener, smaller leaves and higher rates of photosynthesis under chilling stress. The proportion of genotypic variance explained by the detected associations ranged from 34.4 to 67.4%. The observed pattern of allele response suggests that the alleles responsible for shoot growth confer tolerance to only one temperature extreme. A combination of inbred lines carrying alleles, which are superior under extremes of temperature should lead to a complementary effect in the hybrid and would lead to adaptation to a wider range of temperature. Genes adjacent to those alleles are appropriate candidates for testing this approach.

INTRODUCTION

As a result of advanced breeding strategies, thermophilic maize (*Zea mays* L.) is increasingly cultivated in more temperate regions. In cool temperate climates, maize is sown as early as possible to ensure a high and consistent yield. Fast emerging varieties with early development under cool conditions are valuable in regions where cool spring temperatures hamper early development of the seedling. Therefore, chilling tolerance is an important feature of well adapted maize cultivars. With the predicted changes in global weather, earliness may become even more important to avoid heat and drought during flowering (*cf.* BARNABAS *et al.* 2008) in an increasing number of target environments.

High temperature during the seedling stage rarely affects temperate maize. However, high temperature may hinder plant productivity; as shown for rice grain yields declined by 10% with each 1°C increase in minimum temperature during the growing season (PENG *et al.* 2004). Furthermore, early maize hybrids are already considered to be potential second main season crops, i.e., in southern regions of central Europe where winter barley (*Hordeum vulgare* L.) is early harvested. Then, young, isolated maize seedlings surrounded by bare soil, can be exposed to very high temperature. Since heat and chilling stress can affect plant growth in one life cycle, adaptation of the genotype to these conditions is required.

Chilling affects the assimilation rate and phloem transport (SOWINSKI *et al.* 1999) due to downstream effects of disturbed photosynthesis. Physiological changes help to prevent injury to the plant due to temperature stress. Such adaptive changes include the capacity to activate the antioxidant system and changes in lipid composition (ALLEN and ORT 2001). It is essential to determine whether the response to stress is specific or unspecific. Although plants may respond similarly to different types of stress, their responses are often specific, such as that of stress-related protein production (TIMPERIO *et al.* 2008 and references therein). The development of heat shock proteins (*Hsp*) and glutathione S-transferase (*Gst*) are considered to be unspecific, because both responses occur under heat and chilling stress. In contrast, an unsaturation of membrane lipids is reported to enhance the stability of the photosynthetic machinery under low temperature (MOON *et al.* 1995) but not under high temperature (WADA *et al.* 1994). Furthermore, DEAD box RNA helicase (*Drh*) encodes an enzyme involved in RNA metabolism which plays a key role in mRNA export under abiotic stress (*cf.* CHINNUSAMY *et al.* 2007)

Temperate hybrids, grown in northern and central Europe, are usually crosses between inbred lines of the flint and dent heterotic groups (SHAW 1988). Early breeding programs, beginning in the 1950s, grew inbred lines derived from European flint landraces and combined them with lines of Corn Belt dent. The flint lines contributed chilling tolerance, while the dent lines contributed high yield potential (HALLAUER 1990). Both groups were genetically separated at the start of the breeding programs in Europe and are still separated today (ANDERSEN *et al.* 2005; REIF *et al.* 2005). However, the allelic constitution has changed over time (REIF *et al.* 2005), indicating that the breeding had fixed different alleles in each heterotic group. Therefore, the effect of population structure and environment are essential (ANDERSEN *et al.* 2005) to confirm the relationship of an allele to one heterotic group and to a certain environment.

The genetic basis of tolerance of photosynthesis in maize to cold has been investigated by means of QTL studies based on biparental crosses (FRACHEBOUD *et al.* 2002; HUND *et al.* 2004; JOMPUK *et al.* 2005). These studies clearly confirmed that photosynthesis-related traits are quantitatively inherited and that many loci are involved. Traditional QTL mapping, e.g., of biparental crosses, is often limited in mapping resolution and the number of sampled alleles. To overcome these shortcomings, QTLs can be mapped by association analyses based on linkage disequilibrium (LD). Applicable in unrelated germplasms (KRAAKMAN *et al.* 2004), this method offers the advantage that a high number of alleles can be captured simultaneously at a high resolution (FLINT-GARCIA *et al.* 2003). A disadvantage is the risk of spurious associations (false positives) due to an unknown population structure. So far, little effort has been made to trace the effect of an allele throughout the whole range of temperatures, to which maize seedlings may be exposed, depending on the conditions of cultivation and climate. Therefore, the goal was a genome-wide association mapping of the response of seedlings to temperature in a temperate population of maize. Specific questions were: i) Do seedlings show a differential response to low, optimal and high temperature? ii) Are key loci that control the temperature response more frequent in one of the gene pools?

MATERIAL AND METHODS

A set of 74 European maize inbreds was studied, comprising flint (32) and dent (42) lines from the breeding program of the University of Hohenheim. Their genetic background is described in ANDERSEN *et al.* (2005) and SCHRAG *et al.* (2006).

Plant growth:

Plants were tested under chilling stress of 16°C and mild heat stress of 36°C, temperature extremes, and at 28°C, i.e. close-to-optimal conditions. These temperature regimes were selected according to preliminary studies of a wider range of favorable and unfavorable conditions (data not shown).

Seeds were imbibed over night at room temperature, surface-sterilized with 2.5% sodiumhypoclorite (NaOCl (aq)) for 10 min, rinsed thoroughly with distilled water, and germinated on filter papers (∅ 70 mm, Macherey-Nagel AG, Oensingen, Switzerland) in an incubator at 27°C. Seedlings with a similar radicle length were transferred to growth pouches (HUND *et al.* 2009) and cultivated until the respective V2 stage (Figure 2.1), indicated by a fully visible collar on the second leaf (further details see Chapter 3). To establish the seedlings, they were first grown under optimal conditions (28°C) for two days. The photoperiod throughout the whole experiment was 12 h at PPFD 350 µmol m^{-2} s^{-1} and the relative humidity 60%. The temperature treatments were commenced two days after transplanting when the lateral roots had appeared.

Figure 2.1 Growth containers with plants in growth pouches at the V2 stage.

Physiological measurements:

Leaf greenness (SPAD) was measured with a SPAD meter (SPAD 502, Minolta Corporation, Ramsey, NJ, USA). For each replicate four measurements of one leaf were averaged. The operating quantum efficiency of the photosystem II (Φ_{PSII}, GENTY *et al.* 1989) was measured with a PAM-2000 fluorometer (Walz, Effeltrich, Germany) equipped with a leaf clip holder 20030-B. Leaves were cut at the coleoptilar node and the leaf area was measured with a portable area meter (LI-3000A, LICOR, Inc., Lincoln, NE, USA). The shoot material was dried at 60°C to constant weight and the dry matter determined. Specific leaf area (SLA) was calculated as the leaf area divided by the leaf dry weight.

Experimental design and statistics:

The experimental design in each temperature environment (t_j) was an alpha lattice (BARRETO *et al.* 1997) with eight biological replications, i.e., four independent replications per environment (r_{jk}) and two blocks (b_{jkl}) per growth chamber, each containing a full set of inbred lines ($\breve{g}_i$). The 74 inbred lines in each block were assigned to eight incomplete blocks (c_{iklm}). They were distributed in four sections of two growth containers. The final model to obtain the best linear unbiased estimates (BLUEs) of genotypes was:

$$Y_{ijklm} = \mu + \breve{g}_i + t_j + \breve{g}t_{ij} \mid \breve{g}tr_{ijk} + r_{jk} + b_{jkl} + c_{jklm} + e_{ijklm}, \quad (1)$$

where Y_{ijklm} is the effect of the *i*th inbred line in the *j*th temperature treatment, the *k*th growth chamber run, the *l*th block and the *m*th growth container; e_{ijklm} is the residual error and μ the intercept. The terms to the left and right of the vertical bar (|) are considered to be fixed and random, respectively. Analysis of variance was made by the asreml-R package (ASReml release 2.0, GILMOUR *et al.* 2006) and the best linear unbiased estimates (BLUEs), extracted for each genotype-by-treatment combination, and were used as the input values for the association mapping.

Analysis of variance of the heterotic groups, flint and dent, and for the heterotic group-by-environment interaction was:

$$Y_{ijklmn} = \mu + t_j + h_n + th_{jn} \mid \breve{g}_i + \breve{g}t_{ij} + \breve{g}tr_{ijk} + r_{jk} + b_{jkl} + c_{jklm} + e_{ijklmn}, \quad (2)$$

where Y_{ijklmn} is the effect of the *i*th inbred line in the *n*th heterotic group, in the *j*th environment, the *k*th growth chamber run, and the *l*th block and *m*th container; *h* is the *n*th heterotic group (flint or dent) and all other parameters are the same as in model 1. If not stated, then the effects of the temperatures extremes on the trait are always given compared to the close-to-optimum temperature.

Heritability on an entry means (HOLLAND *et al.* 2003) for each treatment was calculated as:

$$h^2 = \frac{\sigma^2_{\breve{g}}}{\sigma^2_{\breve{g}} + \frac{1}{j}\sigma^2_{\breve{g}t} + \frac{1}{jk}\sigma^2_{\breve{g}tr} + \frac{1}{jkl}\sigma^2_{r}}, \qquad (3)$$

where $\sigma^2_{\breve{g}}$ is the genetic variance, $\sigma^2_{\breve{g}t}$ the variance of the genotype-by-temperature interaction, $\sigma^2_{\breve{g}tr}$ the variance of the genotype-by-temperature-by-run interaction, and σ^2_{r} the residual error variance. *j*, *k*, and *l* denote the number of treatments (3), runs (4), and blocks (2), respectively; $\sigma^2_{\breve{g}}$ is the genetic variance after correcting for effects of the heterotic group.

Association mapping approach:

Genome-wide association mapping was performed with 74 maize inbred lines, genotyped with 1415 AFLPs, of which 748 were mapped to one of the ten chromosomes on the Keygene integrated map. The remaining markers are mapped to pseudo chromosomes. First, we analyzed the population structure of the lines. Then, the main marker effects and marker-by-temperature interaction effects were determined for the growth traits of the seedlings. To detect markers linked to genome regions associated with a specific stress response, markers showing significant interactions with the environment were classified according to their allele substitution effects. Finally, we attempted to shed light on the distribution of alleles, which increase tolerance in the heterotic groups.

Analysis of population structure

This analysis was based on 163 SSRs (SCHRAG *et al.*, 2010) using the R Statistics Software (R DEVELOPMENT CORE TEAM 2008). The Rogers' distance (RD) was calculated according to ROGERS (1972). Associations among the 74 inbred lines were revealed by a principal coordinate analysis (GOWER 1966) based on RD estimates between pairs of inbreds. Analysis

of the first principal coordinate (PC1) revealed a clear separation of the heterotic groups, flint and dent, confirming that they are two distinct groups.

The combined analysis of adjusted entry means (BLUEs) across environments obtained from model (1) did not enable us to infer entry-by-environment interactions (*cf.* PIEPHO 2000). Nevertheless, the results of STICH *et al.* (2008a) indicate that the power for detection of marker-phenotype associations with a two-step approach based on adjusted entry means for each environment is only slightly lower than with a one-step approach. Therefore, the analyses were based on the adjusted entry means calculated for each environment. The PK_{opt} method, described by STICH *et al.* (2008b), was used to detect the AFLP phenotype associations:

$$M_{ijp} = \mu + \sum_{u=1}^{z} P_{iu} v_u + l_j + a_p + (al)_{jp} + \breve{g}_i + e_{ijp}, \qquad (4)$$

where M_{ijp} is the adjusted entry mean of the *i*th maize inbred at the *j*th environment carrying the *p*th allele, μ an intercept, v_u the effect of the *u*th column of the population structure matrix **P**, l_j the effect of the *j*th environment, a_p the effect of allele *p*, $(al)_{jp}$ the effect of the interaction of the *p*th allele with the *j*th environment, and $\breve{g}_i$ the genetic effect of the *i*th entry, with the exception of a_p, and e_{ijp} the residuals.

According to ZHAO *et al.* (2007), the first two principal components (*z*=2) of the SSR allele frequency matrix, which explained 28.8% of the variance, were used as the **P** matrix.

The variance of the random effects $\breve{g} = \{\breve{g}_1,...,\breve{g}_{74}\}$ and $e = \{e_{1,\,1,\,1},...,\, e_{74,\,3,\,2}\}$ was assumed to be $\mathrm{Var}(\breve{g}) = 2\mathbf{K_{opt}}\sigma^2_{\breve{g}}$ and $\mathrm{Var}(e) = \mathbf{R}\sigma^2_r$, where $\mathbf{K_{opt}}$ was a 74×74 matrix of kinship coefficients that define the degree of genetic covariance between all pairs of entries and **R** 222 × 222 the identity matrix. Genetic variance, $\sigma^2_{\breve{g}}$ and residual variance, σ^2_r were both estimated by REML. For each examined trait, $\mathbf{K_{opt}}$ was calculated according to STICH *et al.* (2008b) using the SSR markers.

To solve the multiple test problem, the Bonferroni-Holm procedure (HOLM 1979) was applied to detect AFLPs with significant ($P < 0.05$) (1) main effects across environments and (2) AFLP × environment interactions. The proportion of genotypic variance, explained by one marker, was calculated from the reduction of the genetic variance in a model with marker effects compared to the genetic variance in a model without marker effects. The total proportion of genotypic variance explained by all AFLPs with significant main effects was

obtained by fitting a model, which included all markers. All mixed-model calculations were performed with ASReml release 2.0 (GILMOUR *et al.* 2006).

Test for group specificity:

Since the flint and dent heterotic groups were clearly separated, the population structure matrix P was used to avoid detection of spurious associations. It is, therefore, unlikely that traits controlled by alleles associated with the heterotic group were detected. However, it was determined, whether the detected associations were partly associated with the heterotic group. Thus, the frequency of alleles in the flint group was assessed for trait-associated markers. The frequency was expressed as the ratio of the number of flints carrying the allele to the total number of genotypes carrying the allele. The frequency was 0 when the allele was absent in the flint group, and was 1 when the allele was detected in the flints but not in the dents. A χ^2 two sample test was conducted to determine whether the heterotic groups differed in the frequency of alleles, i.e. whether the alleles were group-specific. The average effect of the flints (Effect flint, Tables 2.2 and 2.3) on the traits of a virtual flint-by-dent hybrid was qualified based on the allele substitution effect and the frequency of alleles in the flint pool. In the case of the loci with association-by-temperature interactions, the "effect flint" revealed the relative change in the allele effect at temperature extremes compared to the control. For example, a positive "effect flint" was recorded when α½ changed positively from the optimum towards the extreme and the trait-increasing allele was more frequent in the flints (Table 2.2).

The detected associations were projected on the IBM2 2008 Neighbors Frame genetic map (SCHAEFFER *et al.* 2008) obtained from the Maize Genetics and Genomics Database (MaizeGDB, LAWRENCE *et al.* 2005). This was performed by the software BioMercator (ARCADE *et al.* 2004) using 135 common SSR markers. A collocation of associations of different traits was considered to be positive when the additive effects had the same algebraic sign (+ or −) and negative when the signs were opposite. Genes involved in temperature tolerance in the ± 20 cM region around the detected associations were selected from the IBM2 2008 Neighbors Frame map (MaizeGDB: http://www.maizegdb.org/) to pinpoint the most interesting associations.

Classification of allele responses:

The allele substitution effect (α1/2) is given as the additive effect of replacing allele 1 by allele 2. To obtain the relative allele substitution effects, we set the absolute α1/2 relative to the adjusted means (BLUEs). Figure 2.2 shows the allele responses to temperature. Allele-by-temperature treatment interaction effects are shown for close-to-optimal (here 28°C) and extreme (here 16°C and 36°C) temperature. Allele 2 (A2) shows two possible reactions of one allele in relation to the reference allele 1 (A1). The allele confers tolerance to only one of the temperature extremes (a), both temperature extremes (b), or indifferent (c). Classes are subdivided into those with interactions (a_x, b_x) and those without interactions ($a_{hea,}$ $a_{cold,}$ $b_{opt,}$ b_{ex}). Class (a) displays the response of an allele to either chilling or heat stress while (b) illustrates a similar response to the temperature extremes. Furthermore, the subscript "x" denotes "interaction". Classes without interactions illustrate a response to heat- (a_{heat}), chilling- (a_{cold}), optimal- (b_{opt}) and extreme conditions (b_{ex}). Subclasses of c show either a similar response to optimal and heat (c_{heat}) or to optimal and chilling (c_{cold}) temperature.

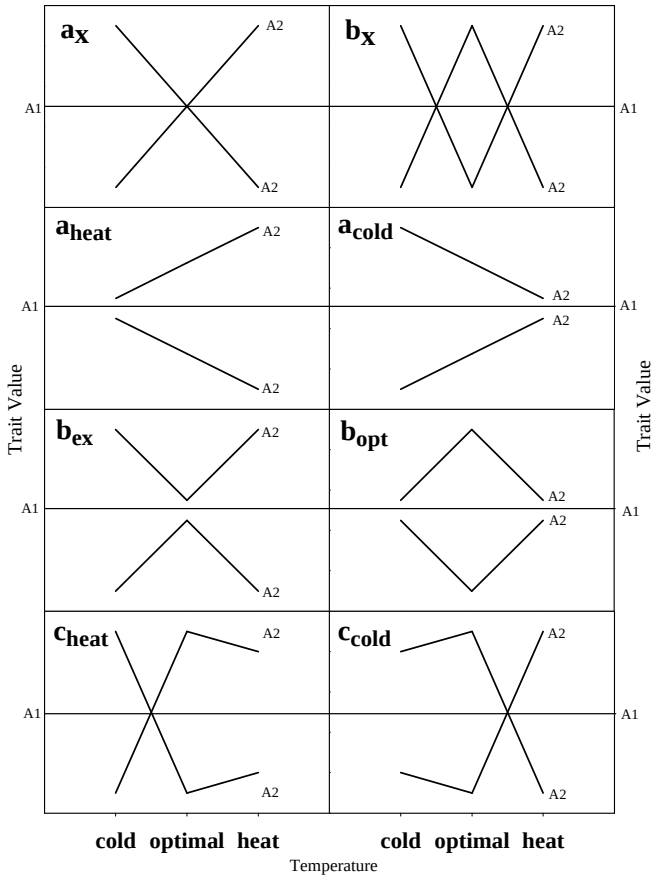

Figure 2.2 Classification of AFLP allele response based on the relative allele substitution effects (α1/2) in each temperature treatment. A2 shows two possible reactions of one allele in relation to the reference allele (A1 zero line). Alleles confer tolerance to temperature extreme (a), or to both temperature extremes (b), and indifferent (c). Classes are subdivided into crossover interactions (a_x, b_x) and no crossover interactions but responsive to heat (a_{heat}), chilling (a_{cold}), optimal (b_{opt}) and extreme conditions (b_{ex}). Subclasses of c show either a similar response to optimal heat (c_{heat}) or to optimal chilling (c_{cold}) conditions.

RESULTS

Seedling growth was strongly affected by chilling and moderately affected by heat:

The temperature treatments had significant effects on the growth of seedlings for all the evaluated traits (Table 2.1, Figure 2.3). Plants grown under chilling conditions developed paler leaves and showed a lower photosynthetic activity. Under chilling, leaf greenness (SPAD) decreased by 33% and the operating quantum efficiency of the photosystem II (Φ_{PSII}) decreased by 35.2% compared to the close-to-optimum temperature. In contrast, the SLA and root-to-shoot dry weight (DW_{RtSt}) increased by 25 and 19%, respectively, under chilling stress. The surface area ratio of roots to leaves decreased considerably under high and low temperature, whereas other traits were hardly affected by heat. Average heritability (h^2) was 0.74. Exceptions were Φ_{PSII} (0.29) and SLA (0.57) owing to low genotypic variance and the strong effect of treatment and run interactions (G×T×R) (Table 2.1). Heritability increased for the flints (0.79), while it decreased for the dents (0.64) when calculated separately for the heterotic groups. The decreased heritability of the dents was most apparent for SLA and was caused by a lower genotypic variance (data not shown). Compared to the flints, the dents had a higher G×T and G×T×R for SLA, indicating a strong response to environmental changes.

The flint heterotic group was genetically separated from the dents, had greener and smaller leaves and a higher rate of photosynthesis under chilling:

The first two principal components of the SSR allele frequency matrix separated the inbred lines into two major subgroups (Figure 2.4) coinciding with the flint and dent heterotic groups. This justifies a separate analysis of each group and a confirmation of their genetic separation due to breeding. For most traits, differences between the flints and dents were small across all three environments (Table 2.1). However, significant effects on the SPAD and shoot dry weight (DW_{St}) were found in each group. The flints maintained comparably greener leaves, while the dents accumulated more dry matter in all three environments (Table 2.1). The groups differed slightly with respect to Φ_{PSII} and leaf area. Temperature-by-heterotic group interactions were found for leaf dry weight (DW_{Leaf}) and the surface area ratio of roots and leaves. The dents outperformed the flints in the high temperature environment for both

traits. The dry weight of the leaves was also greater compared to optimal conditions. Heterotic group-by-temperature interactions were found for leaf area and Φ_{PSII} ($P < 0.1$), because the leaf area of the dents was greater under high temperature, while the flint maintained photosynthesis (Φ_{PSII}) better at low temperatures (Table 2.1).

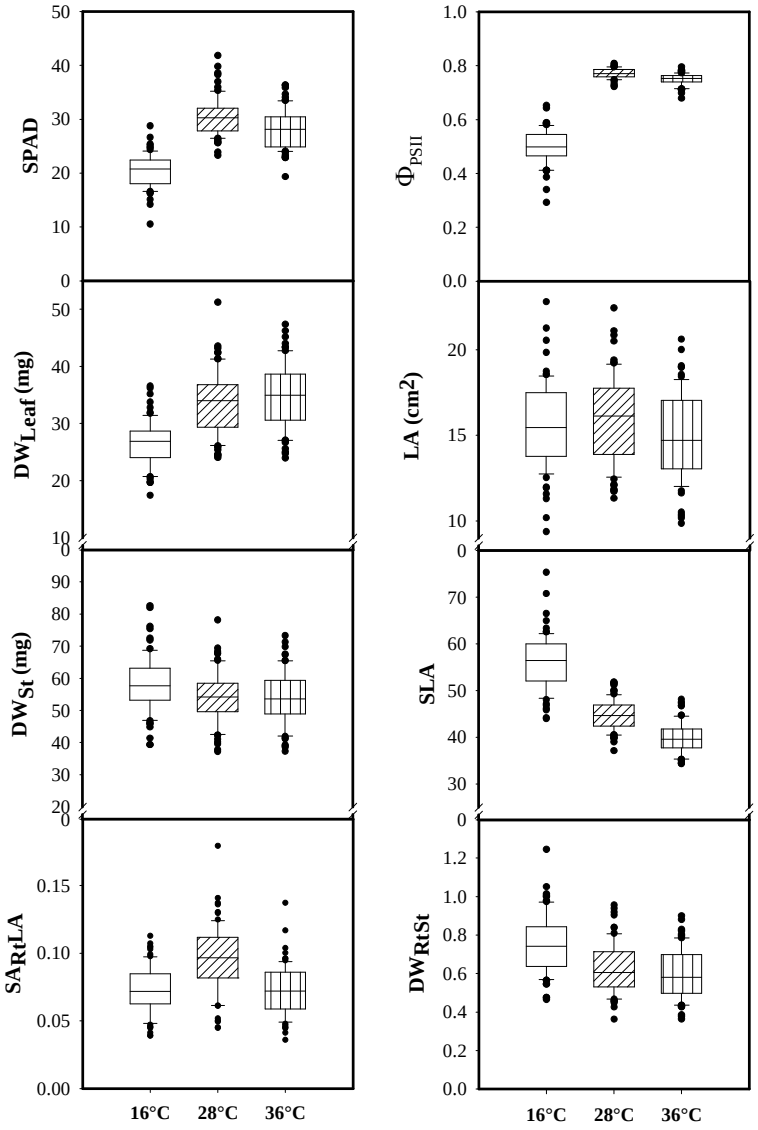

Figure 2.3 Box-Whisker-Plots for temperature effects on leaf greenness (SPAD), operating quantum efficiency of photosystem II (Φ_{PSII}), dry weight of leaves (DW_{Leaf}), total dry weight of shoots (DW_{St}), specific leaf area (SLA), ratio of surface area of roots and leaves (SA_{RtLA}), and ratio of dry weight of root and shoot (DW_{RtSt}).

Table 2.1 Adjusted means for the heterotic groups (flint and dent) within temperature treatments for leaf greenness (SPAD), operating quantum efficiency of photosystem II (Φ_{PSII}), leaf area (LA), dry weight of leaves (DW_{Leaf}), total dry weight of shoots (DW_{St}), ratio of surface area of roots and leaves ($SA_{Rt}LA$), ratio of dry weight of root and shoot (DW_{RtSt}), and specific leaf area (SLA). Proportion of total variance for genotype (G), genotype-by-treatment interaction (G×T), and genotype-by-treatment-by-run interaction (G×T×R) as well as heritability estimates (h^2). ANOVA results for the effect of treatment (T), and heterotic group (HetGr) and their interaction.

		SPAD	Φ_{PSII}	LA	DW_{Leaf}	DW_{St}	$SA_{Rt}LA$	DW_{RtSt}	SLA
				cm^2	mg	mg	cm^2/cm^2	mg/mg	m^2/kg
Heterotic Group									
16°C	flint	22.6	0.526	15.4	26.6	57.1	0.0728	0.779	54.7
	dent	18.6	0.478	15.6	25.7	59.1	0.0700	0.700	56.7
28°C	flint	32.9	0.773	15.2	31.4	51.4	0.0927	0.629	45.0
	dent	28.4	0.771	16.7	34.7	56.1	0.0924	0.604	44.1
36°C	flint	29.5	0.754	14.1	32.4	50.6	0.0645	0.621	40.5
	dent	26.8	0.747	15.5	36.4	56.8	0.0749	0.557	39.1
Variance components									
	G	0.605	0.042	0.376	0.330	0.473	0.576	0.828	0.168
	G×T	0.140	0.125	0.118	0.118	0.111	0.157	0.171	0.17
	G×T×R	0.259	0.220	0.138	0.100	0.091	0.051	0.0734	0.319
	h^2	0.85	0.29	0.8	0.79	0.85	0.85	0.89	0.57
ANOVA									
	T	***	***	**	***	***	***	***	***
	HetGr	***	.	.	NS	*	NS	NS	NS
	T×HetGr	NS	.	.	***	NS	*	NS	NS

., *, **, ***, NS indicate significance level of P <0.1, <0.05, <0.01, <0.001 and not significant, respectively.

Association studies:

The analysis yielded 16 marker-trait associations with main effects for seven traits (Table 2.2). Seven of the 16 associations were observed for AFLPs, which have not yet been mapped to one of the ten chromosomes on the Keygene integrated map (NA, Table 2.2). Twenty-three marker-by-temperature interactions for four traits were detected (Table 2.3). Nine of the 23 markers have not yet been mapped to one of the ten chromosomes on the Keygene integrated map (NA, Table 2.3). Not considering population structure, the association analysis yielded 115 associations with main effects and 24 association-by-temperature interactions (data not shown). The number of significant associations ranged from one for DW_{Leaf}, DW_{St} and SLA to five for SPAD. The genetic variance explained by all the markers ranged from 34.4% for DW_{Leaf} to 67.4% for SPAD. Single marker contributions ranged from 23.3 to 37.8%. Marker-by-temperature interactions ranged from one for SPAD to 11 for SLA (Table 2.3).

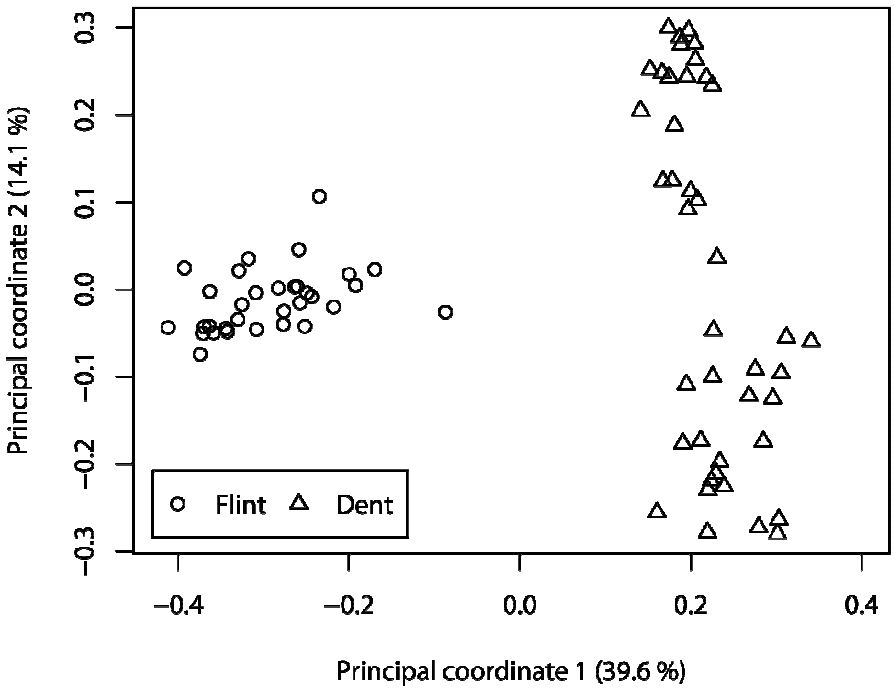

Figure 2.4 Principal coordinate analysis based on Rogers' distance estimates. Flint lines (open circle) dent lines (triangle).

Collocations of important traits describing shoot growth:

The detected associations were projected on the IBM2 2008 Neighbors Frame genetic map. Collocations of marker-trait associations were detected on chromosomes 2 and 5 (Figure 2.5). A positive collocation among DW_{Leaf}, leaf area, and DW_{St} was detected in bin 2.09 (Figure 2.5). This collocation coincides with the very high correlations (r ~ 0.85) among these traits. Furthermore, a positive/negative collocation was detected for an association for DW_{RtSt} and SLA in bin 5.05. This relationship cannot be supported by correlations. However, the correlation was the highest for plants grown at 36°C (r = 0.25). A large number of known and unknown genes are in a ± 20 cM region around the detected associations. Of those the most interesting genes with regard to temperature-tolerance mechanisms were selected from map IBM2 2008 Neighbors Frame (MaizeGDB: http://www.maizegdb.org/). In bin 1.02, the cytokinin response regulator (*Crr8*) was 2 cM from a marker-by-temperature interaction for Φ_{PSII}. Furthermore, the heat shock protein (*Hsp26*) was 17 cM away. In bin 3.05, glutathione S-transferases (*Gst7, Gst21, Gst28*) were ~ 4 cM from a marker-by-temperature interaction for Φ_{PSII}. The cytokinin response regulator (*Crr5*) was 9 cM from the interaction association. In bin 3.05, the DEAD box RNA helicase1 (*Drh1*) was ten cM from the marker-by-temperature interaction for SPAD. In bin 6.05, the glutathione S-transferase (*Gst41*) was 15 cM from an association for No_{Leaf}, and *Gst23* was 7 cM from a marker-by-temperature interaction for Φ_{PSII} in bin 7.02.

There are more alleles with main effects on traits in the dent pool:

The aim was to assess whether alleles are group-specific, i.e. whether the allele, which increases a trait or its tolerance to temperature is more frequent in one heterotic group. Group-specificity was found for ten of the 16 associations (Table 2.2, χ^2). In the flints, an allele was fixed in one case but was absent in four cases. The effect of flint on the trait increase was negative at a majority of eight loci where the flints differed significantly from the dents. Thus, the dents carried more alleles, which favor trait values. Based on the smaller leaf area of the flints (Table 2.1), the “effect flint” (Table 2.2) was negative for this trait at the two detected loci. In the case of SPAD, two of the three loci with significant group specificity showed a

negative effect. Based on the consistently higher values for SPAD of the flints (Table 2.1), more flint-specific alleles were expected for this trait.

The response of alleles to temperature extremes usually differed:

The marker-by-temperature interactions were classified according to the allele response to temperature (Figure 2.2). The allele substitution effect for each trait and treatment was of a similar magnitude for all the detected associations. However, the effects of alleles differed strongly with respect to temperature and trait. Marker-by-temperature interactions for Φ_{PSII} were mainly affected by chilling, marker-by-temperature interactions for DW_{RtSt} were mainly affected by heat, and those for SLA and SPAD were affected by both temperature extremes. Most of the responses were those with at least one crossover interaction (Table 2.4, a_x b_x, c_{heat} or c_{cold}); allele 2 had a positive effect at one temperature and a negative effect at the opposite one. This was especially apparent for Φ_{PSII} and SLA where the majority of cases classified a_x with divergent responses of the alleles to the two temperature extremes. Only the marker-by-temperature interactions for SPAD were clearly of the type b_x, because the underlying alleles showed a positive effect at the optimum temperature but a negative effect at both extremes or *vice versa*.

Flints exclusively carried alleles that increase chilling tolerance of Φ_{PSII}:

Group specificity was also observed for the marker-by-temperature interactions (Table 2.3, χ^2). The allocation of the alleles to one heterotic group compared to the other was significant for 65% of the associations. In the flint group an allele was fixed in only one case and one allele was absent in 12 cases. In summary, the flint pool was genetically less diverse at these loci compared to the dent pool. The alleles with significant group specificity were tested for the conferring of chilling or heat tolerance. This can be examined best for the two traits with the highest number of detected associations, i.e. Φ_{PSII} and SLA. In the case of Φ_{PSII}, an allele was absent in the flints four times and was fixed only once. The flints carried the allele conferring chilling tolerance more frequently, thus contributing to the relative increase in $\alpha 1/2$ between 28 and 16°C (Table 2.3, effect flint: cold). This supports the sizable difference between the heterotic groups at low temperature and the interaction between temperature and

the heterotic group (Table 2.1). In contrast, the alleles conferring heat tolerance of Φ_{PSII} were balanced between the heterotic groups (Table 2.3, effect flint: heat).

In the case of SLA, an allele was absent in the flints seven times. The flints most frequently carried alleles decreasing SLA under chilling but increasing SLA under high temperature and, thus, showed an a_x-type response (Table 2.4). Since the mean values of SLA decreased from low temperature to optimal conditions to high temperature (Figure 2.2) this response pattern of the alleles indicates that the flints carried the alleles, which kept SLA most stable throughout temperatures. However, this pattern of associations was not confirmed by the interaction between temperature and the heterotic group for SLA (Table 2.1).

Table 2.2 List of marker-trait associations with main effects. See Table 2.1 for abbreviations of traits. AFLP marker according to Keygene; marker position on the Keygene integrated map (unpublished) (Pos. KG) and the IBM2 2008 Neighbors Frame (Pos. IBM); proportion of genotypic variance explained by each marker (p_g (%)) including total variance as explained by all significant markers; allele substitution effect (α1/2) as the additive effect of replacing allele 1 with allele 2; χ^2 two sample test for allele distribution between flint/dent; ratio of number of flints carrying the allele vs. the total number of genotypes carrying the allele (Ratio Flint); algebraic sign of the effect of the more frequent allele in the flint group with respect to chilling or heat tolerance (Effect).

Associations with main effects							χ^2 two sample test Flint/Dent	Ratio Flint		Effect Flint on trait increase
Trait	Marker	Pos. KG (cM)	Pos. IBM (cM)	Bin	p_g (%)	a½		Allele 1	Allele 2	
No_{Leaf}	489	42.6	189	1.02	25.6	-1.70	NS	0.38	0.48	-
	486	181	1120	1.12	23.3	1.78	NS	0.5	0.38	-
	919	72.6	300	6.05	26.7	-1.91	NS	0.37	0.58	-
	593	NA	NA	NA	25.6	1.84	NS	0.31	0.51	+
			total		48.3					
DW_{Leaf}	834	151	676	2.09	34.4	-0.21	***	0.12	0.68	-
LA	834	151	676	2.09	33.2	-9.50	***	0.12	0.68	-
	1611	NA	NA	NA	32.8	-13.6	***	0	0.84	-
			total		42.3					
DW_{St}	834	151	676	2.09	34.9	-8.40	***	0.12	0.68	-
SPAD	769	58.6	277	3.04	33.2	-5.64	NS	0.45	0.42	+
	57	61.3	301	3.05	31.6	-6.22	**	0.28	0.67	-
	92	NA	NA	NA	30.7	6.02	*	0.82	0.38	-
	888	NA	NA	NA	29.8	-5.81	NS	0.43	0.42	+
	1722	NA	NA	NA	37.8	8.48	*	0	0.47	+
			total		67.4					
DW_{RtSt}	767	93.9	409	5.05	35.2	-19.8	*	0	0.51	-
	1356	NA	NA	NA	31.5	22.3	***	0.65	0	-
			total		53.1					
SLA	604	NA	NA	NA	41.2	-0.16	*	1	0.4	+

*, **, ***, NS indicate significance level of P <0.05, <0.01, <0.001 and not significant, respectively, based on a χ2 two sample test for allele distribution between the heterotic groups.

[NA]: Marker is not yet mapped to one of the ten chromosomes on the Keygene integrated map.

Table 2.3 List of marker-by-temperature interactions. See Table 2.1 for abbreviations of traits. AFLP marker according to Keygene; marker position on the Keygene integrated map (unpublished) (Pos. KG) and the IBM2 2008 Neighbors Frame (Pos. IBM); allele substitution effect (α1/2) as the additive effect of replacing allele 1 with allele 2; χ^2 two sample test for allele distribution between flint/dent; allele response class; ratio of number of flints carrying the allele vs. the total number of genotypes carrying the allele (Ratio Flint); algebraic sign of the effect of the more frequent allele in the flint group with respect to chilling or heat tolerance (Effect).

Associations with temperature treatment interaction effects					α½			allele response class	χ^2 two sample test Flint/Dent	Ratio Flint		Effect Flint	
Trait	Marker	Pos. KG (cM)	Pos. IBM (cM)	Bin	16°C	28°C	36°C			Allele 1	Allele 2	cold	heat
SPAD	479	73.4	362	3.05	-2.33	1.85	-1.84	b_x	*	0.32	0.7	-	-
Φ_{PSII}	85	43.7	194	1.02	15.3	-1.11	-2.59	a_x	NS	0.33	0.45	+	-
	1743	86	502	1.06	4.65	-1.55	0.05	b_x	NS	0.33	0.45	+	+
	611	74.3	294	2.04	17.7	-0.70	1.38	b_x	NS	0.37	0.75	+	+
	1128	67.4	335	3.05	22.5	-0.02	-2.35	a_x	NS	0.2	0.44	+	-
	966	54.1	200	5.02	14.0	0.64	1.25	b_{ex}	**	0	0.52	+	+
	943	60.7	288	7.02	14.8	-1.18	-2.15	a_x	*	0	0.48	+	-
	1289	NA	NA	NA	-13.7	1.51	0.72	c_{heat}	*	0.49	0	+	+
	1384	NA	NA	NA	15.1	-1.29	-2.29	a_x	NS	0	0.44	+	-
	1661	NA	NA	NA	-19.8	3.20	3.97	a_x	NS	1	0.4	+	-
DW_{RtSt}	151	83.8	370	8.05	2.87	-3.87	8.71	b_x	***	0	0.6	+	+
	1584	NA	NA	NA	-0.46	-5.03	15.30	c_{cold}	*	0.08	0.52	+	+
SLA	971	56.1	269	1.03	0.091	0.038	0.011	a_{cold}	NS	0	0.48	+	-
	629	67.2	265	5.03	0.136	-0.041	-0.020	c_{heat}	***	0.55	0	-	-
	767	93.9	409	5.05	0.126	0.029	-0.052	a_x	*	0	0.51	+	-
	43	54.1	232	7.02	-0.120	0.018	0.049	a_x	NS	0.15	0.5	-	+
	332	79.1	363	7.03	-0.076	0.101	0.087	c_{heat}	***	0	0.55	-	-
	157	64.1	311	10.04	-0.036	0.046	-0.018	b_x	**	0.69	0.3	+	+
	75	NA	NA	NA	-0.133	0.032	0.033	a_x	**	0.07	0.53	-	+
	133	NA	NA	NA	-0.043	0.044	0.055	a_x	*	0	0.48	-	+
	1350	NA	NA	NA	-0.017	0.000	0.041	a_x	***	0.05	0.58	-	+
	1597	NA	NA	NA	0.189	0.004	-0.006	a_x	*	0	0.53	+	-
	1611	NA	NA	NA	-0.134	-0.048	0.004	a_x	***	0	0.84	-	+

*, **, ***, NS indicate significance level of P <0.05, <0.01, <0.001 and not significant, respectively, based on a χ^2 two sample test for allele distribution between the heterotic groups.

NA: Marker is not yet mapped to one of the ten chromosomes on the Keygene integrated map.

Table 2.4 List of allele response classes for marker-by-temperature interactions. Leaf greenness (SPAD), operating quantum efficiency of the photosystem II (Φ_{PSII}), ratio of dry weight of root and shoot (DW_{RtSt}), and specific leaf area (SLA). Symbols refer to the list of classes in Figure 2.2.

Trait/Symbol	No. sig. marker with environment interaction effects	Percentages of allele response classes							
		a_x	b_x	a_{heat}	a_{cold}	b_{ex}	b_{opt}	c_{heat}	c_{cold}
									
SPAD	1	-	100	-	-	-	-	-	-
Φ_{PSII}	9	56	22	-	-	11	-	11	-
DW_{RtSt}	2	-	50	-	-	-	-	-	50
SLA	11	64	9	-	9	-	-	18	-

DISCUSSION

To obtain a phenotypic and genotypic description of the maize material, temperature-dependent early shoot growth was elucidated by means of photosynthesis-related traits and dry matter accumulation. The flint heterotic group was genetically separated from the dents, as it was also reported by ANDERSEN *et al.* (2005) and STICH *et al.* (2006). One study (CAMUS-KULANDAIVELU *et al.* 2006) reports the separation of the flint and the dent breeding pools, also within other populations. Reif *et al.* (2005) illustrates the clear isolation of the flint and dent parental lines used to breed hybrids during the past 50 years. The composition of alleles in both groups changed, while the genetic separation of the groups did not (REIF *et al.* 2005).

A greater variability in Φ_{PSII} at low temperature compared to optimum and high temperature was found. This is in line with other studies, which report that chilling tolerant and chilling sensitive plants usually show little variation in photosynthesis (Φ_{PSII}) under optimum temperatures and that chilling tolerant plants tend to maintain Φ_{PSII} better under chilling stress (FRACHEBOUD *et al.* 1999; HUND *et al.* 2005). The most striking constitutive difference among heterotic groups was the greener leaves of the flints, in line with the observations of FRACHEBOUD *et al.* (1999). This raises the question as to whether the differences between the two groups manifest partially in constitutive differences in the chlorophyll content per unit leaf area.

LEIPNER *et al.* (1999) emphasized the problem of introducing chilling tolerant material from tropical highlands into European breeding material due to the inherent low specific leaf area. A group-specific impact on Φ_{PSII} appeared only under chilling stress, because electron transport in the flints was slightly better than in the dents. This supports our hypothesis that the flint group can better maintain photosynthesis at low temperature, which is corroborated by the results for chilling tolerant flint lines (FRACHEBOUD *et al.* 1999). At high temperature, Φ_{PSII} was hardly affected and the plants did not seem to respond negatively in contrast to the results of SINSAWAT *et al.* (2004), who reported that the Φ_{PSII} decreased to below 0.4 when the plants were exposed to high temperature for 20 min. The strong effect observed by SINSAWAT *et al.* (2004) was probably due to the short exposure to very high temperature. The heat stress was probably not severe enough to affect photosynthesis. However, rates of root elongation of the same seedlings (Chapter 3) revealed that root elongation stopped when the temperature increased to above 36°C. Since the stress level was defined based on root growth, it is concluded that heat stress had occurred.

Constitutively higher SPAD values and a relatively high number of associations with main effects were detected for the flints, which indicate a constitutive behavior in all the environments. The opposite was found for specific leaf area. There was one association with main effects and 11 marker-by-temperature interaction effects. This suggests that SLA tend to be an adaptive trait, which is, unfortunately, not supported by the ANOVA results. Similar results were obtained for Φ_{PSII}. This trait revealed significant marker-by-temperature interaction effects only.

Despite the observed positive collocations, the expected collocations between leaf greenness and specific leaf area were not detected, as reported by HUND *et al.* (2005). SPAD and SLA, and SPAD and Φ_{PSII} were not collocated and not correlated. Therefore, these traits seemed to be controlled by different mechanisms, which would corroborate the findings of JOMPUK *et al.* (2005), who reported that photosynthetic traits and leaf greenness were only moderately related.

Φ_{PSII} and flints are a measure of high yield in flint x dent crosses:

The chilling-tolerant allele for Φ_{PSII} was consistently associated with the flint pool. Assuming additivity and that all the existing associations were detected, this increases the possibility that

flint × dent crosses derived from this population are very tolerant to chilling stress. The effect of the alleles for chilling tolerance at optimum and high temperature was weak; therefore, their mainly negative effects under these conditions may not have a strong effect on the plant's performance. Similar conclusions were drawn from other selection experiments, where genotypes selected for high and low Φ_{PSII} values under chilling did not show different photosynthetic performance under optimum temperature (FRACHEBOUD *et al.* 1999; HUND *et al.* 2005). This indicates that chilling tolerance of the photosynthetic apparatus can be increased without affecting photosynthesis under optimum conditions. However, during the life of the plants they are exposed to optimal conditions for a much longer period than to chilling stress. This raises the question as to whether weak effects, which are usually insignificant, may add up to a negative effect on yield, especially in years with a warm spring. This would explain why some QTLs detected for chilling tolerance of Φ_{PSII} had a negative effect on grain yield (JOMPUK *et al.* 2005) or why test crosses with the lowest chilling tolerance had the highest yield.

Pattern a_x may indicate specific adaptation strategies:

Most allele effects were strongest at one extreme temperature, becoming weaker at the other one (a_x). Thus, the genetic differences were greatest under chilling stress and marginal under close-to-optimal temperature (FRACHEBOUD *et al.* 2002). The allele response pattern of a_x may indicate specific adaptation strategies. The observed allele response pattern to temperature may reveal alleles, which confer tolerance at one temperature extreme. Therefore, typical candidate genes are those, which are linked to agronomically important traits and activate stress-specific mechanisms.

Specifically expressed proteins may be inferior under the respective opposite temperature extreme. Therefore, a combination of flint and dent genotypes, which have a contrasting pattern of alleles with regard to the target trait, would result in a hybrid, in which both mechanisms are combined and which, thus, possesses alleles, which have a positive effect at both temperature extremes. This, too, would expand the range of temperature, to which the hybrid is tolerant and would reduce intolerance to one of the temperature extremes.

Since the traits were usually controlled by a small number of main markers with strong effects (~ 30%) they are suitable for a maker assisted selection (MAS) (SCHÖN *et al.* 2004; UTZ *et al.* 2000). However, a fine mapping of a candidate gene requires a large sample and a high marker density to obtain a high resolution. Our population may thus, be unsuitable for the fine mapping of candidate genes. However, combining a sample of 74 with a marker density of ~1500 AFLPs it is suitable for a genome wide scan of alleles associated with important agronomic traits.

Associated genes involved in chilling or heat tolerance:

Genes near the detected associations were selected based on their assumed function in the response to chilling or heat stress. The gene *Hsp26* in bin 1.02 is interesting, because heat-shock proteins are involved in several stress response mechanisms. They play a major role in sensing ROS (*cf.* TIMPERIO *et al.* 2008) and, therefore, in protecting the photosynthetic apparatus from oxidative damage. Certain HSPs are induced by low temperature (RENAUT *et al.* 2004).

The genes encoding glutathione S-transferase and its subunits in bins 3.05, 6.05, and 7.02 are involved in gene expression responsive to temperature stress by detoxification of reactive oxygen species. An increase in oxygen-detoxifying enzymes helps to protect maize from damage caused by low temperature (*cf.* REVILLA *et al.* 2005). Both *Gst* and *Hsp* induce unspecific responses to several types of stress, which would anticipate an unspecific pattern (b_x) rather than the specific a_x-type for the related associations. Although the related associations for Φ_{PSII} showed an a_x-type response, the effect of the decrease from optimum to high temperature, was minor. This may indicate that the plants either had to antagonize more ROS under low temperature than under high temperature or that the heat stress was not severe enough.

DEAD box RNA helicase1 gene, detected in bin 3.05, encodes an enzyme involved in RNA metabolism, which is important in mRNA export of Arabidopsis (GONG *et al.* 2005) under abiotic stress (*cf.* CHINNUSAMY *et al.* 2007). In maize, the DEAD box RNA helicase protein interacts with the glycine-rich RNA-binding protein (GENDRA *et al.* 2004), which is also reported to be expressed specifically under cold stress (TIMPERIO *et al.* 2008).

The *cytokinin response regulator* gene encodes cytokinins that influence shoot development by maintaining stomatal opening and by delaying senescence under stress (POSPISILOVA and RULCOVA 1999; TEPLOVA *et al.* 1999). Appropriate amounts of cytokinin would regulate and maintain photosynthesis under temperature stress. *Crr8* (bin 1.02) is a type-B regulator (ASAKURA *et al.* 2003), which activates cytokinin transcription, whereas *Crr5* (bin 3.05) is a type-A regulator (ASAKURA *et al.* 2003), which represses transcription. Thus, selection for genotypes with upregulation of *Crr8* under stress would be the most plausible.

CONCLUSION

The development of seedlings was affected by both temperature extremes but to a lesser extent under high temperature. Dents usually carried alleles that increase the trait values at optimum and high temperature. Flints usually carried the alleles that favor chilling tolerance for Φ_{PSII}. The detected loci usually conferred tolerance specific to low or high temperature. This was most apparent for Φ_{PSII}, for which the more frequent alleles in the flint pool consistently conferred chilling tolerance. Those key loci may be involved in tolerance to heat or chilling stress. A combination of inbred lines carrying alleles, which are superior under extremes of temperature should lead to a complementary effect in the hybrid and would lead to adaptation to a wider range of temperature. The identified candidate genes, which confer chilling tolerance, such as the *cytokinin response regulator8,* could be validated further for the use in MAS.

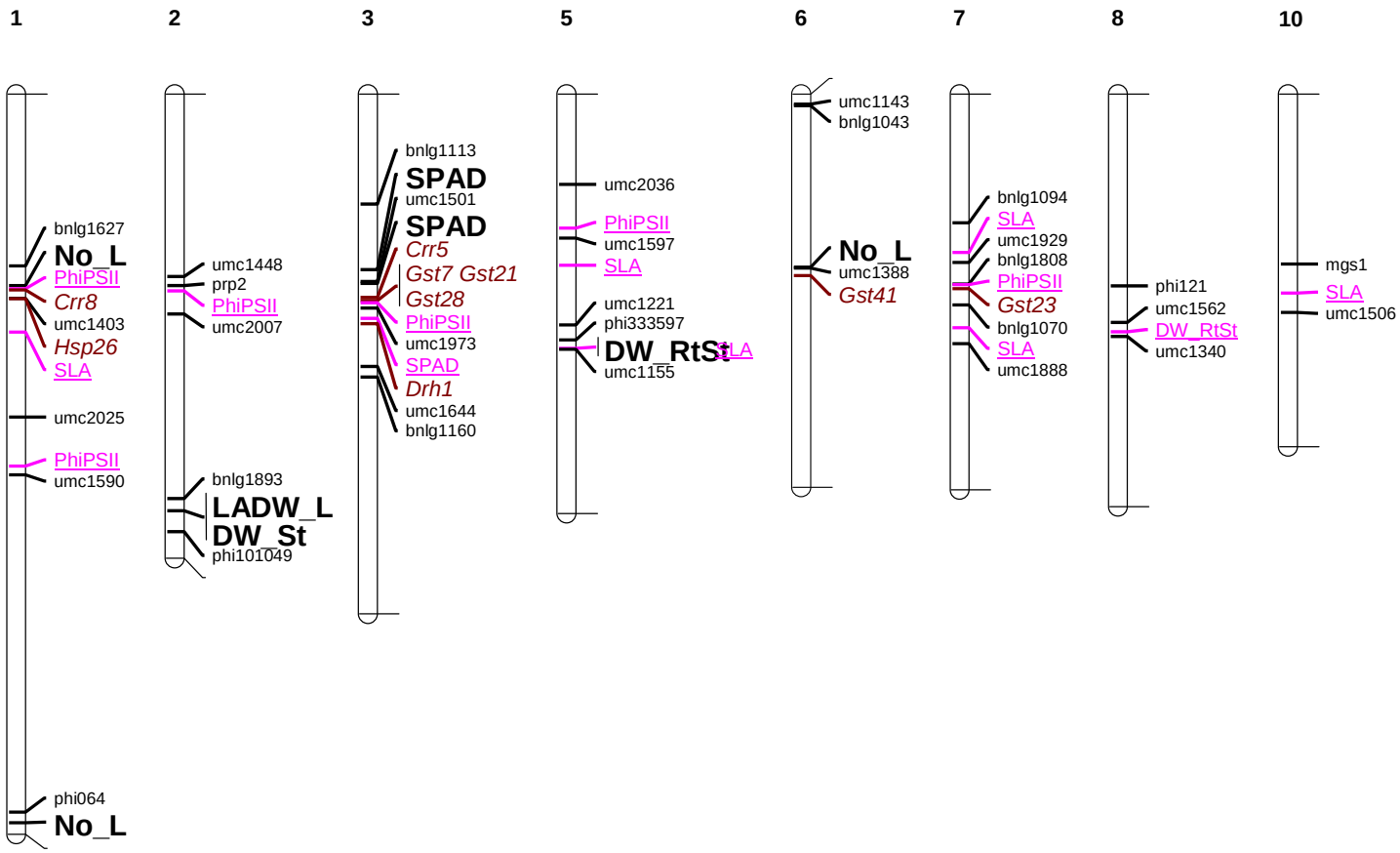

Figure 2.5 Linkage group map. Marker-trait associations with main effects are indicated in bold type; marker-by-temperature interactions are underlined. Positions of traits are displayed next to the closest SSR marker on the IBM2 2008 Neighbors Frame reference map. For the scarce of clarity markers between traits are not shown. Associated genes involved in temperature response mechanisms are indicated in italic, and were selected from the IBM2 2008 Neighbors Frame map (MaizeGDB: http://www.maizegdb.org/).

Chapter 3

Root response to temperature extremes: association mapping of temperate maize (*Zea mays* L.)

* A publication based on this chapter has been submitted.

ABSTRACT

Little is known about the genetic control of the root architecture of maize (*Zea mays* L.) and its response to temperature extremes. An association mapping panel, including 32 flint and 42 dent inbred lines, was characterized for root traits. The growth of axile and lateral roots was assessed non-destructively in growth pouches at 16°C (chilling), 28°C (control) and 36°C (heat). Associations were mapped using the PK_{Opt} mixed-model association-mapping approach. Heat slowed down the development of seedling roots to a lesser extent than chilling, but differences between the heterotic groups were observed mainly at optimal temperature. Of 1415 AFLP markers 70 showed significant marker-trait associations and 90 showed significant marker-trait associations with temperature interaction effects. The dents showed stronger growth of axile roots, especially under optimal conditions, and carried more of the trait-increasing alleles for the length of axile roots. In contrast, the flints accumulated more root dry weight at low temperature and exclusively carried the alleles favoring tolerance to chilling. A combination of inbreds carrying alleles positive for performance under contrasting temperature conditions should lead to a complementary effect in the hybrid and would increase adaptation to a wider range of temperature.

INTRODUCTION

The adaptation of maize to a wide range of environmental conditions including temperature remains a central target of breeding programs. Maize breeders work with inbred lines that are selected for their ability to produce superior, well adapted commercial hybrids. Temperate hybrids in northern and central Europe are usually a cross of inbred lines from the heterotic groups flint and dent (SHAW 1988). Both were established in the 1950s, based on European flint landraces and lines of Corn Belt dent. The flint lines contributed chilling tolerance and the dent lines contributed a high yield potential (HALLAUER 1990).

In cool temperate climates maize is sown as early as possible when soil temperatures are above 7 to 8°C to ensure a high and consistent yield. However, when temperatures are low for a prolonged period of time they have severe negative effects on early development. Chilling decreases the photosynthetic performance of maize seedlings (CHASSOT 2000; HUND 2003; HUND *et al.* 2007) as well as the root growth and leaf expansion (ENGELS 1994; STONE *et al.* 1999). Temperate maize is rarely affected by high temperature during the seedling stage. However, higher temperatures may hamper plant productivity as shown for rice (PENG *et al.* 2004). Early maize hybrids are considered to be a potential second-season crop when winter barley may be harvested earlier in southern regions of central Europe. Accordingly, seedlings may be exposed to chilling stress when sown in spring or to heat stress when sown in summer. A range of physiological and morphological adaptation is required to achieve adaptation to chilling and heat stress. Physiological adaptation to heat and chilling includes activation of the antioxidant system and the accumulation of soluble carbohydrates. Antioxidants prevent damage to the plant caused by reactive oxygen species (NIETOSOTELO and HO 1986; TIMPERIO *et al.* 2008). Furthermore, morphological adaptation may be beneficial to plant productivity, for example through the development of more lateral roots (HUND *et al.* 2008) or an increase in root diameter (CUTFORTH *et al.* 1986). Some of the adaptation mechanism of the plants, as for example the formation of stress related proteins, are, for heat and cold stress, i) the same or similar or ii) stress specific or iii) can have a negative effect under the respective opposite stress. The rapid accumulation of antioxidants or soluble carbohydrates is a similar response, which is required under heat and chilling stress. By observing the allele effects that underlie the response to temperature extremes, the reaction type becomes evident. So far, little effort has been made to trace the effect of an allele over

the whole range of temperatures, to which a maize seedling may be exposed, depending on the environment. Furthermore, there is still little information on the genetic mechanisms controlling root traits.

Quantitative trait loci for root traits of maize were identified in relation to early vigor (HUND *et al.* 2004) as well as for physiological traits and growth under chilling stress (JOMPUK *et al.* 2005). More information exists for seedling root traits at optimal temperature (RUTA *et al.* 2010; TRACHSEL *et al.* 2009b; TUBEROSA *et al.* 2003). All these QTL studies were based on biparental crosses, which have the disadvantage of being limited by the number and the resolution of alleles that can be sampled. Alternatively, in the mapping of marker-trait associations in plant-breeding populations, a high number of alleles can be mapped simultaneously at a high resolution (Flint-Garcia et al. 2003). Statistical methods, to account for population structure minimize the risk of false-positive associations (Pritchard et al. 2000). Our goal was a genome-wide association mapping of root elongation and its response to temperature in a temperate breeding population of maize. Specific questions were: i) Do alleles show a differential response to low, optimal, and high temperatures? ii) Are tolerance alleles more abundant in one of the gene pools indicating their fixation due to selection?

MATERIAL AND METHODS

We used a set of 74 European maize inbreds of flint (32) and dent (42) lines from a breeding program at the University of Hohenheim. Their genetic background was described elsewhere (ANDERSEN *et al.* 2005; SCHRAG *et al.* 2006).

Plant growth:

Plants were tested under chilling stress (16°), close-to-optimal temperature (28°) and mild heat stress (36°). The upper and lower temperatures are considered to be temperature extremes. These temperatures were based on preliminary studies of a wide range of favorable and unfavorable conditions (data not shown).

Seeds were imbibed over night at room temperature, surface sterilised with 2.5% sodiumhypoclorite (NaOCl (aq)) for 10 min, rinsed thoroughly with distilled water, and germinated on filter papers (∅ 70 mm, Macherey-Nagel AG, Oensingen, Switzerland) in an incubator at 27°. Seedlings with a similar radicle length were transferred to growth pouches (HUND *et al.* 2009) and cultivated until the respective V2 stage, indicated by a fully visible collar on the second leaf. The pouches were made of black plastic sheeting and contained blue germination blotting paper (24 × 29.5 cm) (Anchor Paper, St. Paul, MI, USA) and were hung in growth containers (33 cm wide × 132 cm long × 33 cm high). The bottom of the pouch was submerged in nutrient solution (0.23% (v/v) of Wuxal®, Aglukon Spezialdünger GmbH, Düsseldorf, Germany; composition per liter: 100 g N, 100 g P2O5, 75 g K2O, 190 mg Fe, 162 mg Mn, 102 mg B, 81 mg Cu, 61 mg Zn, 10 mg Mo). To establish the seedlinsg, they were grown under optimal conditions (28°) for two days. The photoperiod throughout the experiment was 12 h, the PPFD was 350 µmol m^{-2} s^{-1} and the relative humidity 60%. The temperature treatments were commenced two days after transplanting the seedlings, when lateral roots had appeared. At harvest, the roots were carefully washed and removed from the blotting paper. The root material was dried at 60°C to constant weight and the dry matter determined.

Imaging and analyses:

Images were taken at three specified times by a flatbed scanner (HP scanjet 4600 series, 'see-through', Hewlett-Packard Company): i) before the application of the temperature treatment (t_0) to determine the initial root length, ii) halfway through the treatment period (t_1) to determine the increase of root length as a function of time and iii) at the V2 stage when the plants were harvested (t_2) to determine root morphology depending on the stage. To scan the roots, the pouch was placed on a specially built rack. The front of the pouch was opened and the pouch was fixed; the scanner was in a horizontal position in front of the blotting paper. The acquired 24 bit images were subsequently processed by Adobe Photoshop 7.0 in three steps (Adobe Systems Inc., San Jose, CA, USA). First, the saturation channel was used to obtain 8-bit images with enhanced contrast between roots and the background. Second, the median filter with a radius of three pixels was used to remove noise, which may have been present when detecting spurious roots by WinRhizo 2003b (Regent instruments, Montreal, QC, Canada). Third, binary images were obtained by applying a threshold to the tonal value. These images were manually controlled to ensure quality of the data, which was subsequently processed by WinRhizo, revealing 72 width classes (diameter for roots) ranging from 42.33 µm (1 pixel) to 3.05 mm (72 pixels). The debris removal filter was set to remove objects with an area smaller than 0.02 cm^2 and a length/width ratio lower than 5. The lengths of axile and lateral roots were extracted from the root length in diameter-class distribution (RLDD) obtained by WinRhizo as described by HUND *et al.* (2009). Axile and lateral roots were separated by temperature-dependent thresholds taken from the RLDD. Lateral roots were characterized by root length below this threshold; longer roots were attributed to axile roots.

The elongation rate of the axile roots (ER_{Ax}) was linearly modeled, and the elongation rate of the lateral roots (k_{Lat}) was exponentially modeled. The corresponding models were

$$x(t) = x(t0) \times ER_{Ax} t \; ; \qquad ER_{Ax} = \frac{x(t) - x(t0)}{t} \tag{1}$$

for axile root elongation, where x(t) is the root length at time t after germination, x(*t*0) is the root length at the first scanning day, and Δt is the lag between *t* and *t*0

and

$$x(t) = x(t0) \times e^{k_{lat} t} \; ; \qquad k_{lat} = \frac{\log(x(t) - x(t0))}{t} \tag{2}$$

for lateral root elongation rate, where k_{lat} is the growth constant for lateral roots. The growth constant k is inversely proportional to the doubling time of the lateral roots.

Experimental design and statistics:

The experimental design within each temperature environment (t_j) was an alpha lattice design (BARRETO *et al.* 1997) with eight biological replications, i.e. four independent growth chamber replications per environment (r_{jk}) and two blocks (b_{jkl}) per growth chamber, each containing a full set of inbred lines ($\breve{g}_i$). The 74 inbred lines in each block were distributed across eight incomplete blocks (c_{iklm}), which were distributed in four sections in each of two growth containers. The final model to obtain the best linear unbiased estimates (BLUEs) of genotypes was:

$$Y_{ijklm} = \mu + \breve{g}_i + t_j + \breve{g}t_{ij} \mid \breve{g}tr_{ijk} + r_{jk} + b_{jkl} + c_{jklm} + e_{ijklm}, \quad (3)$$

where Y_{ijklm} is the effect of the *i*th inbred line in the *j*th environment, the *k*th growth chamber run, the *l*th block and the *m*th growth container. e_{ijklm} is the residual error and μ the intercept. The terms to the left and right of the vertical line (|) are considered to be fixed and random, respectively. Analysis of variance was made by the asreml-R package (ASReml release 2.0, GILMOUR *et al.* 2006) and the best linear unbiased estimates (BLUEs), extracted for each genotype-by-treatment combination, were the input values for the association mapping.

The analysis of variance of the heterotic groups, flint and dent, and for the heterotic group-by-environment interaction was made according to the final model:

$$Y_{ijklmn} = \mu + t_j + h_n + th_{jn} \mid \breve{g}_i + \breve{g}t_{ij} + \breve{g}tr_{ijk} + r_{jk} + b_{jkl} + c_{jklm} + e_{ijklmn}, \quad (4)$$

where Y_{ijklmn} is the effect of the *i*th inbred line in the *n*th heterotic group, in the *j*th environment, the *k*th growth chamber run, the *l*th block and the *m*th container. *h* is the *n*th heterotic group (flint or dent); all other parameters are the same as in model 3. If not stated, then the effects of the extreme temperatures on traits are given compared to close-to-optimum temperature.

The heritability based on an entry means (HOLLAND *et al.* 2003) for each treatment was calculated as:

$$h^2 = \frac{\sigma^2_{\breve{g}}}{\sigma^2_{\breve{g}} + \frac{1}{j}\sigma^2_{\breve{g}t} + \frac{1}{jk}\sigma^2_{\breve{g}tr} + \frac{1}{jkl}\sigma^2_{r}}, \quad (5)$$

where $\sigma^2_{\breve{g}}$ is the genetic variance, $\sigma^2_{\breve{g}t}$ the variance of the genotype-by-temperature interaction, $\sigma^2_{\breve{g}tr}$ the variance of the genotype-by-temperature-by-run interaction, and σ^2_{r} the residual error variance. *j*, *k*, and *l* denote the number of treatments (3), runs (4), and blocks (2), respectively. $\sigma^2_{\breve{g}}$ is the genetic variance after correction for effects of the heterotic group.

Association mapping:

A genome-wide association mapping was performed with the 74 maize inbred lines. This approach concluding the analysis of population structure, the test for group-specificity and the classification of allele response was described in detail in Chapter 2.

RESULTS

Chilling had the strongest effect on growth:

Chilling reduced the elongation of axile (ER_{Ax}) and lateral (k_{Lat}) roots by 81 and 72%, respectively. Both traits were affected less by heat stress. At the end of the experiment total root length (L_{Rt}), root diameter, and root surface area had increased in plants grown under extreme temperatures. The root dry weight (DW_{Rt}) and the root-to-shoot dry weight ratio (DW_{RtSt}) decreased from chilling temperature to optimum temperature to high temperature. Thus, shoot growth increased more than root growth when temperature increased. The heritability was high for all the traits (ø 0.81), with the exception of k_{Lat} (0.43) due to low genotypic variance (Table 3.1). When heritability was calculated separately for each heterotic group that of the flints increased slightly (ø 0.85), while that of the dents decreased (ø 0.73). The decrease in heritability in the dents was most apparent for k_{Lat}, No_{Se} and k_{Lat}/ER_{Ax} and was caused by lower genotype variance in the dents (data not shown).

Table 3.1 Adjusted means for population and heterotic groups (flint and dent) within temperature treatments for elongation rate of axile roots (ER_{Ax}), relative elongation rate of lateral roots (k_{Lat}), length of axile roots (L_{Ax}), diameter of axile roots (D_{Ax}), surface area of axile roots (SA_{Ax}), length of lateral roots (L_{Lat}), diameter of lateral roots (D_{Lat}), surface area of lateral roots (SA_{Lat}), number of seminal roots (No_{Se}), dry weight of roots (DW_{Rt}), ratio of dry weight of root and shoot (DW_{RtSt}), total surface area of roots (SA_{Rt}), total length of roots (L_{Rt}) and elongation rate ratio of lateral roots to that of axile roots (k_{Lat}/ER_{Ax}). Proportion of total variance of genotype (G), genotype-by-treatment interactions (G×T) and genotype-by-treatment-by-run interactions (G×T×R) as well as heritability estimates (h^2). ANOVA results for the effect of treatment (T) heterotic group (HetGr) and their interaction.

	ER_{Ax}	k_{Lat}	L_{Ax}	D_{Ax}	SA_{Ax}	L_{Lat}	D_{Lat}	SA_{Lat}	NO_{Se}	DW_{Rt}	DW_{RtSt}	SA_{Rt}	L_{Rt}	k_{Lat}/ER_{Ax}
	$cm\ d^{-1}$	$cm\ d^{-1}$	cm	mm	cm^2	cm	mm	cm^2		mg	mg/mg	cm^2	cm	
Population mean														
16°C	2.62	0.123	57.57	1.00	191.9	22.77	0.317	23.1	1.78	43.3	0.750	218.7	81.4	0.072
28°C	9.35	0.641	56.92	0.85	159.7	19.14	0.250	15.1	1.70	33.3	0.628	179.9	75.3	0.090
36°C	6.55	0.436	57.43	0.94	175.9	25.70	0.306	24.9	1.81	32.1	0.599	206.5	85.3	0.087
Heterotic Group														
16°C flint	2.39	0.122	52.70	1.043	183.2	22.03	0.316	22.4	1.60	44.3	0.779	211.1	76.0	0.074
dent	2.68	0.124	60.34	0.965	195.1	21.73	0.318	22.2	1.91	41.4	0.700	220.8	82.1	0.071
28°C flint	8.16	0.664	50.50	0.890	149.5	17.68	0.253	14.0	1.55	31.7	0.629	169.1	66.8	0.097
dent	10.08	0.611	60.72	0.812	164.1	19.10	0.246	15.1	1.80	34.0	0.604	184.4	78.5	0.084
36°C flint	6.65	0.436	55.67	0.997	178.7	24.12	0.309	23.5	1.65	31.4	0.621	209.5	82.3	0.085
dent	6.22	0.432	57.13	0.900	168.5	25.10	0.302	24.3	1.91	32.0	0.557	198.5	82.9	0.089
Variance components														
G	0.426	0.0774	0.815	0.814	0.785	0.291	0.249	0.289	0.205	0.691	0.828	0.760	0.659	0.101
G×T	0.199	0.117	0.112	0.067	0.099	0.017	0.016	0.015	7.05E-08	0.079	0.171	0.100	0.124	0.112
G×T×R	0.199	0.279	0.105	0.026	0.121	0.231	0.018	0.216	9.29E-08	0.218	0.0734	0.170	0.173	0.192
h^2	0.77	0.43	0.9	0.92	0.9	0.81	0.84	0.82	0.83	0.89	0.89	0.9	0.87	0.52
ANOVA														
T	***	***	NS	***	***	***	***	***	*	***	***	***	***	***
HetGr	NS	NS	NS	***	NS	NS	NS	NS	***	NS	NS	NS	NS	NS
T×HetGr	**	NS	.	NS	.	NS	NS	NS	NS	*	NS	NS	NS	**

., *, **, ***, NS indicate significance level of P <0.1, <0.05, <0.01, <0.001 and not significant, respectively.

Interactions among temperature and heterotic group were due to stronger elongation of axile roots of the dents at optimal temperature:

Only differences in the diameter of axile roots and the number of seminal roots for the flint and the dent groups were significant (ANOVA Table 3.1). On average, the axile roots of the flints were 0.09 mm thicker and the number of seminal roots lower compared to the dents. The number of seminal roots of the dents showed a lower genotypic variance, indicating less diversity among the dent lines for this trait. Heterotic group-by-temperature treatment interactions were found for ER_{Ax}, for the ratio of the elongation rates of axile and lateral roots (k_{Lat}/ER_{Ax}), and for the total root dry weight. Compared to the flints, the dents had a 19% higher ER_{Ax} at optimum temperature, which led to axile roots being longer by 17% at the end of the experiment. In contrast, the relative growth rate of the lateral roots of the flints was higher at optimum temperature, indicated by a wider k_{Lat}/ER_{Ax} ratio. Furthermore, the flints produced more root dry matter under chilling conditions (+7% weight) and less dry matter under close-to-optimal temperatures (-7% weight).

The association analysis yielded 70 marker-trait associations with main effects for 12 traits (Table 3.2). The number of significant associations ranged from one for the surface area of lateral roots (SA_{Lat}), total root length (L_{Rt}), and k_{Lat}/ER_{Ax} to 24 for the median diameter of the axile roots (D_{Ax}). The genetic variance explained by all the markers ranged from about 27% for L_{Rt} to 93% for the number of seminal roots (No_{Se}). The contribution of single markers was highest and lowest for No_{Se} (77.7 and 7.7%, respectively) and averaged 30.6% for all the markers of all traits. A total of 27 of the 70 associations were observed for AFLPs, which have not yet been mapped to one of the 10 chromosomes on the Keygene integrated map (NA, Table 3.2).

Dents carried trait-increasing alleles for length and surface area of axile roots:

The heterotic groups were compared for the frequency of alleles in the detected associations to determine whether some alleles were group-specific, as it was the case for 50% of the associations with main effects, where the frequency of alleles differed among the groups (Table 3.2, χ^2). In the flints, an allele was fixed in seven cases; six of the fixed alleles were for the number of seminal roots (Table 3.2).

An allele was absent in six cases without trait specificity. The flints showed slightly higher ratios for the trait-increasing allele for D_{Ax} ('Effect Flint on trait increase', Table 3.2), but the effects were not significant. The frequency of most of the trait-decreasing alleles at loci controlling axile root length (L_{Ax}), surface area of the axile roots (SA_{Ax}), and total root surface area (SA_{Rt}) was significantly higher in the flints.

Alleles mainly responded to close-to-optimal treatment and, similar to temperature extremes:

The allele substitution effect ($\alpha 1/2$) among each trait and treatment was of a similar magnitude for most detected associations, with the exception of ER_{Ax} (16°). However, $\alpha 1/2$ differed strongly between the temperature treatments for each trait and within the treatments. We classified the detected marker-by-temperature interactions according to the allele response classes based on $\alpha 1/2$ (Figure 2.2). The majority of alleles responded with at least one crossover interaction (Table 3.4, a_x, b_x, c_{heat} or c_{cold}). The type of allele response to temperature can be examined best for the two traits with the highest number of detected associations, i.e. ER_{Ax} (50 associations) and k_{Lat}/ER_{Ax} (28 associations) (Table 3.4). For ER_{Ax}, most of the responses were assigned to scenario 'b' indicating similar allele responses to temperature extremes. Among these, 30% showed an interaction (b_x) and 24% showed sizable effects at optimal temperature (b_{opt}). Accordingly, there were nine loci, where the change in the relative effect on trait values was above 6% at optimal temperatures. These were detected in bins 5.01, 5.03, 7.02, and 10.04, to mention only those mapped to a chromosome. Under chilling, there were four sizable loci, with only one being mapped to a chromosome (bin 7.02). Under high temperature, no sizable locus was detected. For k_{Lat}/ER_{Ax}, all the responses were assigned to b_x (82%) and c_{cold} (18%) (Table 3.4). The effect of most loci was around 20% at the control temperature. A closer look at the c_{cold}-type responses revealed that they were similar to b_{opt}- or b_x-type responses with a large effect at the control temperature and small or even negative effects at extreme temperatures. Thus, the majority of loci showed a clear effect at the control temperature but weak or invers effects at the extremes. One remarkable locus (bin 10.04) caused a particularly strong change in root morphology at extreme temperatures (b_x). A negative collocation was observed for two markers (bin 10.04)

for ER_{Ax} and k_{Lat}/ER_{Ax}. Furthermore, the effect flint (Table 3.3) indicated greater tolerance of ER_{Ax} to temperature extremes but lesser tolerance of k_{Lat} and, accordingly, a decrease in k_{Lat}/ER_{Ax}.

Flints carried alleles favoring chilling tolerance of root dry weight; dents carried alleles for higher k_{Lat}/ER_{Ax} under heat stress:

There were 90 marker-by-temperature interactions for eight traits (Table 3.3), ranging from one for the median diameter of both root types (D_{Ax}, D_{Lat}) to 50 for ER_{Ax}. Thirty-two of the 90 associations were observed for AFLPs, which have not yet been mapped to one of the 10 chromosomes on the Keygene integrated map (NA, Table 3.3). Group specificity was the case for 83.3% of the marker-by-temperature interactions (Table 3.3, χ^2). At most of the group-specific loci, there was a clear association of the tolerance-increasing allele to one of the heterotic groups. For most marker-trait associations, the flint group carried the allele increasing tolerance to heat and cold; for $k_{Lat}/ER_{Ax,}$ the flint group carried the allele decreasing tolerance to heat and cold. Thus, all these associations were clearly trait and group specific.

Response of ER_{Ax} to temperature altered root morphology as indicated by k_{Lat}/ER_{Ax}:

The detected associations were projected onto the IBM2 2008 Neighbors Frame genetic map. Collocations of marker-trait associations were detected on all chromosomes (Figure 3.1). Collocations for association-by-temperature interaction effects were found to a greater extent for axile root traits. Eleven collocations between ER_{Ax} and k_{Lat}/ER_{Ax} appeared on different chromosomes (Figure 3.1). A positive collocation between the ratio k_{Lat}/ER_{Ax} and k_{Lat} was detected in only one case (bin 10.04) (Table 3.3), indicating that a change in ER_{Ax} generally influenced this ratio. This is supported by the close negative correlation between ER_{Ax} and k_{Lat}/ER_{Ax} ($r \sim -0.74$), while k_{Lat} was not correlated with the ratio and, thus, did not influence the ratio. Two collocations for k_{Lat}/ER_{Ax} and axile root length (L_{Ax}) were detected in bins 2.09 (negative collocation) and 10.04 (positive collocation) (Table 3.3, Figure 3.1). Collocations for associations with main effects were found for several traits. On chromosome 5, the surface

area of axile roots (SA_{Ax}) and the total root surface area (SA_{Rt}) collocated positively with the ratio between the dry weight of the root and the shoot (DW_{RtSt}) in bin 5.05. In bin 6.08, SA_{Ax} and SA_{Rt} collocated positively with total root dry weight (DW_{Rt}). This is supported by the high correlations between these traits (r ~ 0.7). In bin 7.02, the surface area of the lateral roots (SA_{Lat}), the length of axile roots (L_{Ax}), and the total root surface area (SA_{Rt}) were collocated. Accordingly, the correlation of L_{Ax} and SA_{Rt} was close (r ~ 0.9), but lateral roots also played a major role in determining root surface area (r ~ 0.7).

Linked genes involved in temperature response mechanisms:

Genes close to the detected association (± 20 cM region), which are involved in temperature-tolerance mechanisms, were selected from the IBM2 2008 Neighbors Frame map (MaizeGDB: http://www.maizegdb.org/). In bin 1.05, glutathione S-transferase *Gst32 and Gst42* were located ~12 cM and *Gst14* was ~5 cM from an association for ER_{Ax}. In bin 8.05, *Gst15* was 2 cM from a marker-by-temperature interaction for ER_{Ax}. In bin 1.04, sucrose synthase (*Sus2)* (pos 329.06 cM) was in 13 cM from marker-by-temperature interactions for ER_{Ax} and k_{Lat}/ER_{Ax} (Figure 3.1). In bin 9.04 *Sus1* was 8 cM from a cluster of ER_{Ax} and k_{Lat}/ER_{Ax} associations. Vacuolar acid invertase2 (*Ivr2)* (bin 5.03, 288 cM) was 3 cM from a marker-by-temperature interaction for ER_{Ax} (type b_{opt} response). The second gene in bin 5.04, cell wall invertase1 (*Incw1)* (376.4 cM), was 1 cM from a marker-by-temperature interaction for ER_{Ax}. *Incw3* (bin 10.04, 272.2 cM), from the same gene family, was 7 cM from a cluster of marker-by-temperature interactions for ER_{Ax}, k_{Lat}, L_{Ax}, and k_{Lat}/ER_{Ax}. *Sus*, *Ivr* and *Incw* all provide sucrose cleavage mechanisms so that sugars can be transported to and utilized in the sink organs.

In bin 1.08, a gene coding for a glycine-rich protein (*Grp1)* was only 2 cM from an association for D_{Lat} and 4 cM from a marker-by-temperature interaction for ER_{Ax}. In bin 5.03, a similar gene, *Grp3* (243.5 cM), was 1 cM from a marker-by-temperature interaction for ER_{Ax} and 2 cM from an association for No_{Se}.

Table 3.2 List of marker-trait associations with main effects. See Table 3.1 for abbreviations of traits. AFLP marker according to Keygene, marker position on the Keygene integrated map (unpublished) (Pos. KG) and the IBM2 2008 Neighbors Frame (Pos. IBM); proportion of genotypic variance explained by each marker (pg (%)) including the total variance explained by all significant markers; allele substitution effect (α1/2) as the additive effect of replacing allele 1 with allele 2; $\chi 2$ two sample test for allele distribution between flint/dent; ratio of number of flints carrying the allele vs. the total number of genotypes carrying the allele (Ratio Flint); algebraic sign of the effect of the more frequent allele in the flint group with respect to chilling or heat tolerance (Effect).

Associations with main effects							χ^2 two sample test Flint/Dent	Ratio Flint		Effect Flint on trait increase
Trait	Marker	Pos. KG (cM)	Pos. IBM (cM)	Bin	p_g (%)	α½		Allele 1	Allele 2	
ER_{Ax}	269	77.4	410	1.05	30.9	-7.65	NS	0.43	0.44	-
	318	126	581	6.08	28.7	-10.1	***	0.31	0.83	-
	927	NA	NA	NA	28.2	-10.1	***	0	0.57	-
	1263	NA	NA	NA	28.4	6.51	NS	0.25	0.49	+
	710	NA	NA	NA	33.9	17.3	***	0.96	0.11	-
				total	79.5					
L_{Ax}	962	51.3	200	7.02	27.9	4.38	***	0.96	0.11	-
	294	56.4	256	7.02	28.3	4.18	***	0.93	0.09	-
	710	NA	NA	NA	31.3	4.89	***	0.96	0.11	-
				total	30.3					
D_{Ax}	1548	57	275	1.03	29.4	4.16	NS	0.41	0.45	+
	972	69.7	359	1.04	25.5	-4.60	NS	0.7	0.4	+
	2169	84.1	361	2.05	30.3	4.43	NS	0.42	0.44	+
	869	51.6	208	3.04	29.7	4.27	NS	0.39	0.47	+
	2036	57.8	269	3.04	29.4	4.16	NS	0.41	0.45	+
	587	59.2	283	3.04	29.4	4.16	NS	0.41	0.45	+
	2133	104	559	3.07	25.6	-3.93	NS	0.44	0.42	+
	753	61.4	286	4.05	30.4	3.85	NS	0.42	0.43	+
	1101	79.4	374	4.06	24.5	3.86	*	0.65	0.33	-
	1113	81.2	350	5.04	31.3	3.81	NS	0.34	0.45	+
	2158	141	622	5.08	29.4	4.16	NS	0.41	0.45	+
	661	44.1	155	6.02	29.4	-4.16	NS	0.45	0.41	+
	336	59.5	281	7.02	25.1	5.24	NS	0.33	0.47	+
	2047	129	544	8.08	26.2	3.74	NS	0.42	0.44	+
	1541	NA	NA	NA	29.4	4.16	NS	0.41	0.45	+
	1829	NA	NA	NA	25.6	3.86	NS	0.4	0.4	=
	2049	NA	NA	NA	25.6	3.93	NS	0.42	0.44	+
	2054	NA	NA	NA	29.7	4.27	NS	0.39	0.47	+
	2058	NA	NA	NA	29.7	4.27	NS	0.39	0.47	+
	2083	NA	NA	NA	29.4	4.16	NS	0.41	0.45	+
	2086	NA	NA	NA	23.4	3.85	NS	0.45	0.42	-
	2089	NA	NA	NA	29.6	4.23	NS	0.42	0.44	+
	2117	NA	NA	NA	29.0	4.07	NS	0.39	0.47	+
	2123	NA	NA	NA	29.4	4.16	NS	0.41	0.45	+
				total	51.5					
SA_{Ax}	767	93.9	409	5.05	28.1	-0.565	*	0	0.51	-
	318	126	581	6.08	24.8	-0.656	***	0.31	0.83	-
	544	55.8	251	7.02	22.4	0.696	***	0.93	0.13	-
	710	NA	NA	NA	28.7	0.906	***	0.96	0.11	-
				total	61.6					

continued:

Associations with main effects							χ^2 two sample test Flint/Dent	Ratio Flint		Effect Flint on trait increase
Trait	Marker	Pos. KG (cM)	Pos. IBM (cM)	Bin	p_g (%)	α½		Allele 1	Allele 2	
D_{Lat}	542	123	773	1.08	30.7	-4.81	NS	0.45	0.38	+
	543	NA	NA	NA	30.7	4.81	NS	0.38	0.45	+
	1365	NA	NA	NA	29.8	4.71	NS	0.38	0.46	+
				total	29.8					
SA_{Lat}	294	56.4	256	7.02	27.3	1.12	***	0.93	0.09	-
No_{Se}	308	75.4	397	1.04	8.78	-13.2	NS	0.67	0.42	+
	129	83.6	475	1.05	51.1	6.80	*	1	0.36	-
	832	151	676	2.09	7.71	-6.56	**	0.92	0.34	+
	1177	58.4	275	3.04	72.5	-1.93	**	1	0.36	+
	1371	140	668	4.09	70.0	2.45	NS	0.48	0.4	-
	930	64	245	5.03	17.0	-5.44	***	0.1	0.34	+
	1253	102	452	5.05	72.2	-2.73	NS	0.13	0.46	-
	1776	63.6	296	7.02	35.1	2.15	**	0.68	0.28	-
	560	102	501	7.04	18.8	-5.89	***	0.81	0.22	+
	1059	68.5	208	9.03	15.2	-11.1	*	1	0.39	+
	1247	NA	NA	NA	31.0	7.08	**	1	0.38	-
	1379	NA	NA	NA	54.7	2.69	NS	0.39	0.83	+
	1382	NA	NA	NA	77.7	3.37	***	0.22	0.91	+
	1465	NA	NA	NA	22.5	12.4	NS	1	0.41	-
	1790	NA	NA	NA	4.61	-5.87	NS	0.51	0.24	+
				total	92.6					
DW_{Rt}	639	91	396	2.06	38.0	-1.72	*	0.07	0.51	-
	467	61.8	232	5.03	22.6	0.84	***	0.65	0.07	-
	318	126	581	6.08	26.4	-0.98	***	0.31	0.83	-
	94	NA	NA	NA	28.8	-1.89	**	0	0.54	-
				total	60.6					
SA_{Rt}	767	93.9	409	5.05	25.4	-0.475	*	0	0.51	-
	318	126	581	6.08	25.7	-0.579	***	0.31	0.83	-
	962	51.3	200	7.02	25.8	0.723	***	0.96	0.11	-
	544	55.8	251	7.02	23.3	0.628	***	0.93	0.13	-
	294	56.4	256	7.02	25.2	0.680	***	0.93	0.09	-
	755	NA	NA	NA	23.2	0.752	***	1	0.13	-
	710	NA	NA	NA	29.8	0.818	***	0.96	0.11	-
				total	58.6					
L_{Rt}	217	85.2	411	3.06	31.5	-0.129	**	0.32	0.8	-
DW_{RtSt}	767	93.9	409	5.05	35.2	-19.8	*	0	0.51	-
	1356	NA	NA	NA	31.5	22.3	***	0.65	0	-
				total	53.1					
k_{Lat}/ER_{Ax}	1379	NA	NA	NA	44.2	5.44	NS	0.39	0.83	+

*, **, ***, NS indicate significance level of P <0.05, <0.01, <0.001 and not significant, respectively, based on a χ^2 two sample test for allele distribution between the heterotic groups.
$_{NA}$: Marker is not yet mapped to one of the ten chromosomes on the Keygene integrated map.

Table 3.3 List of marker-by-temperature treatment interactions. See Table 3.1 for abbreviations of traits. AFLP marker according to Keygene, position of marker on the Keygene integrated map (unpublished) (Pos. KG) and the IBM2 2008 Neighbors Frame (Pos. IBM), allele substitution effect ($\alpha 1/2$) as the additive effect of replacing allele 1 with allele 2; $\chi 2$ two sample test for allele distribution between flint/dent; ratio of number of flints carrying the allele vs. the total number of genotypes carrying the allele (Ratio Flint); algebraic sign of the effect of the more frequent allele in the flint group with respect to chilling or heat tolerance (Effect).

Marker-by-temperature interactions					$\alpha 1/2$			allele response class	χ^2 two sample test Flint/ Dent	Ratio Flint		Effect Flint	
Trait	Marker	Pos. KG (cM)	Pos. IBM (cM)	bin	16°C	28°C	36°C			Allele 1	Allele 2	cold	heat
k_{Lat}	765	60.4	279	10.04	-18.9	14.1	-0.52	b_x	**	0.17	0.6	-	-
	1786	NA	NA	NA	19.6	-21.2	4.01	b_x	**	0	0.52	+	+
ER_{Ax}	31	63.2	316	1.04	-14.4	-10.9	-3.25	a_{cold}	***	0	0.57	-	+
	473	71.2	369	1.04	0.84	5.69	-4.51	c_{cold}	***	0.96	0.15	+	+
	787	71.4	370	1.04	1.83	5.97	-1.58	c_{cold}	***	0.92	0.2	+	+
	657	123	775	1.08	-0.35	6.53	-2.37	b_x	***	0.79	0.23	+	+
	1774	95.9	420	2.07	7.76	-6.21	-0.36	c_{heat}	NS	0.41	0.48	+	+
	715	116	520	2.08	0.60	-7.86	-0.66	c_{heat}	NS	0.22	0.5	+	+
	786	16.2	43	3.01	-4.98	-7.46	2.58	c_{cold}	***	0.04	0.62	+	+
	944	143	801	3.09	4.10	6.78	-1.62	c_{cold}	***	0.86	0.25	+	+
	47	38.7	179	4.03	2.73	-4.07	7.14	b_x	**	0	0.52	+	+
	93	46	212	4.04	3.86	-8.24	3.04	b_x	**	0	0.52	+	+
	1234	59.7	277	4.05	12.3	8.30	0.11	a_{cold}	***	0.93	0.13	-	+
	13	19.9	77	5.01	-2.69	-7.32	-2.13	b_{opt}	NS	0.28	0.5	+	+
	222	37.9	148	5.01	2.13	-7.76	0.63	b_x	***	0.1	0.59	+	+
	344	44.3	169	5.01	-3.97	-10.6	-2.56	b_{opt}	***	0.05	0.58	+	+
	1437	63.9	245	5.03	1.01	8.24	2.22	b_{opt}	***	0.65	0.13	+	+
	313	67	264	5.03	-11.0	-12.7	-7.59	b_{opt}	***	0	0.62	+	+
	1206	71.5	291	5.03	-2.02	-11.4	-5.04	b_{opt}	***	0	0.54	+	+
	174	72.3	296	5.03	-0.59	9.90	3.30	c_{heat}	*	0.5	0.12	+	+
	973	84.5	370	5.04	-0.41	-9.01	0.52	c_{cold}	***	0	0.59	+	+
	538	86	376	5.04	-1.05	-8.89	1.35	c_{cold}	NS	0.3	0.5	+	+
	953	90.3	394	5.05	-1.34	-5.32	3.06	c_{cold}	***	0.08	0.76	+	+
	546	53.9	230	7.02	-6.64	-9.10	-2.19	b_{opt}	***	0.11	0.78	+	+
	1274	55.5	248	7.02	-6.10	-9.37	-2.62	b_{opt}	***	0.11	0.75	+	+
	544	55.8	251	7.02	25.7	12.7	7.62	a_{cold}	***	0.93	0.13	-	+
	280	58.7	197	8.03	2.45	8.92	-1.00	c_{cold}	***	1	0.23	+	+
	24	81.7	355	8.05	-11.4	4.31	-4.88	b_x	*	0.52	0.13	+	+
	1162	77.7	304	9.04	-3.57	-10.8	-2.93	b_{opt}	***	0	0.63	+	+
	754	60.3	278	10.04	3.35	-5.82	3.28	b_x	***	0.04	0.65	+	+
	756	60.4	279	10.04	6.19	-3.15	6.34	b_x	**	0.17	0.6	+	+
	279	60.5	280	10.04	-5.31	-8.67	-0.93	b_{opt}	***	0.08	0.61	+	+
	1119	62.5	297	10.04	-2.07	6.53	-0.24	b_x	***	0.71	0.21	+	+
	474	63.5	306	10.04	-8.38	3.24	-5.83	b_x	**	0.66	0.24	+	+
	11	NA	NA	NA	11.3	-4.04	4.48	b_x	**	0	0.54	+	+
	18	NA	NA	NA	9.69	9.80	3.65	b_{opt}	NS	0.52	0.27	+	+
	164	NA	NA	NA	-2.92	5.46	-1.59	b_x	***	0.74	0.06	+	+
	287	NA	NA	NA	-3.93	-4.53	5.12	c_{cold}	***	0.06	0.73	+	+
	438	NA	NA	NA	-28.9	-14.2	-8.63	a_{cold}	***	0.03	0.82	-	+
	737	NA	NA	NA	-16.9	-13.9	-8.19	a_{cold}	***	0	0.58	-	+
	755	NA	NA	NA	27.5	12.9	7.24	a_{cold}	***	1	0.13	-	+
	927	NA	NA	NA	-22.1	-15.4	-8.90	a_{cold}	***	0	0.57	-	+
	985	NA	NA	NA	2.26	10.4	2.51	b_{opt}	***	0.55	0	+	+
	1041	NA	NA	NA	-3.27	-10.4	-3.25	b_{opt}	***	0	0.59	+	+
	1429	NA	NA	NA	0.90	-7.49	2.32	b_x	***	0.09	0.75	+	+

continued:

Marker-by-temperature interactions					α1/2			allele response class	χ^2 two sample test Flint/ Dent	Ratio Flint		Effect Flint	
Trait	Marker	Pos. KG (cM)	Pos. IBM (cM)	bin	16°C	28°C	36°C			Allele 1	Allele 2	cold	heat
	1471	NA	NA	NA	1.04	-7.94	-2.90	c_{heat}	NS	0.42	0.49	+	+
	1472	NA	NA	NA	-4.28	6.84	1.42	c_{heat}	NS	0.49	0.41	+	+
	1623	NA	NA	NA	6.95	-5.71	4.38	b_x	***	0	0.54	+	+
	1758	NA	NA	NA	13.2	-4.84	5.08	b_x	***	0	0.59	+	+
	1818	NA	NA	NA	10.9	-5.44	3.54	b_x	***	0.11	0.61	+	+
	20	NA	NA	NA	-0.83	6.99	0.74	c_{heat}	**	0.55	0.11	+	+
	625	NA	NA	NA	-14.0	-13.1	-4.74	a_{cold}	***	0.05	0.6	-	+
L_{Ax}	1511	137	611	2.09	-0.13	0.96	-0.83	b_x	***	0.91	0.06	+	+
	756	60.4	279	10.04	0.21	-1.76	0.51	b_x	**	0.17	0.6	+	+
D_{Ax}	1177	58.4	275	3.04	0.91	2.75	-2.42	c_{cold}	**	1	0.36	+	+
D_{Lat}	804	105	504	9.06	1.56	0.71	-1.02	a_x	***	1	0.25	-	+
DW_{Rt}	1138	69.8	360	1.04	0.536	-0.28	0.524	b_x	**	0.19	0.56	+	+
	955	69.9	360	1.04	1.089	0.091	0.727	b_{ex}	***	0	0.54	+	+
	642	133	642	9.07	0.494	-0.39	0.086	b_x	***	0.12	0.7	+	+
	1638	NA	NA	NA	0.705	-0.59	-0.42	c_{heat}	*	0	0.44	+	+
DW_{RtSt}	151	83.8	370	8.05	2.87	-3.87	8.71	b_x	***	0	0.6	+	+
	1584	NA	NA	NA	-0.46	-5.03	15.3	c_{cold}	*	0.08	0.52	+	+
k_{Lat}/ER_{Ax}	31	63.2	316	1.04	0.74	9.96	-1.57	c_{cold}	***	0	0.57	-	-
	7	101	608	1.04	12.9	-7.91	6.18	b_x	NS	0	0.47	+	+
	1774	95.9	420	2.07	-3.72	10.8	-0.44	b_x	NS	0.41	0.48	-	-
	581	105	468	2.07	6.70	-8.07	4.39	b_x	*	0.62	0.31	-	-
	1511	137	611	2.09	4.02	-4.38	8.10	b_x	***	0.91	0.06	-	-
	2	143	637	2.09	0.21	-4.85	5.38	b_x	***	1	0.18	-	-
	726	8.9	4	3.0	-5.46	10.2	-4.11	b_x	***	0	0.67	-	-
	786	16.2	43	3.01	-0.26	11.6	-5.17	b_x	***	0.04	0.62	-	-
	47	38.7	179	4.03	-6.67	8.08	-7.82	b_x	**	0	0.52	-	-
	93	46	212	4.04	-5.66	11.5	-6.08	b_x	**	0	0.52	-	-
	13	19.9	77	5.01	-2.51	9.30	-0.75	b_x	NS	0.28	0.5	-	-
	336	59.5	281	7.02	-0.02	9.81	-3.89	b_x	NS	0.33	0.47	-	-
	24	81.7	355	8.05	4.85	-6.65	5.28	b_x	*	0.52	0.13	-	-
	1162	77.7	304	9.04	0.56	13.4	-0.78	c_{cold}	***	0	0.63	-	-
	754	60.3	278	10.04	-4.97	9.67	-6.03	b_x	***	0.04	0.65	-	-
	756	60.4	279	10.04	-3.68	10.2	-7.43	b_x	**	0.17	0.6	-	-
	279	60.5	280	10.04	0.07	12.1	-2.52	c_{cold}	***	0.08	0.61	-	-
	11	NA	NA	NA	-5.11	8.49	-6.25	b_x	**	0	0.54	-	-
	32	NA	NA	NA	1.04	-4.77	5.89	b_x	***	0.7	0.26	-	-
	287	NA	NA	NA	5.15	10.8	-2.73	c_{cold}	***	0.06	0.73	-	-
	1002	NA	NA	NA	-1.71	7.98	-2.81	b_x	***	0.07	0.73	-	-
	1041	NA	NA	NA	-4.78	10.6	-1.42	b_x	***	0	0.59	-	-
	1273	NA	NA	NA	-7.65	12.6	-7.10	b_x	NS	0.14	0.46	-	-
	1430	NA	NA	NA	-0.77	-13.6	3.93	c_{cold}	NS	0.65	0.36	-	-
	1471	NA	NA	NA	-2.23	12.7	-0.05	b_x	NS	0.41	0.49	-	-
	1472	NA	NA	NA	1.47	-11.7	0.14	b_x	NS	0.49	0.41	-	-
	1818	NA	NA	NA	-6.80	9.02	-5.17	b_x	***	0.11	0.61	-	-
	20	NA	NA	NA	8.44	-4.55	3.14	b_x	**	0.55	0.11	-	-

*, **, ***, NS indicate significance level of P <0.05, <0.01, <0.001 and not significant, respectively, based on a χ^2 two sample test for allele distribution between the heterotic groups.

$_{NA}$: Marker is not yet mapped to one of the ten chromosomes on the Keygene integrated map.

Table 3.4 List of allele response classes for marker-by-temperature interactions. See Table 3.1 for abbreviations of traits. Symbols refer to the list of classes in Figure 2.2.

Trait	No. marker with sig. temperature interaction effects	Percentages of allele response classes							
		a_x	b_x	a_{heat}	a_{cold}	b_{ex}	b_{opt}	c_{heat}	c_{cold}
									
k_{Lat}	2	-	100	-	-	-	-	-	-
ER_{Ax}	50	-	30	-	16	-	24	12	18
L_{Ax}	2	-	100	-	-	-	-	-	-
D_{Ax}	1	-	-	-	-	-	-	-	100
D_{Lat}	1	100	-	-	-	-	-	-	-
DW_{Rt}	4	-	50	-	-	25	-	25	-
DW_{RtSt}	2	-	50	-	-	-	-	-	50
k_{Lat}/ER_{Ax}	28	-	82	-	-	-	-	-	18

DISCUSSION

Although the genetic response of the root system of seedlings had been studied by HUND *et al.* (2004), no attempt had been made to compare the effect of optimum temperature in contrast to high or low temperature. Roots stopped growing at 12°C and 40°C (data not shown), so the temperature extremes were set accordingly at 16°C and 36°C. Roots grew best at 28°C, as described by BARBER *et al.* (1988) and PAHLAVANIAN and SILK (1988).

Morphology:

Fewer seminal roots and a larger median diameter of axile roots was associated with the flints, as observed too by WIGGANS (1916). Wiggans also found that flints had only one to two seminal roots, whereas the dents had three to four seminal roots. This difference was also described by HOECKER *et al.* (2006). Seedlings grown at 15°C had thicker roots with considerably fewer hairs than roots grown at higher temperature (CUTFORTH *et al.* 1986). Therefore, the increased diameter of the flints may be a strategy to achieve tolerance to chilling, because thicker roots enable better water transport under chilling stress due to xylem vessels with a greater diameter (VARNEY *et al.* 1991).

Root elongation vs. final root length:

We found a greater number of marker-by-temperature interactions for traits related to root elongation rates than was found for measurements at the end of the experiment. For example, ER_{Ax} yielded 50 associations compared to L_{Ax}, which had only two. The detection of fewer associations for L_{Ax} may be due to unaccounted differences in germination. These differences can result in large errors and can be overcome by measuring elongation rates (HUND *et al.* 2009). The detection of a greater number of marker-by-environment interactions resulting from the measurement of elongation rates is corroborated by a QTL study of the response of root elongation to water deficit (RUTA *et al.* 2010).

The response of alleles is similar at both temperature extremes:

The relative allele effects were usually strongest at the optimum temperature, decreased towards the extremes (b_{opt}), and sometimes reverted into the opposite effect (b_x). The pattern of allele response of b_x and the subclasses (Figure 2.2) indicates that genotypes are 'equipped' with alleles that are superior or inferior at both temperature extremes in contrast to the optimum. Thus, relative differences in growth rates at extreme temperatures might be due to the activation of stress-response pathways. These may help to maintain organ growth or, alternatively, stop organ growth as we observed. The effect of the greatest genetic differences at optimal temperature is confirmed again by the differences between the heterotic groups. The contribution of the alleles to temperature tolerance is best explained by k_{Lat}/ER_{Ax} and ER_{Ax}, which showed most marker-by-temperature interactions. In the case of k_{Lat}/ER_{Ax}, the inversion of the relative allele effect from the extremes to the close-to-optimal temperature was strong and affected many loci. Furthermore, an increase in k_{Lat}/ER_{Ax} was frequently collocated with a decrease in ER_{Ax}. The relative increase at these loci might be due to the effect of temperature on the growing meristem of the axile root, not on the lateral root. Hund *et al.* (2008) also found that the overall length of the lateral roots was not influenced by temperature. This may be related to apical dominance and to compensation for stress effects on the axile root meristem by subsequent lateral roots. An increase in lateral roots was also observed when roots grew at very high concentrations of PEG, which caused a very low water potential (Trachsel, S.: personal communication). Longer lateral roots have been associated

with better plant performance at low temperature (HUND *et al.* 2007) and are considered to be a key factor in improving early vigor (HUND *et al.* 2008).

In the case of ER_{Ax}, the majority of alleles showed the strongest effects under chilling stress and weaker effects at optimum temperature. This might suggest that alleles responsible for cold tolerance can have a negative effect on plant growth at optimal temperature. This phenomenon has been described for photosynthesis-related traits (JOMPUK *et al.* 2005), but not yet for root elongation.

Allelic composition of heterotic groups:

For almost all traits, the alleles were clearly group-specific, i.e. all trait-increasing alleles tended to be more abundant in one of the heterotic groups. This is remarkable, because these associations were detected, despite the fact that the population structure was taken into account. Thus, only those associations were detected, for which the marker was not fully associated with the heterotic group. When population structure was not taken into account, there was an increase in the number of detected main marker-trait associations (142 compared to 70), probably due mainly to a high number of false positives. In the case of marker-trait associations, which interacted with temperature, taking the population structure into account did not increase the number of detections (90 vs. 89). If population structure is not considered, then the detection of false positive associations cannot be avoided (ANDERSEN *et al.* 2005; CAMUS-KULANDAIVELU *et al.* 2006). On the other hand, fixed alleles for the target trait are closely associated with population structure (heterotic group) and might not be detected if population structure were not considered (ANDERSEN *et al.* 2005; CAMUS-KULANDAIVELU *et al.* 2006).

The detected group specificity is remarkable since it is unlikely that it would happen by chance. But what causes a “synchronized” unequal distribution of the trait-increasing alleles in both heterotic groups? Our results indicate that the heterotic groups may have been selected to allow for a wider adaptation to temperature by the resulting hybrid. The flint contributed alleles for chilling tolerance, and the dent lines contributed to productivity under optimal conditions and, thus, to a high yield potential (HALLAUER 1990). However, little is known about how modern flint and dent lines differ with respect to their allelic contribution to temperature tolerance. MCWILLIAM and GRIFFING (1965) evaluated the temperature-

dependence of heterosis in maize and its contribution to hybrid vigor. They compared a northern flint inbred line with a southern dent inbred line and did not find strong differences among them. However, they noted a genetic defect in the flint line due to inbreeding, which affected the formation of chlorophyll, especially in the cold. This is critical. At the beginning of the hybrid breeding, the genetic burden hampered the evaluation of effects such as the temperature-dependence of heterosis. Inbred selection for hybrid breeding decreased the frequency of such unfavorable alleles in the gene pool. Did it also result in a diversification of selection? Judging from the trend in the genetic diversity of European maize cultivars and their parental components during the past 50 years (REIF *et al.* 2005), this may not be the case. Both heterotic groups were clearly separated at first and developed in parallel thereafter.

Candidate pathways and their genes:

A high proportion of genes located around the detected associations are related to glycolysis, suggesting that this pathway plays a key role in response to temperature. It is striking that three different invertase genes were detected, since, so far, only six forms are known for maize (soluble *Ivr1* and *Ivr2*, insoluble *Incw1, 2, 3 and 4*). Invertase and sucrose synthase are the starting enzymes of the cytosolic glycolysis pathway, which enables essential metabolic adaptability, which facilitates plant development and acclimation to environmental stress (FERNANDES *et al.* 2008). This network seems to play a pivotal role in regulating the response to multiple types of abiotic stress. The expression of stress-specific isozymes may be regulating this pathway (FERNANDES *et al.* 2008) with glucose being the potential signaling molecule (ROITSCH and GONZALEZ 2004). The accumulation of sugars like sucrose is one of the most commonly observed responses to abiotic stress (LUNN and FURBANK 1999) and is also observed under chilling (VERHEUL *et al.* 1995). The root tips accumulate assimilated carbon to a greater extent than at optimal temperature, indicating that they cannot utilize the carbohydrates for growth and respiration (NAGEL *et al.* 2009). An important regulatory role of invertase and sucrose synthase has already been shown for the root elongation of Arabidopsis (SERGEEVA *et al.* 2006). One of our candidate genes, *Ivr2,* was identified as a candidate gene in a study on the genetic control of acclimation of the photosynthetic apparatus to low temperature at night (GUERRA-PERAZA *et al.* 2010).

Genes encoding for glycine-rich proteins were closely linked with root traits like D_{Lat} and ER_{Ax}. Glycine-rich proteins are root-tissue specific and thought to be proteins of the cell wall (GODDEMEIER *et al.* 1998). *Grp* synthesis is induced by external stimuli like abscisic acid (ABA) (DE OLIVEIRA *et al.* 1990; GODOY *et al.* 1990). Since ER_{Ax} is a response association and is usually classified as b_x and b_{opt} and since chilling stress is accompanied by an increase in the ABA concentration, *Grp* might be an appropriate candidate for selecting genotypes with the expression of large amounts of *Grp* in the roots.

CONCLUSIONS

Most of the differences between the heterotic groups were at optimal temperature: the dents grew longer axile roots, and the flints produced a relatively larger proportion of lateral roots. This pattern was also observed for the detected marker-trait associations. The dents carried more alleles increasing ER_{Ax} and more alleles increasing the sensitivity of ER_{Ax} to temperature extremes. In general, the majority of alleles showed a similar response to cold and heat (b_{opt} and b_x). The inverted allele effect (b_x) at many loci indicates that the favorable effect of the different alleles depends on temperature. The development of the heterotic groups was based on the selection of hybrids, i.e. only parents with good combining ability were retained in the groups. This raises the question as to whether the combination of alleles with different responses to temperature would enable the adaptation of the hybrid to a wider range of temperature. A good locus to test this hypothesis is that in bin 10.04, which has a temperature dependent effect on overall root morphology.

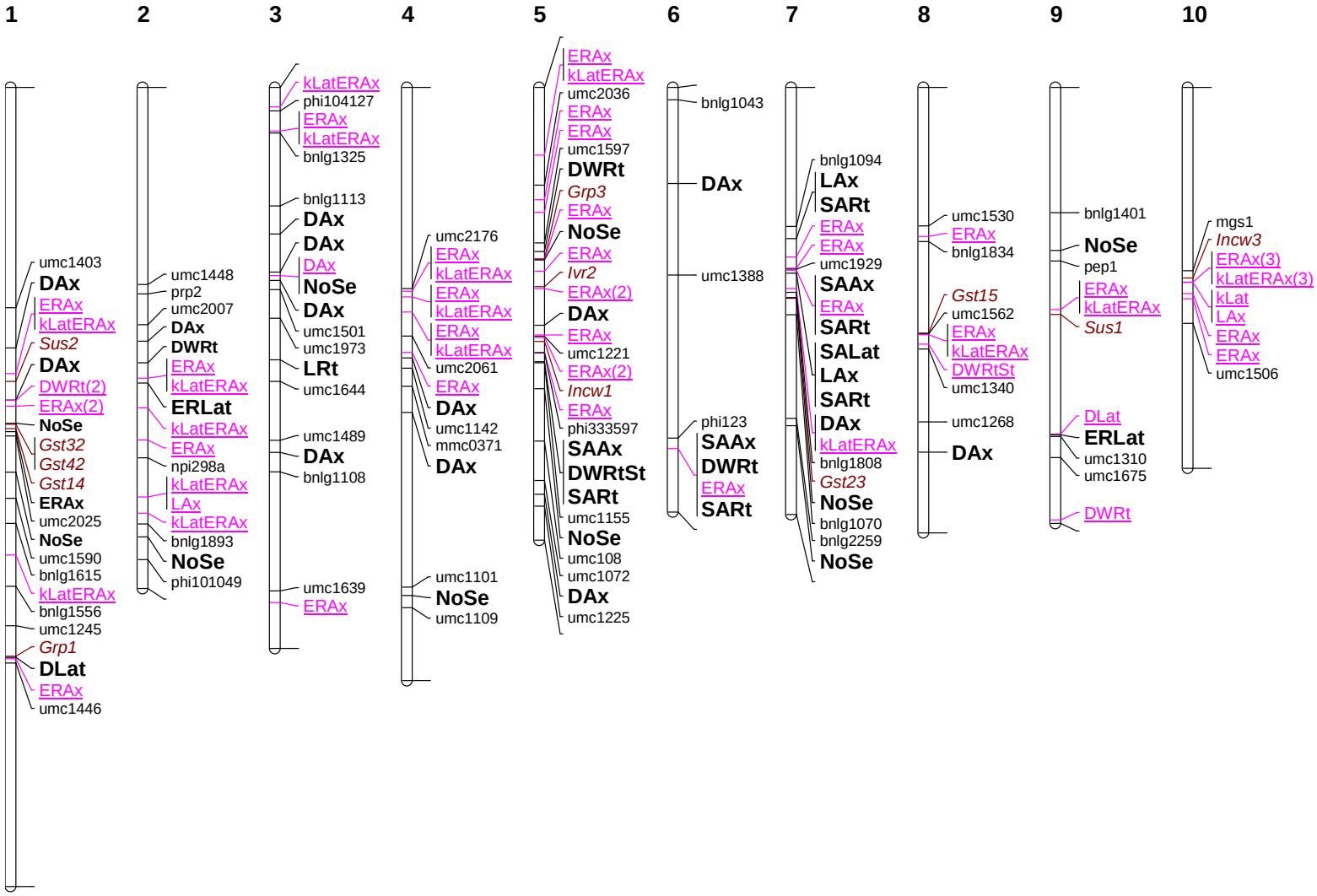

Figure 3.1 Linkage group map. Marker-trait associations with main effects are indicated in bold type; marker-by-temperature interactions are underlined. Positions of traits are displayed next to the closest SSR marker on the IBM2 2008 Neighbors Frame reference map. For the scarce of clarity markers between traits are not shown. Associated genes involved in temperature response mechanisms are indicated in italic, and were selected from the IBM2 2008 Neighbors Frame map (MaizeGDB: http://www.maizegdb.org/).

Chapter 4

Temperature-dependent heterosis for photosynthesis of flint × dent crosses

ABSTRACT

Heterosis occurs when the progeny are able to tolerate environmental stress. Many studies on heterosis in maize have been conducted, but little is known about the dependence of heterosis on temperature. We tested inbred lines, which differed in their response to temperature, to obtain hybrids, which adapt to a wide range of temperature. A complete diallel cross of four European inbred lines, two flint and two dent, was grown under chilling stress, optimum temperature and heat stress until the three-leaf stage (V3). Contrary to our assumptions, only one flint and one dent line were chilling tolerant. Heterosis was greatest at the temperature extremes for photosynthesis-related traits (carbon exchange rate, quantum efficiency of photosystem II, leaf greenness, and maximal quantum efficiency of photosystem II of a dark-adapted leaf) and at optimal temperature for leaf area and shoot dry weight. Some of the hybrids were similar in their expression of heterosis in the different temperature treatments. Heterosis of flint × dent hybrids is explained, in part, by adaptation of the photosynthesis and growth of seedlings to a greater range of temperature.

INTRODUCTION

Heterosis is typically reflected in an increase of yield of the offspring of cross-pollinated plants. In northern and central Europe, the typical maize hybrid is a combination of European flint lines and US dent lines. While northern flints have well adapted to the climatic conditions of central Europe, Corn Belt dents were introduced to central Europe only about 60 years ago. Flint inbred lines contribute chilling tolerance alleles, while dent inbred lines are a source of alleles for potential high yield under close-to-optimal growth conditions (MORENOGONZALEZ *et al.* 1997; SCHNELL 1992). These two gene pools reflect the proven positive correlation between a large genetic distance between the parental lines and the performance of the resulting hybrid (BARBOSA *et al.* 2003; LIU *et al.* 2002a). Heterosis is referred to as mid-parent heterosis (MPH) or better-parent heterosis (BPH). MPH is how the hybrid differs from the mean of both parental lines and BPH is how the hybrid differs from the better parental line.

Heterosis is assumed to be caused by: i) a 'dominance' effect as a result of complementing genes where the most beneficial allele is partially or totally dominant, ii) an 'overdominance' effect, where the heterozygous offspring is better than both of its parents due to overly dominant controlling loci (BIRCHLER *et al.* 2003), and iii) 'epistatic' effects based on allelic interactions. There is little information about the dependence of heterosis on environmental conditions such as temperature. A temperature-dependent pattern of heterosis (MCWILLIAM and GRIFFING 1965) has been explained by enzymatic polymorphism (SCHWARTZ and LAUGHNER 1969) and/or an intergenomic interaction (SRIVASTAVA 2004). Based on these theories, heterosis is the result of greater metabolic diversity, due to which hybrids adapt to a wide range of environmental conditions; accordingly predict that hybrids would outperform their parental inbreds under adverse temperature conditions (LANGRIDGE 1962; MCWILLIAM and GRIFFING 1965). To achieve adaptation to a wide range of temperatures, a combination of alleles, conferring tolerance to heat and cold at multiple heterozygous loci, are necessary.

Our goal was to study the temperature dependence of heterosis at the seedling stage of maize and to determine whether the performance of the hybrid can be predicted form the performance of the inbred lines. The hypothesis was that inbred lines, which respond differently to temperature, result in hybrids that are adapted to a wider range of temperature. We tested i) temperature-dependent combining ability as the basis of adaptation of hybrids to

a wide range of temperature and ii) mid-parent heterosis (MPH) and better-parent heterosis (BPH) as predictors of hybrid performance based on the performance of the inbred lines.

MATERIAL AND METHODS

The study was based on a set of four European maize inbred lines from the breeding program of the University of Hohenheim, Germany.

Table 4.1 Origin of the material: inbred lines and hybrids are accordingly allocated to the intra-pool or inter-pool family.

Name	Type	Pool	Name	Pool
UH002	IL	Flint	**UH002×UH250**	Inter-pool family
UH005	IL	Flint	UH250×UH002	
UH250	IL	Dent	**UH002×UH301**	Inter-pool family
UH301	IL	Dent	UH301×UH002	
UH002×UH005	Intra-pool Flint		**UH005×UH250**	Inter-pool family
UH005×UH002			UH250×UH005	
UH250×UH301	Intra-pool Dent		**UH005×UH301**	Inter-pool family
UH301×UH250			UH301×UH005	

Seeds were imbibed overnight at room temperature, surface-sterilized with 2.5% sodiumhypoclorite (NaOCl (aq)) for 10 min and rinsed thoroughly with distilled water. Seedlings were grown in growth columns (25 cm high, 7 cm in diameter) filled with a 1:1 (v/v) mixture of fine peat and soil (Ricoter, Schweizer Recycling Erden, Aarberg, Switzerland) in a growth chamber (PGW36, Conviron, Winnipeg, Canada).

The photoperiod was 12 h at PPFD 400 µmol m^{-2} s^{-1} and a relative humidity of 40/50% (day/night). To establish the seedlings, an optimal temperature was maintained (26/24°C) until the third leaf tip emerged. Afterwards seedlings were divided among different growth chambers and tested under chilling stress (16/14°C day/night), optimal conditions (26°C/24°C) and mild heat stress (38/34°C). Plants were watered regularly and, after emergence, the seedlings were irrigated with a nutrient solution (0.23% of Wuxal® (Aglukon Spezialdünger GmbH, Düsseldorf, Germany): 100 g N, 100 g P2O5, 75 g K2O, 190 mg Fe, 162 mg Mn, 102 mg B, 81 mg Cu, 61 mg Zn, 10 mg Mo/liter).

Physiological and morphological measurements:

Measurements were conducted at the V3 stage in each treatment, indicated by a fully visible collar of the third leaf. Leaf greenness (SPAD) was measured in the middle of each third leaf with a SPAD meter (SPAD 502, Minolta Corporation, Ramsey, NJ, USA) and is the average of three data points. The same leaf was exposed to full radiation at least 20 min before CER and Φ_{PSII} were measured by a portable, open-flow gas-exchange system (LI-6400, LI-COR) equipped with a 6400-40 leaf chamber fluorometer (LI-COR). The flow rate of air through the chamber and the sample side IRGA was 300 mol s^{-1} at ambient CO_2. To avoid strong fluctuations, the intake air was taken from a buffer volume. Light and temperature in the measuring chamber were the same as in the growth chamber. The rate of carbon exchange (CER) and the fluorescence in the light (F') were recorded when the total coefficient of variation (ΔCO_2 + ΔH_2O+ Δflow) was just below 0.2. A 0.8-second saturation flash (>8.000 µmol quanta m^{-2} s^{-1}) was then applied to determine the maximum fluorescence in the light-adapted state (F_m'). The actinic light was turned off, and the leaf was illuminated with far red light for 3 s to determine the ground fluorescence of light-adapted leaves (F_o'). The chlorophyll fluorescence parameters were calculated according to ROSENQVIST and VAN KOOTEN (2003). The operating quantum efficiency of photosystem II (Φ_{PSII}) was calculated as (F_m'-F')/F_m' (GENTY *et al.* 1989).

The maximum quantum efficiency of photosystem II of a dark-adapted leaf (F_v/F_m) was measured with a PAM-2000 fluorometer (Walz, Effeltrich, Germany) equipped with a leaf clip holder (20030-B). The ground fluorescence of the dark-adapted leaves (F_o) was measured after 30 min in the dark at a light frequency of 600 Hz. The maximum fluorescence yield (F_m) was recorded during a 0.8-second saturation flash (>8.000 µmol quanta m^{-2} s^{-1}) at 20 KHz. The maximum quantum efficiency of PSII primary photochemistry (F_v/F_m) was calculated as (F_m-F_o)/F_m.

Leaves were cut at the coleoptilar node and the leaf area was measured with a portable area meter (LI-3000A, LICOR, Inc., Lincoln, NE, USA). The shoot material was dried at 55°C to constant weight and the weight of the dry matter was determined.

Experimental design and statistics:

The experimental design was a split-plot randomized complete-block design with six biological replications, i.e. three growth chamber replications per temperature treatment (t_k)

and two sets of inbreds (genotypes) (g_i). Therefore, the final model for genotype estimates by ASReml-R (BUTLER 2006) was:

$$Y_{ikr} = t_k + g_i + (gt)_{ik} + b_r + e_{ikr},$$

where t_k is the effect of the kth treatment, g_i the effect of the ith genotype, $(gt)_{ik}$ the interaction between the ith genotype, and the kth treatment, b_r the rth replication, and e_{ikr} the residual error.

Hybrid combinations were assigned as intra-pool or inter-pool hybrid families (Table 4.1). Mid-parent heterosis (MPH) was calculated as the percentage of the parental mean of a certain trait and better-parent heterosis (BPH) as the percentage of the better parent. Individual effects of the F1 progeny were estimated by the reciprocal effects model of (GRIFFING 1956), excluding the crosses within inbreds. Analysis of variance for hybrid effects and effects of hybrid-by-treatment interactions was made with the final model

$$Y_{ijkr} = y + t_k + g_i + g_j + s_{ij} + r_{ij} + (gt)_{ik} + (gt)_{jk} + (st)_{ijk} + (rt)_{ijk} + b_r + (bt)_{rk} + e_{ijkr},$$

where t_k is the effect of the kth treatment, g_i and g_j the combining abilities (GCAs) of the ith and the jth parents, $sij = sji$ the specific combining ability (SCA) of the $i \times j$ crosses, r_{ij} the composite estimate of the extranuclear effects, (where $r_{ij} = -r_{ji}$), $(gt)_{ik}$ and $(gt)_{jk}$ the interactions of the GCAs with the kth treatment, $(st)_{ijk}$ the interaction of the SCA with the kth treatment, $(rt)_{ijk}$ the interaction of the extranuclear effects with the kth treatment, b_r the effect of the rth replication, and e_{ijkr} the residual error. All treatment factors were set as fixed except factors *b*, *bt*, and *e*.

If pure dominance is assumed to explain heterosis, then two hypothetical scenarios for combining contrasting genotypes would lead to the adaptation of the resulting hybrids to a wide range of temperatures: a) the “varying range” scenario and b) the “optimum shift” scenario (Figure 4.1). Accordingly, temperature-dependent heterosis can be explained by two sets of hypothetical genotypes: a) inbred parents, which perform best at the same optimum temperature, but the trait values differ, and which adapt to a different range of temperatures and b) inbred parents, adapted to the same range of temperature with the same values for traits but for which the optimum temperature is different. The resulting hypothetical hybrids (Figure 4.1 a/b, solid line) would always perform well at all temperatures. Temperature-dependent mid-parent heterosis would be highest at the two temperature extremes (Figure

4.1 c/d). Combining inbred lines, which have different responses to temperature, might explain the effects of heterosis: for example, combining the inbred line P1, which, on average, performs well under chilling and heat stress, with the inbred line P2, which performs well at optimal temperature (Figure 4.1 e). The hybrid would, on average, perform well at all temperatures and would be most strongly influenced by the better parent in each temperature regime. Two inbred lines, one performing best at one temperature extreme and the other one performing best at the opposite temperature extreme (Figure 4.1 f), would result in a hybrid, which, on average, performs well at both extremes, assuming that the better parent exerts the greatest influence at the respective temperature extreme.

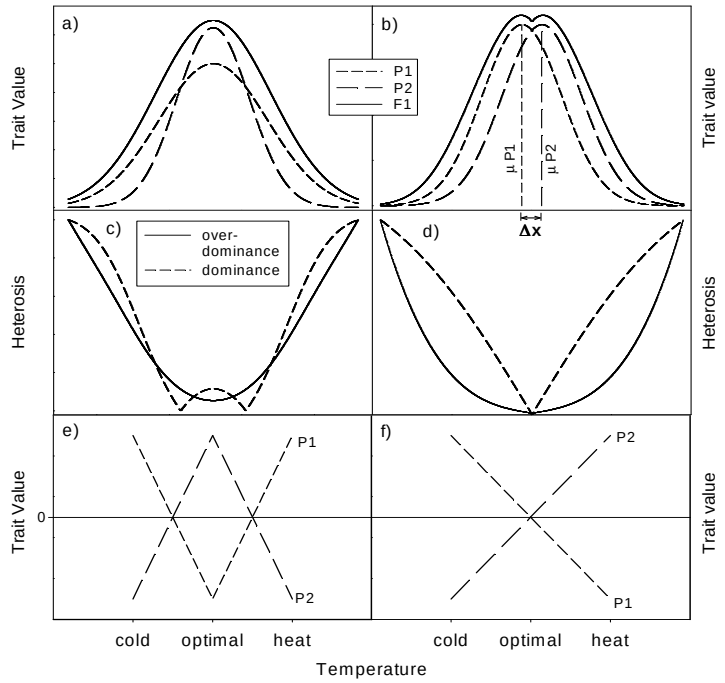

Figure 4.1 Diagram of performance profiles of hypothetical genotypes (P1 and P2) and their F1 hybrid as dependent on growth temperature. It was assumed that the trait value Y decreases symmetrically as the temperatures deviate from the optimum (μ): $Y = Y_{max} \cdot e^{\frac{-(x-\mu)^2}{\sigma}}$, where x is the temperature, Y_{max} the trait value at optimum temperature and σ the operating temperature range. Two cases were considered: a) both inbred lines show the same μ but different σ and $Y_{max,}$ and b) both inbred lines show the same σ and Y_{max} but differ in μ by Δx. Solid lines represent overdominance, where the hybrid exceeds the trait values of the better parent. Temperature-dependent mid-parent heterosis for a) and b) are displayed in figures c) and d), respectively. Values are normalized to fit both cases, i.e. dominance and overdominance, on the same scale. Figure e and f illustrate the deviation of the parents from their parental mean within each of the three extreme environments.

RESULTS

The inbred lines differ at extreme and optimum temperature - UH002 and UH301 were both chilling tolerant:

Both temperature extremes had significant effects on the growth of seedlings (Table 4.2). Effects of genotype-by-treatment interactions were significant for all traits (Table 4.2, ANOVA), indicating that the performance of the inbreds was temperature-dependent.
In general, plants developed light green leaves (SPAD) and had a lower rate of photosynthesis (CER, Φ_{PSII}, F_v/F_m). The effect of chilling was strongest for the carbon exchange rate (CER), which decreased by 43%. These plants had a smaller leaf area and lower dry weight than plants grown at optimum temperature. Heat stress decreased the leaf area and DW_{St} to a much greater extent than chilling stress (Table 4.2), reducing leaf area by 61% compared to optimum conditions. Lines generally performed best at optimum temperature. The flint line UH002 performed best under chilling stress followed by the dent line UH301, while UH250 and UH005 tended to be sensitive to chilling. However, UH005 developed bigger leaves and thus accumulated more dry weight under optimum temperature and showed a good rate of photosynthesis under heat stress. Thus, UH005 was the most vigorous line under more favorable conditions. As well as good performance under chilling stress, UH301 had the highest rate of photosynthesis (CER, Φ_{PSII}) at optimum temperature and the most vigorous growth (leaf area, DW_{St}) under heat stress. UH250 generally performed poorly. Note that the germination of UH250 was usually very slow, which might have influenced its overall performance. UH002 and UH301, with a high CER under chilling stress, showed a relative decrease in CER compared to the mean value of the inbred lines with increasing temperature. The opposite was the case for UH005 and UH250. UH005 produced greener leaves with increasing temperature compared to the mean of the inbreds (Table 4.2). However, this pattern was not found for the other traits. The trait values for the inbred lines decreased or increased from the optimum temperature to the temperature extremes (Table 4.2). Relative differences for Φ_{PSII} and F_v/F_m of the inbreds were found at the temperature extremes and for LA and DW_{St} at optimum temperature.

Table 4.2 Adjusted mean values of UH inbreds as dependent on temperature for carbon exchange rate (CER), quantum efficiency of PSII (Φ_{PSII}), leaf greenness (SPAD), maximum quantum efficiency of PSII (F_v/F_m), leaf area (LA), and dry weight of the shoot (DW_{St}). Wald statistics for effects of genotype (G), effects of temperature (T) and effects of genotype-by-treatment interactions (G×T).

		CER	**Φ_{PSII}**	**SPAD**	**F_v/F_m**	**LA**	**DW_{St}**
		μmol m^{-2} s^{-1}				cm^2	g
Adjusted means							
	16°C/14°C	8.47	0.36	29.3	0.741	80.4	0.225
	26°C/24°C	14.7	0.563	43.4	0.774	111.6	0.276
	38°C/34°C	11.1	0.517	37.3	0.731	43.9	0.123
IL performance							
16°C/14°C	UH002	12.7	0.434	33.1	0.738	103.8	0.275
	UH005	6.0	0.369	28.7	0.741	76.8	0.198
	UH250	3.83	0.21	23.9	0.723	55.5	0.159
	UH301	11.4	0.428	31.7	0.761	85.3	0.267
26°C/24°C	UH002	16.1	0.573	49.3	0.777	136.9	0.323
	UH005	13.2	0.549	44.7	0.768	146.2	0.358
	UH250	12.9	0.553	41.0	0.774	55.8	0.131
	UH301	16.8	0.576	38.7	0.779	107.6	0.29
38°C/34°C	UH002	10.3	0.515	40.1	0.739	50.3	0.138
	UH005	13.9	0.566	42.9	0.759	47.5	0.115
	UH250	9.17	0.446	29.1	0.676	24.7	0.066
	UH301	10.8	0.539	37.2	0.751	53.2	0.173
LSD		2.25	0.027	4.38	0.016	39.3	0.096
ANOVA							
	G	***	***	***	*	***	***
	T	***	***	***	***	***	***
	G×T	***	***	**	***	*	**

*, **, ***; indicate significance level of $P \leq 0.05$, ≤ 0.01, ≤ 0.001, respectively.
LSD: Fisher's least significant differences ($P \leq 0.05$).

Performance of the hybrids:

In general, hybrids performed better than the inbreds with regard to all the measured traits (adjusted means: Tables 4.2 and 4.3). The performance of the hybrid families differed at all temperatures. Under chilling stress the UH002xUH301 family performed best (Table 4.3), as did their parental lines, while intra-pool flint hybrids did not perform as well as their parental lines (Table 4.2). The remaining families were somewhere in between. On average, hybrid performance was best at optimum temperature. The rates of photosynthesis (CER, Φ_{PSII}) and

growth (LA and DW_{St}) of the hybrid family UH005×UH301 were highest at optimal temperature (Table 4.3), the same as for their parental lines (Table 4.2). Under heat stress hybrid families with UH005 and UH301 inbreds performed best. The hybrid family UH002×UH301 developed greener leaves, had more leaf area and higher dry weight, while UH005×UH250 maintained a good rate of photosynthesis (CER and Φ_{PSII}). The CER and Φ_{PSII} of the families differed at the temperature extremes, whereas differences for leaf greenness were found only at optimum temperature (Figure 4.2). For SPAD, all the families followed the same pattern (Figure 4.1 e); chlorophyll content increased or decreased from optimum to extreme temperature. Thus, major differences were observed at optimum temperature, e.g. the SPAD of UH002×UH301 increased towards both extremes relative to the mean of the families. The CER and Φ_{PSII} of some families followed the pattern illustrated in Figure 4.1 f, with the largest differences found at the extremes. All the UH002 families had lower values with increasing temperature and performed better under chilling stress.

Specific combinations of inbreds confer tolerance to chilling or heat stress:

The breeding value of the inbreds differed with regard to GCA when the values for all the hybrids were averaged for each treatment. Thus, it is possible to predict the performance of a hybrid, when a certain inbred line is chosen for all possible combinations with other lines (Table 4.3). The effect of GCA did not usually depend on temperature, indicating that none of the inbred lines is a good combiner for conferring tolerance to heat or chilling stress. Effects of SCA were significant for leaf area and dry weight. More importantly, effects of treatment-by-SCA interactions were significant for all traits except CER, meaning that specific combinations of inbred lines confer chilling or heat tolerance. Extranuclear effects were significant for the morphological traits, indicating that the choice of inbred line as the male or female parent influences performance of the hybrid. This might be due to differences in the reserves in the seed at this early stage.

Table 4.3 Adjusted mean values of hybrid families as dependent on temperature for carbon exchange rate (CER), quantum efficiency of PSII (Φ_{PSII}), leaf greenness (SPAD), maximum quantum efficiency of PSII (F_v/F_m), leaf area (LA), and dry weight of the shoot (DW_{St}). Wald statistics for a diallel mating design for inbreds including reciprocal crosses but not crosses within lines, for effects of temperature (T), general combining ability (GCA), specific combining ability (SCA), extranuclear effects and their effects of treatment interactions.

		CER	**Φ_{PSII}**	**SPAD**	**F_v/F_m**	**LA**	**DW_{St}**
Adjusted means		µmol m^{-2} s^{-1}				cm^2	g
	16°C/14°C	12.4	0.465	34.6	0.765	141.1	0.389
	26°C/24°C	17.1	0.586	45.9	0.788	241.9	0.59
	38°C/34°C	13.5	0.561	40.6	0.763	83.5	0.263
Hybrid performance							
	Intra-pool flint	10.0	0.434	33.5	0.755	126.3	0.33
	UH002×UH250	12.3	0.470	34.2	0.76	140.7	0.384
16°C/14°C	UH002×UH301	13.6	0.486	37.7	0.763	126.6	0.387
	UH005×UH250	12.1	0.451	33.1	0.761	158.2	0.408
	UH005×UH301	13.2	0.466	34.6	0.776	142.2	0.412
	Intra-pool dent	13.2	0.481	34.4	0.774	152.8	0.413
	Intra-pool flint	17.0	0.585	49.2	0.794	227.4	0.52
	UH002×UH250	16.5	0.586	47.2	0.784	260.7	0.558
26°C/24°C	UH002×UH301	16.9	0.581	45.6	0.784	211.3	0.536
	UH005×UH250	17.3	0.585	42.2	0.789	235.5	0.623
	UH005×UH301	17.6	0.591	45.4	0.791	262.9	0.666
	Intra-pool dent	17.3	0.591	45.8	0.787	253.3	0.636
	Intra-pool flint	11.8	0.546	40.6	0.771	77.6	0.204
	UH002×UH250	12.4	0.554	38.4	0.756	90.6	0.263
38°C/34°C	UH002×UH301	13.0	0.545	43.2	0.757	91.9	0.321
	UH005×UH250	15.3	0.59	39.6	0.767	83.7	0.255
	UH005×UH301	13.9	0.555	42.4	0.772	85.7	0.289
	Intra-pool dent	14.7	0.575	39.2	0.757	71.7	0.247
	LSD	2.25	0.033	3.91	0.023	92.7	0.209
ANOVA							
	T	***	***	***	**	***	***
	GCA	**	***	***	***	*	***
	SCA	NS	NS	NS	NS	*	**
	extranuclear effects	NS	NS	*	NS	***	***
	T×GCA	NS	NS	*	NS	*	NS
	T×SCA	NS	***	***	***	**	***
	T×extranuclear effects	NS	NS	*	NS	NS	NS

*, **, ***; NS indicate significance level of $P \leq 0.05$, ≤0.01, ≤0.001 and not significant, respectively.
LSD: Fisher's least significant differences ($P \leq 0.05$).

MPH and BPH were positive for growth at optimum temperature and positive for photosynthesis at the extreme temperatures:

The mid-parent and better-parent regression to the mean values of the genotypes was not significant (Table 4.4), except for F_v/F_m and leaf area. Thus, the performance of the hybrid cannot usually be predicted from the performance of the parents. For F_v/F_m, it was possible to predict the performance of the hybrids under chilling and heat stress from the performance of the better parent. Mid-parent heterosis (MPH) was positive for all the measured traits, with the exception of SPAD, where MPH was negative for UH005×UH250 at optimum temperature and for the intra-pool flint under heat stress. The most positive effect of MPH was found for leaf area and DW_{St} at optimum temperature (Figure 4.3). MPH was most positive for Φ_{PSII} and SPAD under chilling stress and for F_v/F_m under heat stress. The intra-pool dent hybrids and UH005×UH250 and UH002×UH250 had the highest values for these traits, which matched the pattern of temperature-dependent mid-parent heterosis with highest values at the extreme temperatures (Figure 4.1 c/d). Better-parent heterosis (BPH) usually had a positive effect but was slightly negative for CER, Φ_{PSII} and SPAD in hybrid combinations, in which one of the parental lines already had high values for these traits under certain conditions. For leaf area and DW_{St}, heterosis was most pronounced at optimum temperature, where the effects of heterosis were significant for the intra-pool dent family. Φ_{PSII}, SPAD and F_v/F_m of the UH005×UH250 hybrids were superior under chilling stress, and heterosis had the most positive effects on growth-related traits at the temperature extremes.

Table 4.4 Mid-parent- and better-parent regressions (r^2) on genotypic mean values of the resulting hybrids. See Table 4.2 for abbreviations of traits.

		CER	Φ_{PSII}	SPAD	F_v/F_m	LA	DW_{St}
MP							
	16°C/14°C	0.03^{NS}	0^{NS}	0.29^{NS}	0.27^{NS}	0.38*	0.03^{NS}
	26°C/24°C	0.01^{NS}	0.03^{NS}	0.27^{NS}	0.4*	0.07^{NS}	0.31^{NS}
	38°C/34°C	0^{NS}	0.15^{NS}	0.16^{NS}	0.31^{NS}	0.02^{NS}	0.09^{NS}
BP							
	16°C/14°C	0^{NS}	0.07^{NS}	0.13^{NS}	0.53**	0.3^{NS}	0.02^{NS}
	26°C/24°C	0^{NS}	0.01^{NS}	0.19^{NS}	0.02^{NS}	0.02^{NS}	0^{NS}
	38°C/34°C	0.03^{NS}	0.03^{NS}	0.03^{NS}	0.54**	0^{NS}	0.13^{NS}

*, **, ***; NS indicate significance level of $P \leq 0.05$, ≤ 0.01, ≤ 0.001 and not significant, respectively.

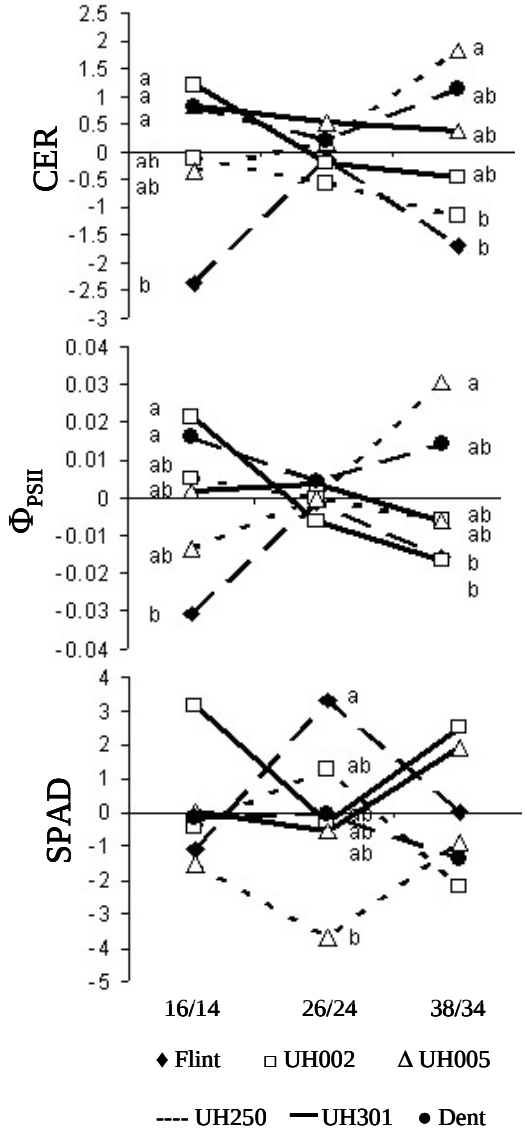

Figure 4.2 Performance of the hybrid family relative to the adjusted families mean for quantum efficiency of PSII (Φ_{PSII}), carbon exchange rate (CER), and leaf greenness (SPAD). Inter-pool hybrid families are represented by a symbol (square, triangle) and a line (dashed, solid); each intra-pool hybrid is represented by a specific symbol. Inbreds with the same letter within temperatures are not significantly different ($P \leq 0.05$) and genotypes within treatments without letters are not significantly different. Each point represents 12 replications.

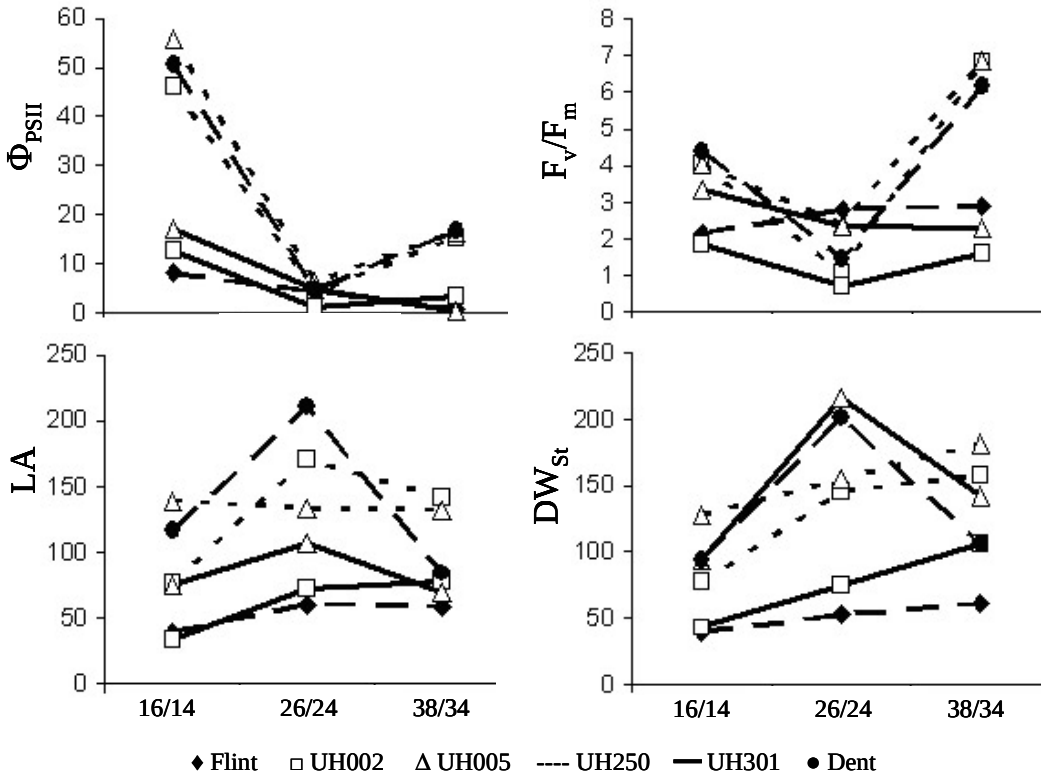

Figure 4.3 Mid-parent heterosis for quantum efficiency of PSII (Φ_{PSII}), F_v/F_m, leaf area (LA), and dry weight of the shoot (DW_{St}). Inter-pool hybrid families are represented by a symbol (square, triangle) and a line (dashed, solid); each intra-pool hybrid is represented by a specific symbol. Each point represents 12 replications.

DISCUSSION

The hypothesis that flint inbreds perform better at low temperatures compared to dent inbreds, as shown for old inbreds of both types (STAMP 1984), was not verified with the small subset in this study; the dent UH301 was quite tolerant to chilling, and the rate of photosynthesis of flint UH005 was exceptionally high under heat stress. However, the leaf area and shoot dry weight of UH005 decreased under heat stress, indicating that different factors determine growth and photosynthesis. Root growth may have been limited by heat stress, because the temperature regime was the same for the shoot- and root zone. This might impair synthesis of cytokinin in the roots, resulting in lower levels of cytokinins in the shoots, which would, thus, limit growth (LIU *et al.* 2002b; UDOMPRASERT *et al.* 1995). The hybrid family UH005×UH301 grew best (leaf area, DW_{St}) at close-to-optimum temperatures (Table 4.3). Extranuclear effects of an inbred line, as the female or male parent, were highly significant only for LA and DW_{St} (Table 4.3).

In the case of UH002×UH301, this may have caused the below-average growth, because UH002 is an unsuitable female parent (personal communication UHOH).

Are the requirements for temperature-dependent heterosis, as based on dominance effects, met?

According to deductions based on the hypothetical genotypes, it should be possible to design hybrids, which are well adapted to a wide range of temperatures, by selecting inbreds, which show a contrasting temperature-dependent performance. Assuming that the resulting hybrid always performs at least as good as the best parent, it would be possible to achieve better adaptation to high and low temperature. The prerequisites for testing this theory were i) inbred-by-treatment interaction for a target trait and ii) significant better-parent offspring regressions or at least a significant temperature-dependent GCA or SCA. While the former prerequisite was met, i.e. the performance of the inbreds depended on temperature, the latter one was not. None of the combinations of inbreds constantly conferred chilling or heat tolerance. The only significant proof of a positive effect of F_v/F_m on a better-parent-to-offspring regression did not reveal relevant differences in the performance of the hybrid families at the extreme temperatures. However, the treatment-by-SCA interactions were significant for most traits, indicating that a specific combination of two inbred lines resulted in a temperature-dependent SCA and that one of the two conferred chilling or heat tolerance. The low parent-to-offspring correlation might be due to the inclusion of the intra-pool hybrids. When these hybrids were omitted from the regression analysis, the coefficients of determination (R^2) increased (data not shown); this would justify a separate analysis of the intra-pool and inter-pool crosses. The combination of the chilling tolerant UH301 and the heat tolerant UH005 resulted in a hybrid with above-average performance at the temperature extremes and average or better than average performance at optimum temperature, indicating an overall improvement in performance independent of the temperature. The same was true when the chilling tolerant UH002 was crossed with the generally chilling sensitive UH250.

Positive effects of heterosis on photosynthesis at the extreme temperatures:

The growth parameters of the hybrids were highest at optimum temperature, in contrast to earlier studies, which reported the most positive effects of heterosis on plant growth under temperature stress (MCWILLIAM and GRIFFING 1965). On the other hand, heterosis had the

most positive effects on photosynthesis-related traits at extreme temperature. This confirms a general pattern of the temperature dependence of heterosis (Figure 4.1 c/d), as reported in earlier studies (LANGRIDGE 1962; MCWILLIAM and GRIFFING 1965), where the positive effect of heterosis was much more pronounced in extreme environments (PARSONS 1971). Negative effects of heterosis were found for a few combinations such as UH002xUH301, where the BPH was negative for CER and SPAD at optimum temperature. Since its parental inbreds performed best with regard to SPAD or CER, the physiological limit may have already been reached.

The strongest effects of MPH and BPH were found for photosynthesis (Φ_{PSII}, SPAD) for UH005xUH250 under chilling stress. HOECKER *et al*. (2006) also observed positive MPH effects on the length of the primary root for UH005×UH250 under controlled conditions (26°C). Fast development of the primary root is also favorable under chilling stress and may have contributed to the positive effect on the performance. However, the parental inbreds did not perform well under chilling stress, which may explain why the performance of the hybrids was not much better. A reverse pattern of heterosis has also been described, where low-performance × low-performance combinations showed the strongest effects (MOLL *et al.* 1965).

Is there any proof that the hypothetical scenarios contributed to adaptation of the hybrids to a wider range of temperature?

Advantageous crossing of inbreds might result in hybrids that adapt to a wider range of environmental conditions, thus leading to better physiological and morphological performance under stress conditions as a result of the “optimum shift” or “varying range” scenarios. Since the physiological and morphological traits differed depending on the environmental conditions, under which heterosis occurred, it is assumed that there are a number of reasons for these differences. In the case of CER and Φ_{PSII}, the response of the inbreds to temperature more or less followed the same pattern as the “optimum shift” scenario (Figure 4.1 b), with the optimum temperature for an individual line being shifted towards the high or low temperature extreme. The same pattern was found at an earlier stage for alleles at loci controlling the temperature tolerance of Φ_{PSII} (Chapter 2). In the case of the morphological traits, the response of the inbred lines to temperature tended to follow the

pattern of the “varying range” scenario (Figure 4.1 a), where the flints showed better growth compared to the dents at optimum temperature but both showed similar growth at the temperature extremes. The same pattern was found at an earlier stage for alleles controlling the temperature tolerance of morphological traits (Chapter 2). However, in the latter case, the dents grew better at optimal temperature. This discrepancy is probably due to the small sample size (four inbred lines) in this study. In general, none of the crosses were above average in any of the temperatures treatments. Good performance at one temperature extreme was not matched at the other extreme. Similarly, good performance at optimum temperature often resulted in poor performance at the temperature extremes.

CONCLUSIONS

There are indications that the hypothetical “optimum shift” and “varying range” scenarios contributed to the adaptation of the hybrids to a wider range of temperature and that they are useful in explaining the dependence of heterosis on temperature.

If the goal is to make use of the effect of heterosis, then it is important to know that traits of photosynthesis follow the pattern of “optimum shift” and morphological traits the pattern of “varying range”.

Chapter 5

An algorithm to separate axile and lateral roots of maize based on diameter classes

INTRODUCTION

The axile and lateral root types differ in origin and time of appearance. The axile root system described in here includes the embryo-borne primary and seminal roots and postembryonic underground shoot-borne crown roots (FELDMAN 1994). While the primary root becomes visible two or three days after germination (HOCHHOLDINGER *et al.* 2004b) followed by the seminal roots, the crown roots develop in later stages. Lateral roots of 1st order are initiated approximately four days after germination (HOECKER *et al.* 2006) and emerge from the pericycle of all axile growing roots. Because of their large metaxylem, laterals are considered mainly responsible for water and nutrient uptake (*cf.* HOCHHOLDINGER 2009). HUND *et al.* (2004) demonstrated that the root system of maize can be separated into lateral and axile roots using the root length in diameter-class distribution (RLDD). The results were based on destructive sampling, followed by manual separation of axile and lateral roots. The data suggested that the diameter of both populations of roots, were normally distributed and that the two peaks were clearly distinguishable. This approach, proved also to be feasible to classify roots non-destructively via root system images taken from growth pouches (HUND *et al.* 2009). However, the threshold to distinguish between axile and lateral roots varied dependent on experimental factors. For example, it is well known that root diameter increases at low temperature (CUTFORTH *et al.* 1986; KIEL and STAMP 1992) and, accordingly, temperature-dependent thresholds were necessary to separate into lateral and axile roots (Chapter 3). Furthermore, slight differences in optical properties during the scanning procedure made individual threshold for each independent experiment necessary. Accordingly, we applied thresholds for each temperature-by-run combination. Beside that, there are indications that diameters also depend on the genotype and even on the root type. For example, diameter of the primary roots of the parent of a QTL mapping population (Lo964) was considerably larger as compared to the diameter of the other parent (Lo1016)

(HUND *et al.* 2004). This implies that there is a need to establish individual thresholds for each genotype-by-temperature-by-run combination. Furthermore, there usually appeared additional dips and peaks within the bimodal RLDD profile, which are artifacts generated by the image processing software (HUND *et al.* 2009; ZOBEL *et al.* 2007). These artifacts make it difficult to identify the trough between the two main peaks. Non-parametric kernel density estimation (SILVERMAN 1986) may be used to smooth the RLDD profile and determine the trough with higher accuracy. However, it may be difficult to set the smoothing parameter of these functions in an optimal way to avoid detection of spurious peaks in every case. Alternatively, general optimization for a bimodal distribution may be used to smooth and interpolate the data (NELDER and MEAD 1965). Accordingly, our objectives were to develop a method to determine the threshold of axile and lateral roots for a large number of individual experimental units of a designed experiment using non-parametric or parametric approaches.

MATERIAL AND METHODS

WinRhizo usually delivers the distribution of measured root length, within diameter classes. This so-called root length in diameter-class distribution (RLDD) can be used to extract information about root diameters or the length of different classes of roots. In case of maize seedling, there are at least two root classes distinguishable: the large-diameter axile roots and their first order laterals (HUND *et al.* 2009). The process involves the separation of the RLDD into diameters most likely belonging to the population of axile and lateral roots. For this study a dataset was used, derived from an experiment aiming to determine the response of maize roots to temperature (Chapter 3). A set of 74 inbred lines was grown in growth pouches exposed to three temperature regimes within four independent replications. In the original study a separate threshold for each replication within temperature was applied. The thresholds were determined based on the average RLDD profiles.

Large-diameter axile roots and small-diameter lateral roots are distinguished using a mixture model:

Non-parametric and parametric methods were evaluated to detect the trough between the peak belonging to the axile roots and the one belonging to the lateral roots. A first approach to

detect the position of the trough was to use non-parametric kernel density estimates implemented in the R-function density() (R DEVELOPMENT CORE TEAM 2008). The bandwidth was determined either using the normal reference bandwidth (width = "nrd") according to Silverman 's 'rule of thumb' (SILVERMAN 1986, p 48) or the Sheather-Jones 'direct plug-in' (width = "SJ-dpi") (SHEATHER and JONES 1991) using pilot estimation of derivatives.

A second approach to detect the trough was applied by fitting a Gaussians mixture model of two normal distributions. The model was fitted as described by VENABLES and RIPLEY (2002, pp 436-444) using the Nelder-Mead method implemented in the R-function optim() (R DEVELOPMENT CORE TEAM 2008). The log-likelihood function for the mixture model is

$$L(\pi,\mu_1,\sigma_1,\mu_2,\sigma_2)=\sum_{i=1}^{n}\log\left[\frac{\pi}{\sigma_1}\phi\left(\frac{y_i-\mu_1}{\sigma_1}\right)+\frac{1-\pi}{\sigma_2}\phi\left(\frac{y_i-\mu_2}{\sigma_2}\right)\right] \quad (1)$$

The parameters $\pi,\mu_1,\sigma_1,\mu_2,\mu_2$ were estimated by minimizing $-L$. where μ and σ are the mean and the standard deviation of each normal distribution, respectively, and the subscripts identify the distribution of the lateral roots (1) and axile roots (2). π is the proportion of the overall root length attributed to lateral roots and y_i (i = 1,2, …,n) the diameter classes in mm. The accuracy of the model was assessed using a Q-Q plot. The plot was produced by solving for the quantiles by using the reduced-step Newton method as described by VENABLES and RIPLEY (2002, p 440).

The estimated parameters were used to determine the threshold to separate the RLDD into diameter classes most likely representing lateral roots and those most likely representing axile roots. The threshold diameter was chosen in a way that the same proportion of roots was falsely classified for both root types. The equation was accordingly:

$$TrSD=\mu_1+\frac{(\mu_2-\mu_1)}{1+\frac{\sigma_2}{\sigma_1}} \quad (2)$$

The experimental design within each temperature environment (t_j) was an alpha lattice design (BARRETO *et al.* 1997) with 8 biological replications, i.e. four independent growth chamber replications per environment (r_{jk}) and two blocks (b_{jkl}) per growth chamber, containing a full set of inbred lines (g_i) each. The 74 inbred lines within each block were distributed to eight incomplete blocks (c_{iklm}). These were distributed in four sections within two growth containers. Therefore the final model was:

$$Th_{LatAx\,\mathrm{ijklm}} = \mu + g_i + t_j + gt_{ij} + gtr_{ijk} \mid + b_{jkl} + c_{jklm} + \varepsilon_{ijklm} \quad (3)$$

where $Th_{LatAxijklm}$ is the effect of the *i*th inbred line in the *j*th environment, *k*th growth chamber run, *l*th block and *m*th growth container, ε_{ijklm} the residual error and μ the intercept. The term left and right of the vertical line (|) are considered fixed and random, respectively. Analysis of variance was made by ASReml-R (BUTLER 2006). The best linear unbiased estimates (BLUEs), extracted for each genotype-by-treatment-by-run combination, were used to obtain the estimates of the Th_{LatAx}. In order to get more robust estimates for subsequent analyses, 10% outliners based on standardized residuals were removed from the analysis. These missing data were subsequently re-estimated based on the fitted model.

RESULTS

In the original dataset the thresholds were chosen manually for each replication within each treatment. This resulted in thresholds of 0.63, 0.63, 0.63 and 0.63 for the chilling, 0.46, 0.63, 0.63 and 0.46 for the optimum and 0.63, 0.63, 0.39 and 0.51 for the heat treatment and averaged at 0.57. Genotype-specific troughs were not taken into account. However, the median diameters determined from the RLDDs of the peaks of axile and lateral roots, where highly heritable and showed differences among heterotic groups (Chapter 3) indicating that genotype-specific thresholds would be appropriate.

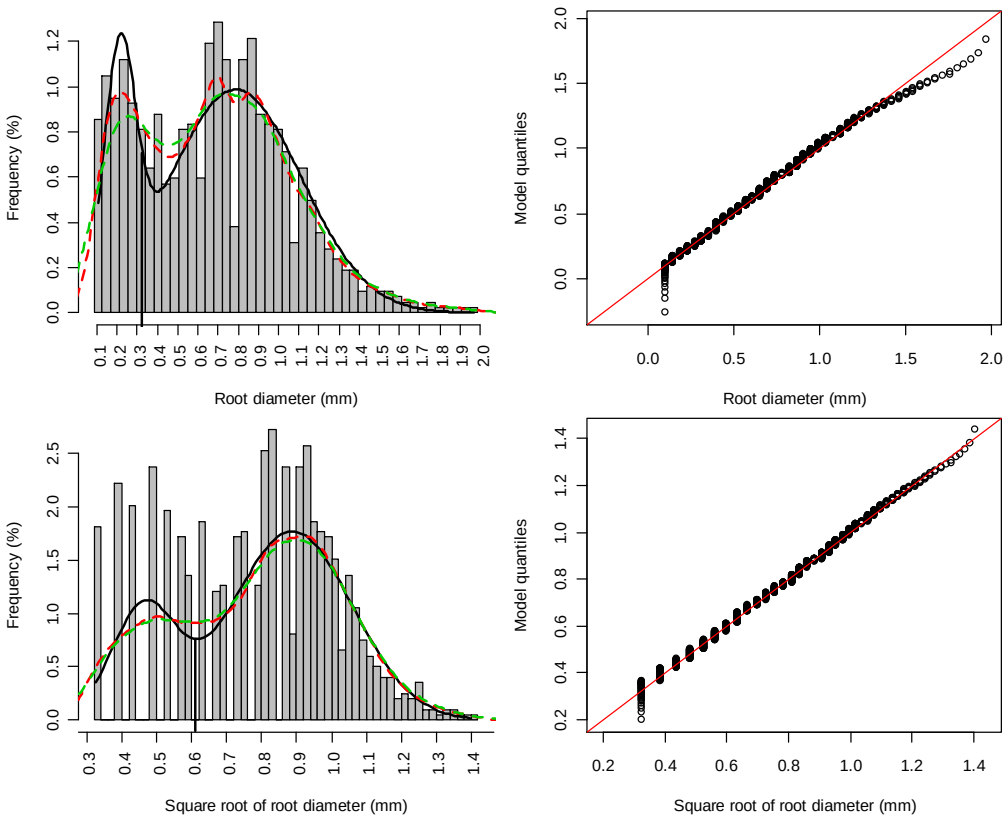

Figure 5.1 Histogram of the root length in diameter-class distribution (RLDD) untransformed (top) or square root transformed (bottom) of the average of the control treatment plants (left). Superimposed on the histograms are i) a mixture model of two normal components (solid black), and ii) kernel estimates estimated with a kernel function and normal bandwidth (dashed, green), and the Sheather-Jones 'direct plug-in' (dotted, red). Q-Q plots of observed diameter, measured by WinRhizo against quantiles of the mixture model (right). Quantiles were solved using a reduced-step Newton method as described by VENABLES and RIPLEY. (2002, p 440). Vertical black line indicates the determined threshold value to distinguish axile from lateral roots.

When applying the kernel density functions to individual plots (data not shown), many plots yielded multiple dips and peaks making it difficult to automate the detection of the trough. The normal reference bandwidth resulted in a smoothing that was too strong in many cases while the Sheather-Jones 'direct plug-in' did not smooth strong enough to remove the artifacts (e.g. Figure 5.1, dashed lines). The mixture model between two normal distributions, one for the lateral, one for the axile roots (Equation 1), proved a good solution to the problem (Figure 5.1, solid lines). The model was forced to detect two peaks, disregarding additional dips caused by artifacts generated by WinRhizo. When the model was run on the untransformed RLDD (Figure 5.1, top, left), it resulted in a rather low threshold to separate into axile and lateral roots (Th_{LatAx}) of 0.32 for the control treatment plants. Furthermore, the Q-Q plot showed a fat upper tail of the distribution indicating suboptimal model fit

(Figure 5.1, top, right). The square root transformation significantly improved the distribution, resulting in a higher Th_{LatAx} and a Q-Q plot suggesting a normal distribution of the data and a good model fit (Figure 5.1, bottom, right). In the transformed RLDD the Th_{LatAx} fell proximately to the trough between the two peaks while for the untransformed RLDD this threshold was lower (Figure 5.1, left, vertical line). Out of the total of 1700 plots analyzed, the model failed to detect a Th_{LatAx} in the range between 0 and 2 mm for 20 plots. Using equation 3, we tested the effect of the genotype *i,* treatment *j* and run *k* on the determined threshold value between axile and lateral roots. There was a significant interaction between every treatment combination indicating that individual threshold values were necessary (data not shown). The significant run effects were not surprising since we expected random effects related to differences in handling and scanning. Since there were only two observations per genotype-by-treatment-by-run combination, keeping the term in the model resulted in an imprecise model fit. Therefore, the term *gtr* was dropped from the model. To avoid that poor adjustment of the mixture model, which had a strong influence on subsequent analyses we identified 10% of the outliers based on standardized residuals (Figure 5.2). This way, 102 outliers were detected and set as missing. The 102 outliers and the 20 plots, where the model failed to detect a trough in the expected range, were re-estimated by running reduced Equation 3 again. The resulted thresholds fell within a range between 0.2 and 0.8 mm (Figure 5.3). The application of the mixture model to the means of the RLDDs across treatments, revealed a temperature-dependent shift in the modes of the two peaks and in the trough between them. Trough and modes were lowest at optimal temperature and highest at the temperature-extremes (Figure 5.4)

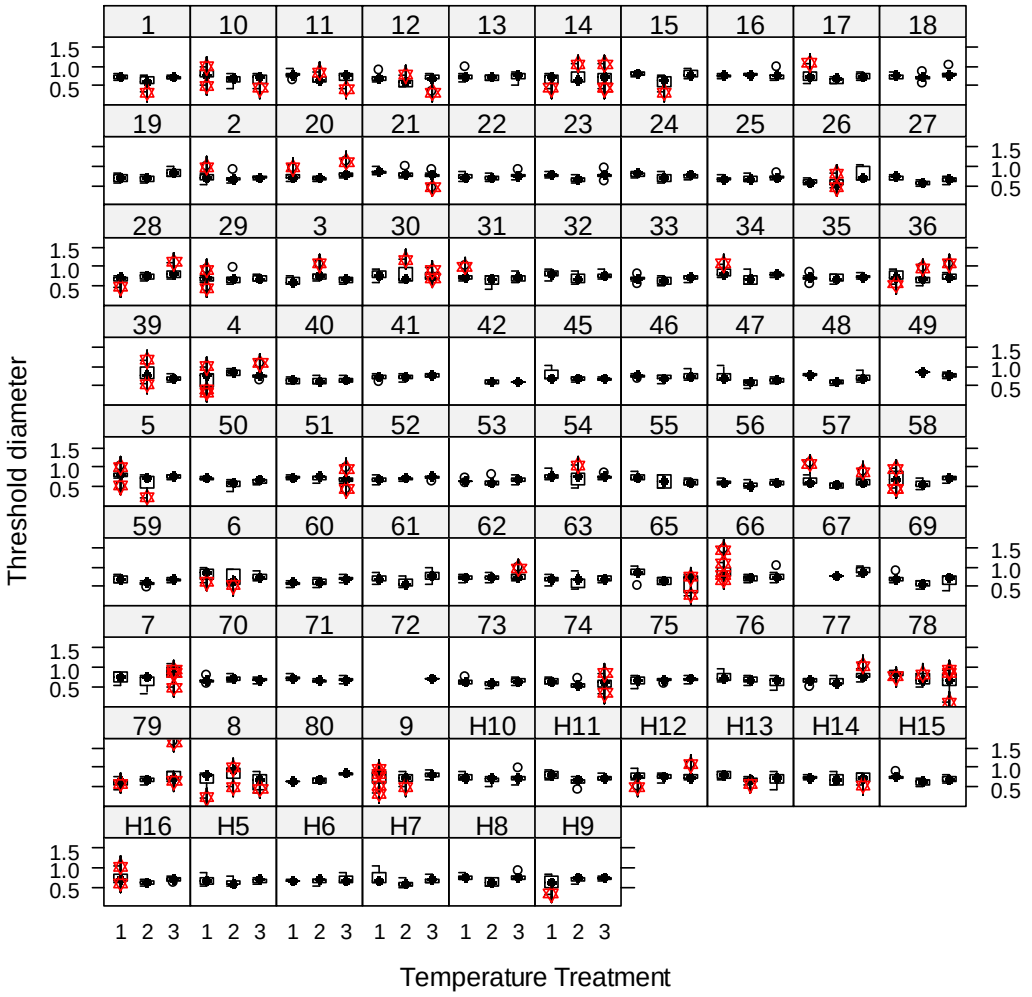

Figure 5.2 Box-Whisker-Plots of the threshold diameters (square root transformed) to separate lateral from axile roots dependent on the temperature treatment (1 = chilling, 2 = optimal, 3 = heat), separated for each genotype. Superimposed stars (red) indicate 10% outliers based on standardized residuals. The quantile function was used to determine the threshold to identify outliers based on standardized residuals.

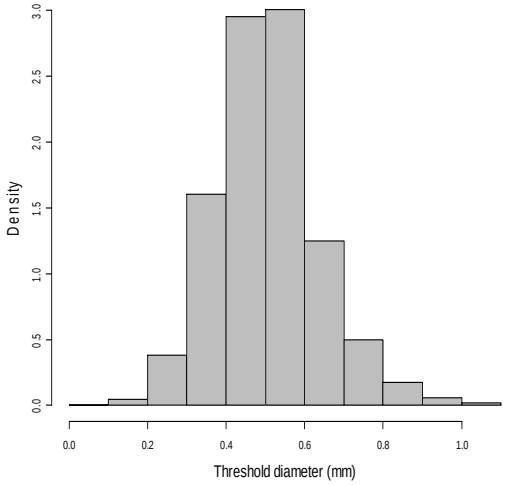

Figure 5.3 Histogram of the thresholds between axile and lateral roots (Equation 3) after re-estimating 10% outliers based on the fitted model of the remaining observations.

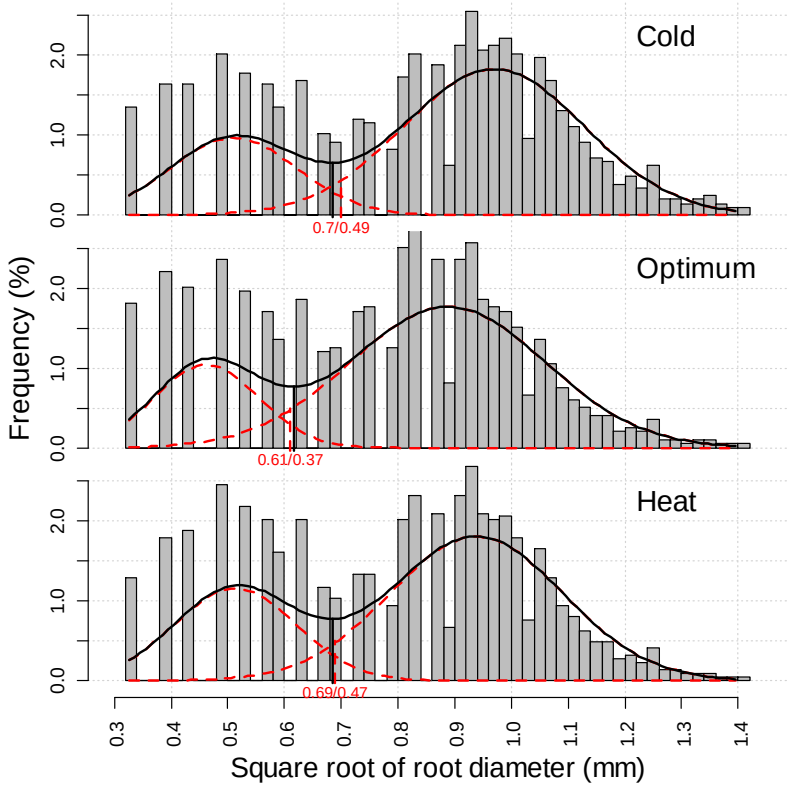

Figure 5.4 Histogram of the square root transformed root length in diameter-class distribution (RLDD) based on mean values within the three temperature treatments. Superimposed on the histograms are i) the mixture model of two normal components (solid black) fitted to the RLDD, and ii) the two underlying normal components (dashed). Vertical lines indicate the threshold values where for both distributions the same proportion of observations was discarded (dashed, red); corresponding values represent the threshold for transformed and untransformed data, respectively.

DISCUSSION

The assessed averaged threshold of 0.57 obtained with the kernel density functions is similar to the threshold of 0.55 obtained in drought stress experiments (RUTA 2008; TRACHSEL 2009a). As the thresholds ranged from 0.39 to 0.63 for the treatment and run combination an even more detailed analysis is suggested. Therefore, as an improvement, each genotype should be taken into account. We therefore aimed for a more flexible approach, extracting the trough between the axile and lateral roots based on genotypes within treatments and runs.

The main problem in determining the trough between the putative peaks of the axile and lateral roots was the presence of additional dips and peaks in the density plot generated by WinRhizo. The dips and peaks were detected at the same place for every environment for each individual last image (Figure 5.4). ZOBEL (2008) examined the nature of the artifacts and summarised that the observed dips occur every 3 to 4 pixel (occasionally two and five) widths along the abscissa (diameter-class distribution). It appeared that an individual bandwidth was necessary making the compromise between smoothing enough to remove the artifacts and not smoothing too much to smear out the real peaks. Automatic bandwidth selection using the "second generation" rules such as Sheather-Jones, seems to be preferable and close-to-optimal (JONES *et al.* 1996). However, in our case the algorithm was too sensitive and the resulting kernel density estimates tended to follow the artificial dips and peaks in the density plot.

The alternative optimization of the mixture model of two normal distributions seemed to be a better solution to determine the threshold between axile and lateral roots. The assumption of a normal distribution of the diameters of each root type is supported by the observation of HUND *et al.* (2004). Normal distribution of diameters was the case, when roots were separated manually and spread on a scanner with minimal amount of overlapping or parallel orientation of roots. However, in growth pouches, where roots remain intact during the scanning process, parallel rooting and crossing can not be ruled out. Therefore, diameters in growth pouches were overestimated due to a certain proportion of roots growing in parallel. This effect may be the cause of the fat upper tail of the density distribution.

Re-estimating the 10% outliers using the fitted model for the remaining values resulted in thresholds lying in the expected range between 0.2 and 0.8 mm. This diameter range is consistent with the range reported to hold the majority of lateral roots of maize (VARNEY *et al.* 1991),

even though we have to note, that the system was not calibrated to measure the true diameter of the roots. Several factors can possibly influence the root diameters. Especially root hairs may cause an effect of enlarged apparent root diameters. This can be avoided by a washing step of the pouch just before image acquisition.

Apart from determining the threshold value to separate between axile and lateral roots, the parameters estimates derived from a mixture model may directly be used as target traits. The diameters and the standard deviations of the two root types may be valuable key traits to determine differences among genotypes and their response to the environment. This approach was used by ZOBEL *et al.* (2007), who employed a non-linear model to determine if root diameters of very fine roots changed dependent on the nutrient concentration based on the derived model parameters.

The more precise the separation of axile and lateral roots is the more accurate following assessments based on that data become. In example temporal root observation for both root types separately are interesting parameters to study in changing environments. These parameters are well suitable for an association mapping approach on roots as we reported in Chapter 3.

Chapter 6

General conclusions

Maize breeding for challenging environments:

Maize cultivation is increasing year by year. As a main cattle forage crop, the production of maize needs to keep up with the increasing demand for meat. Furthermore, the development on the biogas market increases the demand for energy maize. While the cropping area is decreasing due to soil sealing and growth conditions are challenging, yields are expected to rise. Though, the full yield potential of a plant can only be realized at optimal growing conditions. Abiotic stresses like chilling or heat are severely disturbing this optimum. Maize cultivation has been extended to areas in cooler regions where its high temperature requirement is not always fulfilled. Accordingly, breeding for chilling tolerance is the main focus of many breeding programs. Early maize seedling development is usually not affected by heat stress. However, current climate models forecast an average temperature increase and strong temperature fluctuations to cold and heat temperature extremes. Therefore, tolerance to heat stress is becoming increasingly important, too.
Considering the fluctuations as a challenge, breeders aim to adapt crops to a wide range of environmental conditions. However, little efforts have been made so far to study the response of maize to the whole range of possible temperatures. To allow for a better adaptation of plants to fluctuating temperature it is necessary to understand how allele effects vary with temperature regimes.

Chilling and heat stress effects:

This study sheds light on the genetic control of temperature response in temperate maize. The results indicate that heat stress diminished seedlings development less severe than chilling stress. This was mainly expressed for the shoot traits. The high amount of detected association-by-temperature interactions for ER_{Ax} indicates that axile roots seemed to be more temperature sensitive than lateral roots. The numerous collocations to the ratio k_{Lat}/ER_{Ax} indicate that the relative increase at these loci was due to the temperature effect on developing

axile roots. In general, the root elongation traits had a greater power to detect marker-trait associations than the traits describing end lengths, indicated by the higher number of detected associations. This suggests that root elongation over time should not be neglected in future association mapping approaches for temperature tolerance of roots.

Phenotypic and genotypic results corroborated for the observed differences between the heterotic groups. The flints accumulated more root dry weight, maintained the rate of photosynthesis at chilling stress and carried exclusively alleles favoring chilling tolerance for root dry weight and Φ_{PSII}. The dents grew axile roots better under optimum and heat conditions and carried trait increasing alleles for the length of axile root, the root surface area and for heat tolerance of the ratio k_{Lat}/ER_{Ax}. Alleles underlying the observed root traits could mostly be classified as b_x, as they showed similar responses to both temperature extremes. This indicates that changes in temperature away from the optimum initiate general response pathways. In contrast, the shoot parameters mostly followed the a_x pattern, indicating a response to either temperature. Those underlying alleles may be involved in true tolerance to chilling or heat stress.

How are shoot and root growth parameters related? Do they depend on temperature and heterotic group?

The different allele-response pattern of roots and shoots indicate different genetic control of the two organs concerning temperature tolerance. Since neither root nor shoot traits alone are reliable indicators for tolerance strategies, their relatedness has to be identified. The best positive relationships for root dry matter accumulation were found for leaf area and for total shoot dry weight. Most intriguing correlation for Φ_{PSII} to root traits was found for k_{Lat} ($r = 0.3$, 0.52, 0.43; chilling, optimum, heat). This positive relationship between Φ_{PSII} and k_{Lat} suggested that a strong photosynthetic performance is important for early lateral root elongation or *vice versa*. However, only at chilling the flints ($r = 0.46$) deviated from the dents. A weak positive relationship for Φ_{PSII} and root dry weight was only found under heat stress ($r = 0.355$).

All correlations though between shoot and root traits, were moderate to weak and their use as a measure for inferring root development from shoot development is limited. Furthermore, it can't be completely ruled out that population structure played a role. On the genetic level, a selection for SLA could probably go along with ER_{Ax} since closely located associations were

detected in bin 5.03 and 7.02. However, only very low positive correlations were found for this parameter combination, meaning that a high SLA is not necessarily associated with fast axile root elongation.

Was the phenotyping methodology suitable to meet the requirements of an association mapping for root response to temperature?

For this study a genetically diverse germplasm set was chosen. This set is used in breeding programs tackling different breeding questions of major agricultural importance. The phenotyping in growth pouches allowed for a precise application of the desired temperature stress and a high throughput screening of the material as it is required for an association mapping approach. The new insights on temperature-dependent root growth and its genetic control would possibly not have been observed in solid media such as sand or soil. Root elongation rates could be measured non-destructively correcting for differences in root length at the beginning of the stress experiment. This led to a greater precision of the measurements, which was possibly the reason for the greater number of associations detected for the elongation rates. A more flexible and precise approach to separate axile from lateral roots after digital image analysis was developed for future applications. Furthermore, TRACHSEL (2009a) discussed the transferability to more natural growth conditions and reported the pouch system root growth parameters as sufficient indicators for root development at later stages in more natural substrates.

Outlook:

The association-by-temperature interaction model was successful in detecting significant associations. However, in this approach, temperature was modeled as a factor rather than a covariate. Alternatively, temperature could be modeled as an environmental gradient described by a non-linear function (e.g. by a Gaussian distribution). The individual parameters of this function could be used as “traits” themselves. This approach would be similar to the mixture model of two normal distributions to evaluate the threshold between axile and lateral roots (Chapter 5). For example, if the temperature-response curves would satisfy some sort of normal distribution, the parameters could be mean and standard deviation of this function.

Accordingly, the concept of “optimum shift” vs. “varying range” scenarios (Chapter 4) would be testable in a much more precise manner. This approach would not demand for a higher number of replications since the number of replication per temperature could be reduced with increasing the number of different temperature conditions. The wider range of tested temperature conditions would also solve the problem that the sensitivity to temperature stress depends on the target trait (Chapter 2 and 3). In a further step, it needs to be tested if the combination of inbred lines with different temperature optima or ranges leads to a hybrid with a broadened temperature tolerance. This approach was already taken with a limited set of genotypes (Chapter 4) and the results indicate that it is worth up scaling this experiment. Those plants would be able to realize their full yield potential even at changing and challenging environments. Since association mapping bears the risk of discovering false-positives due to unaccounted population structure, the most promising loci should be further confirmed in QTL experiments using biparental crosses. Most promising parental lines for these crosses are those which are divergent at the loci of interest and/or differ in their response to temperature.

References

AL-KHATIB, K., and G. M. PAULSEN, 1999 High-temperature effects on photosynthetic processes in temperate and tropical cereals. Crop Science 39: 119-125.

ALLEN, D. J., and D. R. ORT, 2001 Impacts of chilling temperatures on photosynthesis in warm-climate plants. Trends in Plant Science 6: 36-42.

ANDERSEN, J. R., T. SCHRAG, A. E. MELCHINGER, I. ZEIN and T. LUBBERSTEDT, 2005 Validation of Dwarf8 polymorphisms associated with flowering time in elite European inbred lines of maize (Zea mays L.). Theoretical and Applied Genetics 111: 206-217.

ARCADE, A., A. LABOURDETTE, M. FALQUE, B. MANGIN, F. CHARDON *et al.*, 2004 BioMercator: integrating genetic maps and QTL towards discovery of candidate genes. Bioinformatics 20: 2324-2326.

ASAKURA, Y., T. HAGINO, Y. OHTA, K. AOKI, K. YONEKURA-SAKAKIBARA *et al.*, 2003 Molecular characterization of His-Asp phosphorelay signaling factors in maize leaves: Implications of the signal divergence by cytokinin-inducible response regulators in the cytosol and the nuclei. Plant Molecular Biology 52: 331-341.

BARBER, S. A., A. D. MACKAY, R. O. KUCHENBUCH and P. B. BARRACLOUGH, 1988 Effects of soil-temperature and water on maize root-growth. Plant and Soil 111: 267-269.

BARBOSA, A. M. M., I. O. GERALDI, L. L. BENCHIMOL, A. A. F. GARCIA, C. L. SOUZA *et al.*, 2003 Relationship of intra- and interpopulation tropical maize single cross hybrid performance and genetic distances computed from AFLP and SSR markers. Euphytica 130: 87-99.

BARNABAS, B., K. JAGER and A. FEHER, 2008 The effect of drought and heat stress on reproductive processes in cereals. Plant Cell and Environment 31: 11-38.

BARRETO, H.J., G.O. EDMEADES, S.C. CHAPMAN and J. CROSSA, 1997. The alpha lattice design in plant breeding and agronomy: Generation and analysis. pp. 544-551 *In* G.O. EDMEADES *et al.*, eds. Developing drought and low N-tolerant maize. Proceedings of a symposium, El Batan, Mexico. 25-29 March 1996. CIMMYT, Mexico D.F.

BASSIRIRAD, H., M.M. CALDWELL and K.A. MOTT, 1991 Effect of root cooling on photosynthesis of artemisia tridentata seedlings under different light levels. Botanica Acta 106: 223-227.

BIRCHLER, J. A., D. L. AUGER and N. C. RIDDLE, 2003 In search of the molecular basis of heterosis. Plant Cell 15: 2236-2239.

BROWSE, J., and Z. G. XIN, 2001 Temperature sensing and cold acclimation. Current Opinion in Plant Biology 4: 241-246.

BUTLER, D., 2006 asreml: asreml() fits the linear mixed mode. R package version 2.00.

CAMUS-KULANDAIVELU, L., J. B. VEYRIERAS, D. MADUR, V. COMBES, M. FOURMANN *et al.*, 2006 Maize adaptation to temperate climate: Relationship between population structure and polymorphism in the Dwarf8 gene. Genetics 172: 2449-2463.

CHASSOT, A., 2000 Early growth of roots and shoots of maize as affected by tillage-induced changes in soil physical properties. Diss. ETH No. 13907, Zurich.

CHINNUSAMY, V., J. ZHU and J. K. ZHU, 2007 Cold stress regulation of gene expression in plants. Trends in Plant Science 12: 444-451.

COLLARD, B. C. Y., M. Z. Z. JAHUFER, J. B. BROUWER and E. C. K. PANG, 2005 An introduction to markers, quantitative trait loci (QTL) mapping and marker-assisted selection for crop improvement: The basic concepts. Euphytica 142: 169-196.

COLLINS, R. P., P. J. GREGORY, H. R. ROWSE, A. MORGAN and B. LANCASHIRE, 1987 Improved methods of estimating root length using a photocopier, a light box and a bar code reader. Plant and Soil 103: 277-280.

CUTFORTH, H. W., C. F. SHAYKEWICH and C. M. CHO, 1986 Effect of soil-water and temperature on corn (Zea-Mays-L) root-growth during emergence. Canadian Journal of Soil Science 66: 51-58.

DE OLIVEIRA, D. E., J. SEURINCK, D. INZE, M. VAN MONTAGU and J. BOTTERMAN, 1990 Differential expression of five Arabidopsis genes encoding glycine-rich proteins. Plant Cell 2: 427-436.

DONG, S. F., D. NEILSEN, G. H. NEILSEN and M. WEIS, 2003 A scanner-based root image acquisition technique for measuring roots on a rhizotron window. Hortscience 38: 1385-1388.

DUNCAN, W. G., and J. D. HESKETH, 1968 Net photosynthetic rates relative leaf growth rates and leaf numbers of 22 races of maize grown at 8 temperatures. Crop Science 8: 670-&.

DWYER, L.M., D.W. STEWART and D. BALCHIN, 1987 Rooting characteristics of corn, soybeans and barley as a function of available water and soil physical characteristics. Canadian Journal of Soil Science 68: 121-132.

ENGELS, C., and H. MARSCHNER, 1990 Effect of sub-optimal root zone temperatures at varied nutrient supply and shoot meristem temperature on growth and nutrient concentrations in maize seedlings (*Zea mays* L.). Plant and Soil 126: 215-225.

ENGELS, C., 1994a Effect of root and shoot meristem temperature on shoot to root dry matter partitioning and the internal concentrations of nitrogen and carbohydrates in maize and wheat. Annals of Botany 73: 211-219.

ENGELS, C., 1994b. Nutrient acquisition by plants and its limitations by low temperatures in maize. pp. 503-510 *In* K. DÖRFFLING *et al.*, eds. Crop adaptation to cool climates COST 814 workshop. ECSP-EEC-EAEC. Brussels.

FELDMAN, L., 1994. The maize root. pp. 29-37 *In* M. FREELING *et al.*, eds. The Maize Handbook Springer-Verlag. New York, Inc.

FERNANDES, J., D. J. MORROW, P. CASATI and V. WALBOT, 2008 Distinctive transcriptome responses to adverse environmental conditions in Zea mays L. Plant Biotechnology Journal 6: 782-798.

FLINT-GARCIA, S. A., J. M. THORNSBERRY and E. S. BUCKLER, 2003 Structure of linkage disequilibrium in plants. Annual Review of Plant Biology 54: 357-374.

FOYER, C. H., H. VANACKER, L. D. GOMEZ and J. HARBINSON, 2002 Regulation of photosynthesis and antioxidant metabolism in maize leaves at optimal and chilling temperatures: review. Plant Physiology and Biochemistry 40: 659-668.

FRACHEBOUD, Y., P. HALDIMANN, J. LEIPNER and P. STAMP, 1999 Chlorophyll fluorescence as a selection tool for cold tolerance of photosynthesis in maize (Zea mays L.). Journal of Experimental Botany 50: 1533-1540.

FRACHEBOUD, Y., J-M. RIBAUT, M. VARGAS, R. MESSMER and P. STAMP, 2002 Identification of quantitative trait loci for cold-tolerance of photosynthesis in maize (*Zea mays* L.). Journal of Experimental Botany 53: 1967-1977.

FRACHEBOUD, Y., C. JOMPUK, J-M. RIBAUT, P. STAMP and J. LEIPNER, 2004 Genetic analysis of cold-tolerance of the photosynthesis in maize. Plant Molecular Biology 56: 241-253.

GENDRA, E., A. MORENO, M. M. ALBA and M. PAGES, 2004 Interaction of the plant glycine-rich RNA-binding protein MA16 with a novel nucleolar DEAD box RNA helicase protein from Zea mays. Plant Journal 38: 875-886.

GENTY, B., J. M. BRIANTAIS and N. R. BAKER, 1989 The relationship between the quantum yield of photosynthetic electron-transport and quenching of chlorophyll fluorescence. Biochimica Et Biophysica Acta 990: 87-92.

GILMOUR, AR., BJ. GOGEL, BR. CULLIS and R. THOMPSON, 2006 ASReml user guide release 2.0. VSN International Ltd, Hermel Hempstead.

GODDEMEIER, M. L., D. WULFF and G. FEIX, 1998 Root-specific expression of a Zea mays gene encoding a novel glycine-rich protein, zmGRP3. Plant Molecular Biology 36: 799-802.

GODOY, J. A., J. M. PARDO and J. A. PINTORTORO, 1990 A Tomato Cdna Inducible by Salt Stress and Abscisic-Acid - Nucleotide-Sequence and Expression Pattern. Plant Molecular Biology 15: 695-705.

GONG, Z. Z., C. H. DONG, H. LEE, J. H. ZHU, L. M. XIONG *et al.*, 2005 A DEAD box RNA helicase is essential for mRNA export and important for development and stress responses in Arabidopsis. Plant Cell 17: 256-267.

GOWER, J. C., 1966 Some distance properties of latent root and vector methods used in multivariate analysis. Biometrika 53: 325-&.

GREGORY, P. J., D. J. HUTCHISON, D. B. READ, P. M. JENNESON, W. B. GILBOY *et al.*, 2003 Non-invasive imaging of roots with high resolution X-ray micro-tomography. Plant and Soil 255: 351-359.

GRIFFING, B., 1956 Concept of general and specific combining ability in relation to diallel crossing system. Australian Journal of Biological Sciences 9: 463-493.

GUERRA-PERAZA, O., J. LEIPNER, R. REIMER, H. T. NGUYEN, P STAMP *et al.*, 2010 Temperature at night affects the genetic control of acclimation to cold in maize seedlings. Submitted to Euphytica.

HALLAUER, A. R., 1990 Methods used in developing maize inbreds. Maydica 35: 1-16.

HOCHHOLDINGER, F., W.J. PARK, M. SAUER and K. WOLL, 2004a From weeds to crops: genetic analysis of root development in cereals. Trends in Plant Science 9: 42-48.

HOCHHOLDINGER, F., K. WOLL, M. SAUER and D. DEMBINSKY, 2004b Genetic dissection of root formation in maize (Zea mays) reveals root-type specific developmental programmes. Annals of Botany 93: 359-368.

HOCHHOLDINGER, F., 2009. The maize root system: morphology, anatomy, and genetics. pp. 145-160 *In* Handbook of Maize: Its Biology.

HOECKER, N., B. KELLER, H. P. PIEPHO and F. HOCHHOLDINGER, 2006 Manifestation of heterosis during early maize (Zea mays L.) root development. Theoretical and Applied Genetics 112: 421-429.

HOLLAND, JB, WE NYQUIST and CT CERVANTES-MARTÍNEZ, 2003. Estimating and interpreting heritability for plant breeding: an update. pp. 9-112 *In* JANICK J, ed, Plant Breeding Reviews John Wiley & Sons, Inc.

HOLM, S., 1979 A simple sequentially rejective multiple test procedure. Scandinavian Journal of Statistics 6: 65-70.

HOWARTH, C.J., 2005. Genetic improvements of tolerance to high temperature. pp. 277-300 *In* M. ASHRAF *et al.*, eds. Abiotic stresses. Plant resistance through breeding and molecular approaches.

HUND, A., 2003. Genetic analysis of the response of maize (Zea mays L.) seedlings to long-term mild chilling stress: a morpho-physiological approach. Diss. ETH No. 15181, Zurich.

HUND, A., Y. FRACHBOUD, A. SOLDATI, E FRASCAROLI, S. SALVI *et al.*, 2004 QTL controlling root and shoot traits of maize seedlings under cold stress. Theoretical and Applied Genetics 109: 618-629.

HUND, A., E. FRASCAROLI, J. LEIPNER, C. JOMPUK, P. STAMP *et al.*, 2005 Cold tolerance of the photosynthetic apparatus of maize: pleiotropic relationship between chlorophyll content and specific leaf area. Molecular Breeding 16: 321-331.

HUND, A., W. RICHNER, A. SOLDATI, Y. FRACHEBOUD and P. STAMP, 2007 Root morphology and photosynthetic performance of maize inbred lines at low temperature. European Journal of Agronomy 27: 52-61.

HUND, A., Y. FRACHEBOUD, A. SOLDATI and P. STAMP, 2008 Cold tolerance of maize seedlings as determined by root morphology and photosynthetic traits. European Journal of Agronomy 28: 178-185.

HUND, A., S TRACHSEL and P. STAMP, 2009 Growth of axile and lateral roots of maize: I development of a phenotying platform. Plant and Soil 325: 335-349.

ISHIKAWA, H., and M. I. EVANS, 1995 Specialized zones of development in roots. Plant Physiology 109: 725-727.

JOMPUK, C., Y. FRACHEBOUD, P. STAMP and J. LEIPNER, 2005 Mapping of quantitative trait loci associated with chilling tolerance in maize (Zea mays L.) seedlings grown under field conditions. Journal of Experimental Botany 56: 1153-1163.

JONES, M. C., J. S. MARRON and S. J. SHEATHER, 1996 A brief survey of bandwidth selection for density estimation. Journal of the American Statistical Association 91: 401-407.

KIEL, C., and P. STAMP, 1992 Internal root anatomy of maize seedlings (Zea-Mays L) as influenced by temperature and genotype. Annals of Botany 70: 125-128.

KOCHHAR, S., and V. K. KOCHHAR, 2005 Expression of antioxidant enzymes and heat shock proteins in relation to combined stress of cadmium and heat in Vigna mungo seedlings. Plant Science 168: 921-929.

KRAAKMAN, A. T. W., R. E. NIKS, PMMM VAN DEN BERG, P. STAM and F. A. VAN EEUWIJK, 2004 Linkage disequilibrium mapping of yield and yield stability in modern spring barley cultivars. Genetics 168: 435-446.

LANGRIDGE, J., 1962 Genetic and molecular basis for heterosis in Arabidopsis and Drosophila. American Naturalist 96: 5-&.

LAWRENCE, C. J., T. E. SEIGFRIED and V. BRENDEL, 2005 The maize genetics and genomics database. The Community Resource for Access to Diverse Maize Data. Plant Physiology 138: 55-58.

LEIPNER, J., Y. FRACHEBOUD and P. STAMP, 1997 Acclimation by suboptimal growth temperature diminishes photooxidative damage in maize leaves. Plant Cell and Environment 20: 366-372.

LEIPNER, J., A. STEHLI and A. SOLDATI, 1999 Photosynthetic performance of exotic maize (Zea mays L.) germplasm from tropical highlands at low and high temperature. Journal of Applied Botany 73: 20-24.

LIEDGENS, M., and W. RICHNER, 2001 Minirhizotron observations of the spatial distribution of the maize root system. Agronomy Journal 93: 1097-1104.

LIU, X. C., K. ISHIKI and W. X. WANG, 2002a Identification of AFLP markers favorable to heterosis in hybrid rice. Breeding Science 52: 201-206.

LIU, X. H., B. R. HUANG and G. BANOWETZ, 2002b Cytokinin effects on creeping bentgrass responses to heat stress: I. Shoot and root growth. Crop Science 42: 457-465.
LUNN, J. E., and R. T. FURBANK, 1999 Sucrose biosynthesis in C-4 plants. New Phytologist 143: 221-237.
LYNCH, J., 1995 Root architecture and plant productivity. Plant Physiology 109: 7-13.
MALOOF, J. N., 2003 QTL for plant growth and morphology. Current Opinion in Plant Biology 6: 85-90.
MALOOF, J. N., 2006 Quantitative genetics - Small but not forgotten. Heredity 96: 1-2.
MANSCHADI, A. M., G. L. HAMMER, J. T. CHRISTOPHER and P. DEVOIL, 2008 Genotypic variation in seedling root architectural traits and implications for drought adaptation in wheat (Triticum aestivum L.). Plant and Soil 303: 115-129.
MCCULLY, M. E., and M. J. CANNY, 1988 Pathways and processes of water and nutrient movement in roots. Plant and Soil 111: 159-170.
MCWILLIAM, J.R., and B. GRIFFING, 1965 Temperature-dependent heterosis in maize. Australian Journal of Biological Sciences 18: 569-&.
MIEDEMA, P., 1982 The effects of low temperature on *Zea mays*. Advances in Agronomy 35: 93-128.
MIEDEMA, P., J. POST and P. J. GROOT, 1987 The effects of low temperature on seedling growth of maize genotypes. Verslagen van Landbouwkundige Onderzoekingen (Agricultural Research Reports): 1-124.
MOLL, R. H., LONNQUIS.JH, J. V. FORTUNO and E. C. JOHNSON, 1965 Relationship of heterosis and genetic divergence in maize. Genetics 52: 139-&.
MONK, C., 1966 Ecological importance of root/shoot ratios. Bulletin of the Torrey Botanical Club 93: 402-&.
MOON, B. Y., S. I. HIGASHI, Z. GOMBOS and N. MURATA, 1995 Unsaturation of the membrane-lipids of chloroplasts stabilizes the photosynthetic machinery against low-temperature photoinhibition in transgenic Tobacco plants. Proceedings of the National Academy of Sciences of the United States of America 92: 6219-6223.
MORENOGONZALEZ, J., F. RAMOSGOURCY and E. LOSADA, 1997 Breeding potential of European flint and earliness-selected US corn belt dent maize populations. Crop Science 37: 1475-1481.
MULDOON, D. K., J. L. WHEELER and C. J. PEARSON, 1984 Growth, mineral-composition and digestibility of Maize, Sorghum and Barnyard Millets at different temperatures. Australian Journal of Agricultural Research 35: 367-378.
NAGEL, K. A., B. KASTENHOLZ, S. JAHNKE, D. VAN DUSSCHOTEN, T. AACH *et al.*, 2009 Temperature responses of roots: impact on growth, root system architecture and implications for phenotyping. Functional Plant Biology 36: 947-959.
NELDER, J. A., and R. MEAD, 1965 A simplex method for function minimization. The Computer Journal 7: 308-313.
NIETOSOTELO, J., and T. H. D. HO, 1986 Effect of heat-shock on the metabolism of glutathione in maize roots. Plant Physiology 82: 1031-1035.
PAHLAVANIAN, A. M., and W. K. SILK, 1988 Effect of temperature on spatial and temporal aspects of growth in the primary maize root. Plant Physiology 87: 529-532.
PARSONS, P. A., 1971 Extreme-environment heterosis and genetic loads. Heredity 26: 479-&.
PENG, S. B., J. L. HUANG, J. E. SHEEHY, R. C. LAZA, R. M. VISPERAS *et al.*, 2004 Rice yields decline with higher night temperature from global warming. Proceedings of the National Academy of Sciences of the United States of America 101: 9971-9975.

PIEPHO, H. P., 2000 A mixed-model approach to mapping quantitative trait loci in barley on the basis of multiple environment data. Genetics 156: 2043-2050.

POSPISILOVA, J., and J. RULCOVA, 1999 Can synthetic cytokinins alleviate water stress in Phaseolus vulgaris leaves? Biologia Plantarum (Prague) 42: S77.

PRITCHARD, J.K., M. STEPHENS, N.A. ROSENBERG and P. DONNELLY, 2000 Association mapping in structured populations. American Journal of Human Genetics 67: 170-181.

R DEVELOPMENT CORE TEAM, 2008 R: A language and environment for statistical computing. R Foundation for Statistical Computing, Vienna, Austria.

REIF, J. C., S. HAMRIT, M. HECKENBERGER, W. SCHIPPRACK, H. P. MAURER *et al.*, 2005 Trends in genetic diversity among European maize cultivars and their parental components during the past 50 years. Theoretical and Applied Genetics 111: 838-845.

RENAUT, J., S. LUTTS, L. HOFFMANN and J. F. HAUSMAN, 2004 Responses of poplar to chilling temperatures: Proteomic and physiological aspects. Plant Biology 6: 81-90.

REVILLA, P., A. BUTRON, M. E. CARTEA, R. A. MALVAR and A. ORDAS, 2005. Breeding for cold tolerance. pp. 301-398 *In* M. ASHRAF *et al.*, eds. Abiotic stresses. Plant resistance through breeding and molecular approaches.

RIBAUT, J. M., and D. HOISINGTON, 1998 Marker-assisted selection: new tools and strategies. Trends in Plant Science 3: 236-239.

RICHNER, W., A. SOLDATI and P. STAMP, 1996 Shoot-to-root relations in field-grown maize seedlings. Agronomy Journal 88: 56-61.

ROGERS, J. S., 1972 Measures of genetic similarity and genetic distance. Wheeler, Marshall R. (Ed.). Studies in Genetics, Vol. 7. No. 7213. 354p. Illus. University of Texas: Austin, TX., USA: 145-153.

ROITSCH, T., and M. C. GONZALEZ, 2004 Function and regulation of plant invertases: sweet sensations. Trends in Plant Science 9: 606-613.

ROSENQVIST, E., and O. VAN KOOTEN, 2003. Chlorophyll fluorescence: a general description and nomenclature. pp. 31–77 *In* J.R. DEELL *et al.*, eds. Practical applications of chlorophyll fluorescence in plant biology. Kluwer Academic Publishers. Dordrecht.

RUTA, N., 2008 Quantitative trait loci controlling root and shoot traits of maize under drought stress. Diss. ETH No. 17900

RUTA, N., M. LIEDGENS, Y. FRACHEBOUD, P. STAMP and A. HUND, 2010 QTLs for the elongation of axile and lateral roots of maize in response to low water potential. Theoretical and Applied Genetics 120: 621-631.

SANGUINETI, M. C., M. M. GIULIANI, G. GOVI, R. TUBEROSA and P. LANDI, 1998 Root and shoot traits of maize inbred lines grown in the field and in hydroponic culture and their relationships with root lodging. Maydica 43: 211-216.

SCHAEFFER, M.L., H. SANCHEZ-VILLEDA and E. COE, 2008 Neighbors 2008. Maize Genetics and Genomics Database.

SCHNELL, F.W., 1992. Maiszüchtung und die Züchtungsforschung in der Bundesrepublik Deutschland. pp. 27-44 Vortrag Pflanzenzüchtung.

SCHÖN, C. C., H. F. UTZ, S. GROH, B. TRUBERG, S. OPENSHAW *et al.*, 2004 Quantitative trait locus mapping based on resampling in a vast maize testcross experiment and its relevance to quantitative genetics for complex traits. Genetics 167: 485-498.

SCHRAG, T. A., A. E. MELCHINGER, A. P. SORENSEN and M. FRISCH, 2006 Prediction of single-cross hybrid performance for grain yield and grain dry matter content in maize using AFLP markers associated with QTL. Theoretical and Applied Genetics 113: 1037-1047.

SCHRAG, T. A., J. MÖHRING, A. E. MELCHINGER, B. KUSTERER, B. S. DHILLON *et al.*, 2010 Prediction of hybrid performance in maize using molecular markers and joint analyses of hybrids and parental inbreds. Theoretical and Applied Genetics **120:** 451-461.

SCHWARTZ, D., and W. J. LAUGHNER, 1969 A molecular basis for heterosis. Science 166: 626-&.

SERGEEVA, L. I., J. J. B. KEURENTJES, L. BENTSINK, J. VONK, L. H. W. VAN DER PLAS *et al.*, 2006 Vacuolar invertase regulates elongation of Arabidopsis thaliana roots as revealed by QTL and mutant analysis. Proceedings of the National Academy of Sciences of the United States of America **103:** 2994-2999.

SHARP, R.E., and W.J. DAVIES, 1979 Solute regulation and growth by roots and shoots of water-stressed maize plants. Planta 147: 43-49.

SHAW, R. H., 1988 Climate Requirement. pp. 609-638 *In* Corn and Corn Improvement, Third Edition, G. F SPRAGUE and J. W. DUDLEY (Eds). American Society of Agronomy, Madison, Wisconsin, USA.

SHEATHER, S. J., and M. C. JONES, 1991 A reliable data-based bandwidth selection method for kernel density-estimation. Journal of the Royal Statistical Society Series B-Methodological 53: 683-690.

SILVERMAN, B.W., 1986 Density estimation for statistics and data analysis. Chapman and Hall: London.

SINSAWAT, V., J. LEIPNER, P. STAMP and Y. FRACHEBOUD, 2004 Effect of heat stress on the photosynthetic apparatus in maize (Zea mays L.) grown at control or high temperature. Environmental and Experimental Botany 52: 123-129.

SMIT, A. L., and J. GROENWOLD, 2005 Root characteristics of selected field crops: Data from the Wageningen Rhizolab (1990-2002). Plant and Soil 272: 365-384.

SOWINSKI, P., A. DALBIAK, A. SOWINSKA, Z. KROLIKOWSKI, J. ADAMCZYK *et al.*, 1998 Root architecture and field characteristics in maize seedlings of flint and dent type adapted to Polish climate. Plant Breeding and Seed Science 42: 101-108.

SOWINSKI, P., A. DALBIAK, J. TADEUSIAK and P. OCHODZKI, 1999 Relations between carbohydrate accumulation in leaves, sucrose phosphate synthase activity and photoassimilate transport in chilling treated maize seedlings. Acta Physiologiae Plantarum 21: 375-381.

SRIVASTAVA, H. K., 2004 Mitochondria-nuclear interaction in male sterility and heterosis for productivity enhancement in crop plants. Journal of Sustainable Agriculture 23: 51-72.

STAMP, P., 1984 Chilling tolerance of young plants demonstrated on the example of maize (*Zea mays* L.). *In* Advances in Agronomy and Crop Science 7. Paul Parey Berlin.

STAMP, P, 1986. Chilling stress in maize. *In* O. DOLSTRA *et al.*, eds. Breeding of Silage maize. Pudoc Wageningen.

STAMP, P., B. FEIL, M. SCHORTEMEYER and W. RICHNER, 1997. Responses of roots to low temperatures and nitrogen forms. pp. 143-154 *In* H.M. ANDERSON *et al.*, eds. Plant roots - from cells to systems. Kluver Academic Publishers, Netherlands.

STICH, B., A. E. MELCHINGER, M. FRISCH, H. P. MAURER, M. HECKENBERGER *et al.*, 2005 Linkage disequilibrium in European elite maize germplasm investigated with SSRs. Theoretical and Applied Genetics 111: 723-730.

STICH, B., H. P. MAURER, A. E. MELCHINGER, M. FRISCH, M. HECKENBERGER *et al.*, 2006 Comparison of linkage disequilibrium in elite European maize inbred lines using AFLP and SSR markers. Molecular Breeding 17: 217-226.

STICH, B., A. E. MELCHINGER, M. HECKENBERGER, J. MÖHRING, A. SCHECHERT *et al.*, 2008a Association mapping in multiple segregating populations of sugar beet (Beta vulgaris L.). Theoretical and Applied Genetics 117:1167-1179.

STICH, B., J. MOHRING, H. P. PIEPHO, M. HECKENBERGER, E. S. BUCKLER *et al.*, 2008b Comparison of mixed-model approaches for association mapping. Genetics 178: 1745-1754.

STONE, P.J., I.B. SORENSEN and P.D. JAMIESON, 1999 Effect of soil temperature on phenology, canopy development, biomass and yield of maize in a cool-temperature climate. Field Crops Research 63: 169-178.

TEPLOVA, I., R. FARKHUTDINOV, A. MITRICHENKO and G. KUDOYAROVA, 1999 Changes in zeatin and ABA content and water relations in wheat seedlings as influenced by elevated temperature. Biologia Plantarum (Prague) 42: S78.

THOMASHOW, M. F., 1999 Plant cold acclimation: Freezing tolerance genes and regulatory mechanisms. Annual Review of Plant Physiology and Plant Molecular Biology 50: 571-599.

TIMPERIO, A. M., M. G. EGIDI and L. ZOLLA, 2008 Proteomics applied on plant abiotic stresses: role of heat shock proteins (HSP). Journal of Proteomics 71: 391-411.

TRACHSEL, S., 2009a Genetic analysis of root morphology and growth of tropical maize and their role in tolerance to desiccation, aluminium and high temperature. Diss. ETH No. 18243.

TRACHSEL, S., R. MESSMER, P. STAMP and A. HUND, 2009b Mapping of QTLs for lateral and axile root growth of tropical maize. Theoretical and Applied Genetics **119:** 1413-1424.

TUBEROSA, R., S. SALVI, M. C. SANGUINETI, P. LANDI, M. MACCAFERRI *et al.*, 2002 Mapping QTLs regulating morpho-physiological traits and yield: Case studies, shortcomings and perspectives in drought-stressed maize. Annals of Botany 89: 941-963.

TUBEROSA, ROBERTO, SILVIO SALVI, MARIA CORINNA SANGUINETI, MARCO MACCAFERRI, SILVIA GIULIANI *et al.*, 2003 Searching for quantitative trait loci controlling root traits in maize: a critical appraisal. Plant and Soil 255: 35-54.

UDOMPRASERT, NAWARAT, PAUL H. LI, DAVID W. DAVIS and ALBERT H. MARKHART, III, 1995 Root cytokinin level in relation to heat tolerance of Phaseolus acutifolius and Phaseolus vulgaris. Crop Science 35: 486-490.

UTZ, H. FRIEDRICH, ALBRECHT E. MELCHINGER and CHRIS C. SCHON, 2000 Bias and sampling error of the estimated proportion of genotypic variance explained by quantitative trait loci determined from experimental data in maize using cross validation and validation with independent samples. Genetics 154: 1839-1849.

VARNEY, G. T., M. J. CANNY, X. L. WANG and M. E. MCCULLY, 1991 The branch roots of Zea .1. 1st order branches, their number, sizes and division into classes. Annals of Botany 67: 357-364.

VENABLES, W.N., and B.D. RIPLEY, 2002. Modern applied statistics with S. Springer, Berlin.

VERHEUL, M. J., P. R. VANHASSEL and P. STAMP, 1995 Comparison of maize inbred lines differing in low-temperature tolerance - effect of acclimation at suboptimal temperature on chloroplast functioning. Annals of Botany 76: 7-14.

VERHEUL, M.J., C. PICATTO and P. STAMP, 1996 Growth and development of maize seedlings under chilling conditions in the field. European Journal of Agronomy 5: 31-43.

WADA, H., Z. GOMBOS and N. MURATA, 1994 Contribution of membrane-lipids to the ability of the photosynthetic machinery to tolerate temperature stress. Proceedings of the National Academy of Sciences of the United States of America 91: 4273-4277.

WALTER, A., H. SPIES, S. TERJUNG, R. KUSTERS, N. KIRCHGESSNER *et al.*, 2002 Spatio-temporal dynamics of expansion growth in roots: automatic quantification of diurnal course and temperature response by digital image sequence processing. Journal of Experimental Botany 53: 689-698.

WIGGANS, R G, 1916 The number of temporary roots in cereals. Journal of the American Society of Agronomy 8: 31-37.

XU, Q. Z., and B. R. HUANG, 2001 Lowering soil temperatures improves creeping bentgrass growth under heat stress. Crop Science 41: 1878-1883.

ZHAO, K. Y., M. J. ARANZANA, S. KIM, C. LISTER, C. SHINDO *et al.*, 2007 An Arabidopsis example of association mapping in structured samples. PloS Genetics 3.

ZOBEL, R. W., T. B. KINRAIDE and V. C. BALIGAR, 2007 Fine root diameters can change in response to changes in nutrient concentrations. Plant and Soil 297: 243-254.

ZOBEL, R. W., 2008 Hardware and software efficacy in assessment of fine root diameter distributions. Computers and Electronics in Agriculture 60: 178-189.

Acknowledgments

„Keine Schuld ist dringender, als die, Dank zu sagen.“ (Marcus Tullius Cicero)

I would like to thank Prof. Dr. Peter Stamp for providing me the opportunity to work in his group, for his guiding advice and permanent support throughout my PhD studies. I am further grateful to my adviser Dr. Andreas Hund for introducing me into the hidden world of roots, for sharing his knowledge, for discussing challenging questions and of course for his great statistical and editorial support. I would also like to thank Prof. Dr. Albrecht E. Melchinger for offering his expertise as external co-examiner.

Thank you to Dr. Benjamin Stich for computing the association mapping and for constructive discussions at the MPI in Cologne and on the telephone and to Dr. Tobias Schrag as my contact person and seed provider at Hohenheim.

Gratitude goes to my ‘root gang’- members Andi, Dr. Nathinee Ruta as my pouch producing partner and lab mate during the experimental phase, Dr. Samuel Trachsel who built the growth containers together with me and Ms. Susanne Hochmann who offered technical support during the experimental phase.

I would like to thank Mr. Bruno Aeschbacher for managing the ‘Heterosis’-experiment, Mr. Miroslav Kares for taking care of the growth chambers and Mr. Patrick Flütsch for his kind and immediate support in building any types of constructions.

Many thanks go to all current and former members of the office A8 for creating a pleasant working atmosphere during the last years. I would like to thank PD Dr. Jörg Leipner for introducing me to the physiology of cold tolerance and to QTL studies and his warm welcome at the ETH when I first arrived to do my Master thesis. Thanks to Magali, Christophe, Tobi, Michael, André and Jörg for skiing and climbing adventures and to all other group members for the warm and friendly group atmosphere. I would further like to thank my friend Silvi for dragging me to the gym to keep us healthy and in shape during busy times.

My warmest appreciation goes to my boyfriend and partner Mr. Chad Brokopp for his never ending encouragement and his invaluable advice in all aspects of life. Last but not least my deepest heartfelt appreciations are for my parents and my brother for their unconditional love and support.

Marker information and the ‘Keygene integrated map’ were provided by Keygene N.V., P.O. Box 216, 6700 AE Wageningen, The Netherlands